UPPSALA
UNIVERSITET

Digital Comprehensive Summaries of Uppsala Dissertations from the Faculty of Science and Technology 1711

The interplay between quark and hadronic degrees of freedom and the structure of the proton

HAZHAR GHADERI

ACTA
UNIVERSITATIS
UPSALIENSIS
UPPSALA
2018

ISSN 1651-6214
ISBN 978-91-513-0420-5
urn:nbn:se:uu:diva-357911

Dissertation presented at Uppsala University to be publicly examined in 80101, Wednesday, 10 October 2018 at 09:00 for the degree of Doctor of Philosophy. The examination will be conducted in English. Faculty examiner: Prof. Dr. Thomas Gutsche (Institut für Theoretische Physik Eberhard Karls Universität Tübingen).

Abstract
Ghaderi, H. 2018. The interplay between quark and hadronic degrees of freedom and the structure of the proton. *Digital Comprehensive Summaries of Uppsala Dissertations from the Faculty of Science and Technology* 1711. 99 pp. Uppsala: Acta Universitatis Upsaliensis. ISBN 978-91-513-0420-5.

We study the low-energy sector of the strong interaction which is the least understood part of the Standard Model, the theory that describes the interactions of all known particles. The ideal particles for this study are the proton and the neutron, collectively called the nucleon. They make up the nucleus of all the atoms of our world and understanding them has been of high priority ever since their discovery. We show that one cannot neglect the effects of other hadrons, such as neutrons and pions when studying the proton. A large part of the proton's hadronic wavefunction is shown to consist of the wavefunctions of other hadrons. In other words, when probing the proton there is a sizeable probability that one is probing some other hadron surrounding the proton as a quantum fluctuation.

The nucleon itself consists of elementary particles known as quarks and gluons, collectively called partons. Exactly how the properties of these partons make up the properties of the nucleon has been the subject of active research ever since their discovery. Two main issues are the flavor asymmetry of the proton sea and the spin structure of the nucleon. To address these questions we study the interplay between the partonic and hadronic degrees of freedom. We introduce a model based on a convolution between hadronic quantum fluctuations as described by chiral perturbation theory, and partonic degrees of freedom motivated by a physical model of the nucleon having only few physically constrained parameters.

We present the hadronic distribution functions and the parton distribution functions. The results are in agreement with a large set of experimental data. These include the structure functions of the proton and the neutron. Agreement with the sum rules of the spin structure functions offers new insight into the spin structure of the nucleon.

Hazhar Ghaderi, Department of Physics and Astronomy, Nuclear Physics, Box 516, Uppsala University, SE-751 20 Uppsala, Sweden.

ISSN 1651-6214
ISBN 978-91-513-0420-5
urn:nbn:se:uu:diva-357911 (http://urn.kb.se/resolve?urn=urn:nbn:se:uu:diva-357911)

For Siamand & Sara and all my other hearts to follow

List of papers

This thesis is based on the following papers, which are referred to in the text by their Roman numerals.

I **Octet and decuplet contribution to the proton self energy**,
H. Ghaderi,
arXiv:1805.06490, 2018

II **Nucleon parton distributions from hadronic quantum fluctuations**,
A. Ekstedt, H. Ghaderi, G. Ingelman, S. Leupold,
Submitted to Phys. Rev. D (2018), arXiv:1807.06589, 2018

III **Towards solving the proton spin puzzle**,
A. Ekstedt, H. Ghaderi, G. Ingelman, S. Leupold,
Submitted to Phys. Rev. Lett. (2018), arXiv:1808.06631, 2018

My contribution to the papers

Paper I: I am the sole author of this paper.

Paper II & III: I was involved in all conceptual and technical discussions of the project. The formalism that we developed consists of a hadronic and a partonic part. For the hadronic part I derived the formulas that went into the code and the papers. This derivation is only partially documented in the papers, but a more detailed account is given in Chapter 7 of this thesis. On the partonic side I wrote a significant part of the computer code and performed numerical evaluations. I contributed to the writing of all sections of the papers.

Contents

1. Introduction

The search for knowledge and the quest to understand the world around us goes back several thousand years and probably much further back into prehistoric times. The cause of this curiosity has in many cases been driven by survival instincts. And for good reasons. But with the development of larger societies and better agriculture, this 'traditional' view on the need-of-learning slowly but surely changed. For instance in Ancient Greece, institutions allowed for seeking knowledge for the sake of knowledge, that is for sheer curiosity. Historically, only a chosen few per society had this privilege. In modern times, the distribution is much more heterogenous.[1] There are now large and many institutions all around the globe, with students numbering in the hundreds of millions, dedicated to learn more.

Science in general can be sectioned into two large categories. That of the applied sciences and that of the basic sciences. The former can be broadly described as the study of some specific, and in many cases a human-made device or application of some kind. As the name suggests, very often if not always, the main motivation is to perfect the application of said device or natural phenomena, such that in shortest time possible one can reap the benefits from it. In the basic sciences, the philosophy is somewhat different.

In the basic sciences, one seeks to understand and answer problems that ask the most fundamental questions regarding our existence. The main motivation is the yearning for learning.[2] But as evident from modern history, even in the basic sciences the search for knowledge very often also yields a great benefit for the general public in the form of an improved life quality.

In this thesis, we will study the properties of one of the most important building blocks that makes up most of our world, the *proton*. In understanding the proton one also gains knowledge about the properties of the *neutron* which is the sister particle of the proton. Together the proton and the neutron make up the nucleus of every atom around us. That is the air you breathe, the water you drink and so on are all made up of some combination of protons and neutrons. The importance of understanding these building blocks cannot be stressed enough. For instance the energy that the Sun provides us comes about because when protons and neutrons as 'fused' together inside of the Sun, the resulting mass of the new-formed object is slightly lower than the sum of its parts. Some of the mass has transformed into energy, as given by Einstein's

[1] Unfortunately, discrimination still occurs but this is a subject for another thesis.

[2] Although it is worth noting that what is basic science today, can be applied science tomorrow.

famous equation $E = mc^2$, and is radiated away in the form of light. This light is essential for the existence of life here on Earth. Furthermore due to the interaction properties between a proton in motion and human tissue, *proton therapy* has become a widely used tool in treating certain types of cancer [1].

If one takes a look around, one will notice that in large, the physical world consists of objects belonging to different size scales. We are mostly accustomed to 'normal-sized' objects such as ourselves, other human beings, insects, dust, rocks and so on. These objects have similar dynamics. You give them a push, they move (and/or they push you back). Then there are objects so large that the gravitational field they create have tangible effect on other bodies, without any physical contact. But notice that the force due to gravity is in most cases not that strong at all. The non-gravitational force created by a magnet, when acting on an object of small mass, can overcome Earth's gravitational pull on said object! Thus, in *most* cases in the study of small objects, one can safely neglect any effects of gravity.[3]

In addition to gravity, there are three other forces that we know of and have a sound theory to describe them. These are the weak interactions, the electromagnetic interactions and the strong interactions. The theory that best describes all three of these interactions is what is called the Standard Model of particle physics (cf. e.g. [2]). We will get into more detail regarding the Standard Model in Chapter 2.

Within the Standard Model (SM), the weak and the electromagnetic interactions are described by the electroweak theory which represents these forces as a single unified force. The electroweak interactions are mediated by particles which for the *weak* sector are the *massive* Z and $W^{\pm}$ gauge bosons. For the *electromagnetic* sector the interactions are mediated by the *massless* gauge boson called the photon which is denoted by γ. The fact that the gauge bosons of the weak theory are very massive implies that the range of the force in coordinate space is very short. On the same note, the masslessness of the photon implies that the range of the electromagnetic force is infinite, which for all practical purposes is in accordance with observation.

In studying electroweak interactions one can use the weak sector to describe the weak interactions and/or use quantum electrodynamics (QED) to describe the electromagnetic part of the interactions. In other words, the electroweak part of the SM is quite well understood. On the other hand, understanding the strong force offers a formidable challenge.

The part of the SM that describes the strong force is called quantum chromodynamics (QCD). It is a theory of particles called quarks and gluons that carry color charges. In QCD, the gluons mediate the strong force. Gluons are massless, but unlike photons they cannot travel that far. The strong force has a very limited range in coordinate space. Like quarks, gluons are confined

[3]Obviously, in the study of small objects that *do* have a strong gravitational field, such as black holes, gravity plays a central role.

within 'colorless' objects called *hadrons*. Hadrons come in two general categories, those containing three quarks, these are called *baryons* with the proton being the most prominent one. And those containing quark-antiquark pairs, these are called *mesons*.[4]

Now, a very useful method of problem solving is what is called perturbation theory. This is used in problems having one part that is exactly solvable and another part proportional to some small parameter a, that is treated as a perturbation. One then expands the problem in this parameter and solves the equations in order of appearance of this parameter where every order of a^j is much smaller than the previous one. That is, $a^3 \ll a^2 \ll a$ and so on. In many cases, it is then sufficient to approximate the full problem with the first non-trivial appearance of a. That is, one regards the terms proportional to a^2, a^3 and so on to be negligible. If one wants an even more refined answer, one also takes into account the term proportional to a^2, but leaves out a^3. The procedure can be continued to any desired degree of precision and one even has a control over the error one introduces in the answer by leaving out the higher order terms. This method is used in effective theories, something that in some regards also the SM can be categorized as. We will discuss effective theories in more detail in Chapter 3.

Perturbation theory is successfully applied to the SM where for instance in the electric part one expands in the fine-structure constant of electrodynamics $\alpha = e^2/(4\pi)$ where $-|e|$ denotes the electric charge of the electron. Numerically $\alpha \approx 1/137 \approx 0.0073$, thus its square is even yet smaller $\alpha^2 \approx 0.000053$. Therefore, the solutions to many of the problems one attacks in QED, are to a good extent given by the terms proportional to α.

Actually, to be more accurate, the fine-structure constant α is not a constant at all [4]. The value one extracts for it from experiment, depends on the energy-momentum (squared) of one's probe Q^2 in said experiment. In other words $\alpha = \alpha(Q^2)$. The value $\alpha \approx 1/137$ quoted above is the low-energy limit of it $\alpha(0) \approx 1/137$. At higher energies, for instance at the mass of the Z boson, one obtains $\alpha(m_Z^2) \approx 1/128$. The point is that the α of QED is not only very small but it also varies very slowly with the energy scales of present-day and most certainly all future particle physics experiments. This makes perturbation theory the optimal tool to use in solving QED problems.

For good or bad, the same cannot be said for the color dynamics of the gluons and quarks of QCD. The expansion parameter of perturbative QCD (pQCD), denoted by α_s is much more sensitive to the energies used in experiments. Furthermore whereas $\alpha(Q^2)$ grows larger for increasing values of Q^2, $\alpha_s(Q^2)$ grows larger for decreasing values of Q^2 and it actually grows close to unity for small energy-momentum transfers. This means that at small energy-momentum transfers, i.e. in dynamics involving hadrons rather than

[4]The SM also allows for hadrons containing more than 3 quarks. Experimental research in this area is very active, cf. e.g. [3].

the gluons and quarks themselves, pQCD is no longer a viable option because the perturbative expansion breaks down.

One way to proceed here is to put QCD on a lattice and aim for numerical solutions by computers [5]. This is doable in some cases, but this offers more numbers than physical insight. Another option is to make use of a low-energy effective theory of QCD called chiral perturbation theory (ChPT) [6]. In ChPT the degrees of freedom are the hadrons as opposed to the degrees of freedom of QCD, which are the gluons and the quarks collectively called *partons*.

In the intermediate region between small and large energy-momentum transfers QCD is parametrized in terms of so called parton distribution functions (PDFs). These are functions that describe the distribution of quarks and gluons inside hadrons at low energy scales. They depend on the energy-momentum of the probe, but also on what fraction x of the hadron's momentum the parton in question carry. Thus one writes the PDFs at the low energy scales as $f(x, Q_0^2)$. These PDFs are global functions meaning that once they are found for a specific hadron, the proton say, the same PDFs can be used in another reaction containing the proton. Experimentally, the PDFs are generally measured at high values of Q^2. To compare to experiment one therefore has to evolve the PDFs from the low-energy starting scale Q_0^2 to the value of the experimental one. This is possible via the Dokshitzer-Gribov-Lipatov-Altarelli-Parisi (DGLAP) evolution equations [7–9].

The exact form of the PDFs at Q_0^2 is not known from first principles and usually they are parameterized with a large number of free parameters. This is practical but offers no physical insight into the nature of the bound-state hadrons. We will in this work take the minimalistic approach in that we will use as few parameters for $f(x, Q_0^2)$ as possible while still being consistent with proton structure function data. The form of the starting distributions are here motivated by physical intuition in order to get a better understanding of low-energy strong interactions from a physics point of view.

The quantum field theoretical description of physical reality and in particular in describing the proton allows for the existence of quantum fluctuations. These fluctuations can for instance be of hadronic or partonic nature, e.g. meson-baryon fluctuations or quark-antiquark fluctuations. The latter are described by pQCD and the DGLAP equations, while the former are not. In both cases antiquarks appear inside of the proton. Either as an antiquark residing in the meson in the meson-baryon fluctuation or directly if the fluctuations are of partonic origin. Then the obvious question to ask is whether probing the antiquark in the meson-baryon fluctuation vs probing the antiquark in the partonic fluctuation might have any observable consequences. And if this turns out to be the case, how does one describe the observations quantitatively?

In paper I we investigate to what extent the hadronic fluctuations contribute to the self-energy of the proton. We take the approach of describing the physical proton state at low energies $Q^2 \lesssim 1$ GeV^2 by its Fock expansion, writing it

as a bare proton part together with its hadronic baryon-meson (BM) fluctuation part. The same philosophy is also used in papers II & III.

Formally this reads [10–16]

$$|P\rangle = \sqrt{Z}\,|P\rangle_{\text{bare}} + \sum_{BM} \alpha_{BM}\,|BM\rangle\,, \tag{1.1}$$

where $|P\rangle$ is the physical-proton state and the coefficients $\sqrt{Z}$ and α_{BM} are the probability amplitudes for the bare proton and the baryon-meson fluctuations, respectively. This is reasonable from a phenomenological point of view since we know that at the low energies quoted above, the hadrons are the relevant degrees of freedom.

Conversely, at large enough energy scales the relevant degrees of freedom are the partons of QCD hence the hadronic picture needs a cut-off of some kind. This cut-off Λ_H is one of the free parameters in our model and its value comes out to be quite understandable. The remaining parameters in our model are those for the starting PDFs $q(x, Q_0^2)$. These number in 3 plus the starting scale Q_0^2. This is in contrast to global fits of PDFs where a large number of free parameters is used to get a fit as good as possible at the cost of introducing ignorance to the physics of low-energy strong interactions.

QCD is a very successful theory of the strong interactions, but there are some open questions that are related to low-energy physics which naturally cannot be attacked via pQCD. One example is given by the *flavor asymmetry* inside the proton. For instance, due to the fact that the mass of the up and down antiquarks are both much smaller than the QCD scale parameter $\Lambda_{\text{QCD}} \approx$ 200 MeV, one would expect from a pQCD point of view that their momentum distributions inside the proton be nearly the same. Data clearly suggest that this is not the case [17]. Thus, if one is to accept that QCD is *the* theory of the strong interactions, the logical conclusion would be that the asymmetry comes from the low-energy non-perturbative part of QCD. Indeed, this is what we find in Paper II where we also derive and study the strange-quark distribution inside the proton.

One may also ask how the properties of the partons translate to the properties of the proton as a whole. In paper III we investigate what is known as the 'proton spin puzzle' which has been an outstanding problem since the 1980's. Using the same parameter values as in the asymmetry case, we provide a guiding light towards the solution of the proton spin puzzle. The x-shapes thus obtained for the spin-dependent structure functions of the neutron and the proton are consistent with data. Thus so are their integrated values, the so called sum rules.

The thesis is organized as follows. In Chapter 2 we briefly describe the SM of particle physics and its low-energy limits. The modern view of the SM is that of an effective theory. We discuss the general idea of an effective theory and give several examples of such theories in Chapter 3. In Chapter 4 we go through the basics of ChPT which is the effective theory used in the low-

energy part of our model. From the leading-order Lagrangian describing the interaction of Goldstone bosons with octet-baryons and decuplet-baryons we derive the Lagrangian describing the neutron fluctuating into a baryon-meson pair.

In Chapter 5 we describe deep inelastic scattering and the language which best describes it, which is the light-front formalism. We then introduce the structure functions and how they are related to observables. We will also show their form in the parton model and describe briefly how radiative corrections introduce a Q^2 dependence. In the same chapter, the virtual-photon asymmetries and the Bjorken sum rule are presented. We give a brief introduction to the SU(6) model of hadrons, giving a couple of examples on how to extract their constituents' contribution to the spin-dependent PDFs.

In Chapter 6 we collect all the parts of our Hadron-Cloud Model. In Chapter 7 we will get into the full details of the deep inelastic scattering calculation in the Hadron-Cloud Model and present the hadronic distribution functions and the associated fluctuation probabilities $|\alpha_{BM}|^2$ of (1.1). We will briefly discuss the connection between the probabilities to those obtained in the self-energy calculation.

In Chapter 8 we will give our conclusions with an outlook to applications of our model to other reactions involving the nucleon. Chapter 9 is written in Swedish and is a popularized summary of the work.

2. The Standard Model and its low-energy limits

This chapter contains a short overview of the collection of theories collectively known as the Standard Model of particle physics. We will briefly review gauge transformations and we will explain why invariance under gauge transformations is a desired feature of the Standard Model. We will describe QCD and some of its symmetries, in particular the chiral symmetry of QCD. We will conclude with a short prelude to ChPT.

The content of this chapter is standard material. There are many textbooks and lecture notes that deal with the content of this chapter in much more detail. See e.g. Refs. [2, 4, 18–22] for the parts that deal with the Standard Model and gauge theories. For the section on chiral symmetry cf. e.g. Ref. [6].

2.1 The matter particles and gauge bosons of the Standard Model

The ultimate decider of the validity of any statement is the experiment. Oftentimes, when building a model to describe the physical reality, there's more than one way to arrive at an answer consistent with experimental data. How does one proceed to distinguish what is the more correct theory?

There are some tools to make use of regarding this. First, there is the much general Occam's razor principle. This basically states that given two explanations for a problem, usually the simplest one should hold largest weight, i.e. is the 'more correct' one. Then there is the 'rule' of elegance of a theory that holds a lot of weight in the theoretical sciences, in particular in theoretical physics. Of course, non of these need necessarily be true or followed for a particular case, but experience has proven over and again that using them as a guide can be very fruitful.

With these principles in mind, the collection of theories that best describes elementary particles and their interactions is a renormalizable quantum field theory based on local gauge invariance under the group

$$\mathrm{SU}(3)_c \times \mathrm{SU}(2)_L \times \mathrm{U}(1)_Y. \tag{2.1}$$

This is the symmetry group of the SM before spontaneous symmetry breaking due to the Higgs mechanism.

Table 2.1. *All the matter particles (quarks and leptons) of the Standard Model together with the gauge bosons and the quanta of the Higgs field denoted by H. Each generation is a heavier copy of the previous one (in ascending order).*

	Generation		
	1	2	3
Quarks	u up	c charm	t top
	d down	s strange	b bottom

	Generation		
	1	2	3
Leptons	e electron	μ muon	τ tau
	ν_e electron-neutrino	ν_μ muon-neutrino	ν_τ tau-neutrino

Gauge bosons	g	gluons (8 of them)
	γ	gamma (the photon)
	Z	Z boson
	W^+	W^+ boson
	W^-	W^- boson

Higgs	H

The different parts stand for various sectors of the SM. The symmetry group of weak isospin, given by $\mathrm{SU}(2)_L$ and that of weak hypercharge, denoted by $\mathrm{U}(1)_Y$ together gives the electroweak sector[1] $\mathrm{SU}(2)_L \times \mathrm{U}(1)_Y$ which after spontaneous symmetry breaking reduces to the electromagnetic symmetry group $\mathrm{U}(1)_{\mathrm{EM}}$. The QCD sector of the SM is described by the *color* SU(3) gauge group $\mathrm{SU}(3)_c$. All the particles of the Standard Model are collected in Table 2.1.

2.2 Global and local invariance

In a general quantum field theory, the physics is contained in the action S, defined in 4-dimensional spacetime as

$$S = \int \mathrm{d}^4 z \, \mathscr{L}(z), \tag{2.2}$$

where the Lagrangian density $\mathscr{L}(z)$, simply called the Lagrangian for short, is some combination of field operators. In the case of a free Dirac field, it is given by the Dirac Lagrangian[2]

$$\mathscr{L}_{\mathrm{QED}}^{\mathrm{free}} = \bar{\psi}(z) \left(\mathrm{i}\gamma^\mu \partial_\mu - m \right) \psi(z). \tag{2.3}$$

[1] Also referred to as the Glashow-Salam-Weinberg model.

[2] We suppress notation for bare masses etc for now.

A symmetry transformation is a transformation that leaves the action invariant. There are two general types of symmetry transformations. Global and local ones. Global transformations are those that are independent of spacetime. For a simple example of a *global symmetry*, consider multiplying each field operator by a constant phase

$$\psi(z) \to \psi'(z) = \mathrm{e}^{\mathrm{i}\alpha}\psi(z), \tag{2.4}$$

where α is a constant real number. This is a global U(1) transformation. Equation (2.4) implies that

$$\bar{\psi}(z) \to \bar{\psi}'(z) = \bar{\psi}(z)\mathrm{e}^{-\mathrm{i}\alpha}, \tag{2.5}$$

so that the combination (2.3) is invariant and hence so is the action and thus the physics. The main reason this went through is that the constant α and thus the transformation itself is independent of the spacetime coordinate z and thus commutes with the derivative operator $\partial_\mu \mathrm{e}^{\mathrm{i}\alpha} = \mathrm{e}^{\mathrm{i}\alpha}\partial_\mu$.

Things become considerably more involved when we gauge the transformation, i.e. making it local by letting it depend on spacetime. For concreteness let now $\alpha(z)$ be given by a function depending on spacetime and consider the transformation

$$\psi(z) \to \psi'(z) = \mathrm{e}^{\mathrm{i}\alpha(z)}\psi(z). \tag{2.6}$$

We now find that the transformation is not a symmetry of the system because the derivative term is not invariant. We get for this term

$$\partial_\mu \psi \to \partial_\mu \left(\mathrm{e}^{\mathrm{i}\alpha(z)}\psi(z)\right) = \mathrm{e}^{\mathrm{i}\alpha(z)}\partial_\mu \psi + \mathrm{i}\left[\partial_\mu \alpha(z)\right]\mathrm{e}^{\mathrm{i}\alpha(z)}\psi, \tag{2.7}$$

which is different from $\mathrm{e}^{\mathrm{i}\alpha(z)}\partial_\mu\psi$ for a general function $\alpha(z)$. Thus, with our ordinary derivative ∂_μ, we find that the theory is not gauge invariant. The derivative does not transform covariantly. This is not surprising considering the definition of ∂_μ in some direction n^μ [18, 23],

$$n^\mu \partial_\mu \psi(z) = \lim_{\varepsilon\to 0}\frac{1}{\varepsilon}\left(\psi(z+\varepsilon n) - \psi(z)\right). \tag{2.8}$$

Insisting that our theory be invariant under local transformations, we can transform $\psi(z)$ and $\psi(z+\varepsilon n)$ independently and (2.8) would lose its definite meaning as a derivative. We need a derivative operator where $\psi(z)$ and $\psi(z+\varepsilon n)$ transform the same way. This is accomplished by utilizing the techniques of parallel transport. What one finds is the covariant derivative D_μ, which in the case of U(1) gauge theory is given by,

$$D_\mu = \partial_\mu - \mathrm{i}gA_\mu. \tag{2.9}$$

In (2.9) g is a constant and $A_\mu(z)$ is a real vector field that transforms as

$$A_\mu(z) \to A_\mu(z) + \frac{1}{g}\partial_\mu \alpha(z) \tag{2.10}$$

under the transformation (2.6). It is now straightforward to check that $D_\mu\psi$ and ψ transform similarly under (2.6).

Finally, to make $A_\mu(z)$ a dynamical field, one needs to write down a kinetic term for it in the Lagrangian. This kinetic term should be invariant under (2.10). By observing that $D_\mu(D_\nu\psi)$ and $(D_\mu D_\nu - D_\nu D_\mu)\psi$ transform as ψ under (2.10), one constructs

$$[D_\mu, D_\nu] \equiv -\mathrm{i}gF_{\mu\nu}, \tag{2.11}$$

where

$$F_{\mu\nu} \equiv \partial_\mu A_\nu - \partial_\nu A_\mu, \tag{2.12}$$

and $F_{\mu\nu}\psi$ transforms as ψ. The full QED Lagrangian, invariant under U(1) gauge transformations is then given by,

$$\mathscr{L}_{\mathrm{QED}} = -\frac{1}{4}F_{\mu\nu}F^{\mu\nu} + \bar{\psi}(z)\left(\mathrm{i}\gamma^\mu D_\mu - m\right)\psi(z). \tag{2.13}$$

We notice that by requiring the theory to be invariant under gauge transformations, we automatically get interactions in the theory.[3]

The procedure can be repeated for a general non-Abelian gauge group where one finds that the covariant derivative is given by

$$D_\mu = \partial_\mu - \mathrm{i}gT^a A^a_\mu, \tag{2.14}$$

where g is the gauge coupling and the T^a are the generators of the Lie algebra. They satisfy

$$\mathrm{i}f^{abc}T^c = [T^a, T^b], \tag{2.15}$$

where the f^{abc} are the structure constants of the group.

The field strength is constructed analogously to (2.11) by

$$[D_\mu, D_\nu] = -\mathrm{i}gT^a F^a_{\mu\nu}. \tag{2.16}$$

Thus

$$F^a_{\mu\nu} = \frac{\mathrm{i}}{g}[D_\mu, D_\nu]^a = \partial_\mu A^a_\nu - \partial_\nu A^a_\mu + gf^{abc}A^b_\mu A^c_\nu, \tag{2.17}$$

from which the kinetic term can be constructed

$$\mathscr{L} = -\frac{1}{2}\mathrm{tr}\left(F_{\mu\nu}F^{\mu\nu}\right), \tag{2.18}$$

where 'tr' denotes color trace.

Expanding (2.18) one finds terms with three and four gauge fields. This is drastically different from the Abelian case where gauge field self-interactions

[3]This can be seen by expanding Equation (2.13). Doing so one finds terms involving both the photon and the fermion field such as $\bar{\psi}\gamma^\mu A_\mu \psi$.

are absent.[4] This has profound implications for QCD. We will return to this in discussing QCD.

2.3 The electroweak sector of the Standard Model

Since we won't need much details of the weak interactions we won't get into the specifics regarding it. But in summary one can say that using the techniques described above, one can construct the covariant derivative for the electroweak gauge group $\mathrm{SU}(2)_L \times \mathrm{U}(1)_Y$. To describe the dynamics of the massive gauge bosons $W^{\pm}$ and the Z, one might be tempted to add mass terms such as m^2Z^2 to the theory. But such a mass term can be shown to break gauge invariance. This problem is absent in QED since photons are anyway massless and hence don't need any mass term. Also in QED the fermion mass-term is gauge invariant as we have seen. This latter statement is no longer true when one incorporates QED and the weak theory into the unified electroweak theory.

Thus if one insists on keeping a theory invariant under gauge transformations, one has to accept that explicit mass terms are forbidden. One way to generate mass terms is then via spontaneous symmetry breaking and the Brout-Englert-Higgs mechanism [24, 25]. The question is why one should consider gauge theories in the first place. The short answer is that even though one introduces redundancies when one considers gauge invariant quantities, they make life easier w.r.t. the renormalizability of the theory [26–28].

A little more involved suggestion is discussed next.

2.4 Why gauge invariance is a good thing

Some questions naturally spring to mind. Why renormalizable and why gauge invariance? And why do we ultimately want to break the symmetry and in particular why not break it explicitly instead of choosing to introduce the Higgs mechanism and thus break the symmetry hiddenly? All these questions are somewhat related and we refer the reader to [29] for a more in depth discussion on this.

To shed some light on this here, we consider classical electromagnetism as an example. We know that the dynamical fields are those of the electric and magnetic fields, $\vec{E}$ and $\vec{B}$ respectively. It is in terms of these that the original Maxwell equations are formulated.[5] We can actually set up and measure the fields $\vec{E}$ and $\vec{B}$ themselves. So in that sense they are quite physical. Now,

[4] At one-loop QED one might consider the simplest *photon-photon* interaction via a triangle of fermions. But by Furry's theorem these diagrams sum to zero (odd number of photons). The next simplest thing is a box diagram of four fermions in the loop describing photon-photon scattering, cf. Figure 3.1b.

[5] Actually, the original equations of Maxwell are in terms of the components of $\vec{E}$ and $\vec{B}$.

because the electric and magnetic fields are irrotational and divergenceless, respectively, one can reformulate the theory in terms of the *derivatives* of the scalar and vector potentials ϕ and $\vec{A}$ instead. But, due to the nature of derivatives, these functions are uniquely determined only up to additive constants. Thus, already here some redundancy is introduced into the theory. And that is really what a gauge symmetry is. It is a redundancy and not really a symmetry in a physical sense. True symmetries of Nature are global in character, and come in companion with associated conserved charges and Noether's theorem and Ward identities.

In any case, for a long period of time the potentials ϕ and $\vec{A}$ were seen as mere mathematical objects that simplified calculations and not much more. It was the more directly measurable objects $\vec{E}$ and $\vec{B}$ that were considered more fundamental. It was only in the 1950's through phenomena such as e.g. the Aharonov-Bohm effect [30] that it was recognized that the potentials contained more information than did the objects $\vec{E}$ and $\vec{B}$.

For any relativistic quantum mechanics, Galilean invariance is not enough. To the best of our knowledge, and all experimental data support this, the world around us is a Lorentz-invariant one. Hence the relativistic theories we build should respect this. Now, it is possible to press on and construct the theory in terms of say the fields $\vec{E}$ and $\vec{B}$. But this comes with the price of checking that each and every step in our calculations really is Lorentz-invariant. On the other hand, by reformulating the theory in terms of (Lorentzian) scalar products of the even more abstract four-vector potential $A^\mu = (\phi, \vec{A})$, Lorentz-invariance will be manifest. This comes with the price of introducing redundancies into the theory and one must make sure not to overcount any degrees of freedom [31]. The latter alternative is much more easier and useful in practice than is the former.

2.5 QCD

This section is devoted to perhaps the most difficult but at the same time the most fascinating part of the SM. It is about what has been established as the theory of the strong interactions, namely QCD. In contrast to the electromagnetic fine structure parameter,[6] the strong parameter $\alpha_s(\mu^2)$ grows large for low energies < 1 GeV. This running of α_s introduces a scale $\Lambda_{\rm QCD} \approx 200$ MeV where the degrees of freedom of QCD, the quarks and gluon somehow configure themselves into colorless hadrons. Around this scale, the strong coupling is large and pQCD breaks down.

[6] At the Planck scale $1/\sqrt{G_N}$ and perhaps even lower than that, quantum gravity effects are no longer negligible. Also, ordinary QFTs are questionable at these enormous energies. Here G_N is Newton's constant. The electromagnetic parameter α blows up at the Landau pole (LP) which occurs at trans-Planckian energies $E_{\rm LP} \approx 10^{277}$ GeV $\gg 1/\sqrt{G_N} \sim 10^{19}$ GeV.

More specifically, the evolution of $\alpha_s(\mu)$ is described by the renormalization group equation

$$\mu^2 \frac{\partial \alpha_s}{\partial \mu^2} = \beta(\alpha_s), \tag{2.19}$$

where the beta function $\beta(\alpha_s)$ has been computed to four-loop order in pQCD [32] and more recently to five-loop order [33].

The leading order expression for the beta function is given by,

$$\beta_0 = 11 - \frac{2}{3} n_f, \tag{2.20}$$

where n_f is the number of active light-quark flavors. We see that $\beta_0 < 0$ for $n_f \leq 16$ (this property persists to higher orders). This property leads to *asymptotic freedom* [34, 35]. Plugging in β_0 in (2.19), one can solve for α_s,

$$\alpha_s(\mu^2) = \frac{\alpha_s(\mu_0^2)}{1 + \frac{\beta_0}{4\pi} \alpha_s(\mu_0^2) \ln \frac{\mu^2}{\mu_0^2}}, \tag{2.21}$$

which relates α_s at two different scales μ_0^2 and μ^2. It is this running of α_s and the fact that it grows large at scales around Λ_{QCD} that makes pQCD break down around these scales. As is obvious from (2.20), the value of Λ_{QCD} depends on the number of active flavors one is taking into account, but its value is around 200 MeV - 300 MeV.

There are two major alternatives to handle this issue of the non-applicability of pQCD. One is lattice QCD, which emphasizes the numerical computability of QCD. The other major alternative is ChPT which takes into account the hadronic degrees of freedom. We will use the leading-order Lagrangian of ChPT. But in order to get an idea of what ChPT is about, we will first discuss QCD is more detail.

The QCD Lagrangian is given by

$$\mathscr{L}_{\text{QCD}} = -\frac{1}{2} \text{tr}\left(F_{\mu\nu} F^{\mu\nu}\right) + \bar{\psi}\left(\mathrm{i}\not{D} - M_q\right)\psi, \tag{2.22}$$

where the quark fields are collected in the object ψ and M_q is the (diagonal in flavor space) mass matrix $M_q = \text{diag}(m_u, m_d, m_s, m_c, m_b, m_t)$. The field strength is given by Equation (2.17). QCD is invariant under non-Abelian gauge transformations $U(z) \in \text{SU}_c(3)$, but due to confinement the range of the force is short as opposed to infinite as in the Abelian case of QED. The demand that only gauge-invariant objects are observable, hints at why particles carrying color, such as the gluons and the quarks, arrange themselves into color-white objects.

QCD has several exact global symmetries, such as baryon-number conservation and flavor-number conservation. The former forbids decays such as

alpha-particles (Helium nucleus) into pions

$$\mathrm{He}^{2+} \nrightarrow \pi^+\pi^+\pi^0 \quad \text{(forbidden by baryon-number conservation in QCD)}, \tag{2.23}$$

while flavor-number conservation forbids strong decays such as,[7]

$$K^+ \nrightarrow \pi^+\pi^0 \quad \text{(not allowed in QCD)}. \tag{2.24}$$

QCD has also several approximate global symmetries. These are SU(2) isospin and flavor $\mathrm{SU}(3)_f$. This can be shown if one approximates the QCD Lagrangian by ignoring the mass differences of the lightest quarks. For instance, the up and down quarks have the masses $m_u \approx 3$ MeV and $m_d \approx 5$ MeV. The difference of their mass is not small compared to the absolute value of their masses, but it is small relative the typical hadronic scale of the proton mass $m_P \approx 1$ GeV. If one ignores the mass difference between the two lightest quarks, the u and d in the QCD Lagrangian, it becomes invariant under SU(2) isospin transformations. Now, because the said mass difference is not exactly zero, but rather small, we don't expect the symmetry to be exact, but rather good. The consequence of this invariance is that the three conserved (isospin) charges commute with the Hamiltonian hence we get a degeneracy in the hadronic spectrum. This is also what is found in Nature, namely the proton and the neutron are nearly degenerate in mass and form an isospin doublet called the nucleon. The pions are nearly degenerate in mass and form an isospin vector. The isospin quartet corresponding to $I = 3/2$ are the four Delta baryons $\Delta^{++}, \Delta^+, \Delta^0$ and Δ^-. All these mentioned hadrons are major players in this thesis.

One can press on and approximate the QCD Lagrangian by taking the mass difference of the three lightest quarks u, d and s to be negligible. Then the obtained Lagrangian is invariant under flavor $\mathrm{SU}(3)_f$ transformations, but we don't expect this symmetry to be as good as the isospin symmetry previously considered. This is due to the fact that the mass of the strange quark, $m_s \approx 100$ MeV, is considerably larger than that of the u and d. In any case, it is still an order of magnitude smaller than the typical hadronic scale. The degeneracy in the hadronic spectrum due to this allows one to classify the low-lying hadrons into multiplets, as shown in Figure 2.1.[8]

In this thesis, we include all the Goldstone bosons corresponding to the spontaneously broken $\mathrm{SU}(3)_A$ symmetry of the chiral Lagrangian, a topic we now turn to.

[7] This parity-violating decay can proceed via the weak interactions yielding a much longer lifetime for the K^+.

[8] Historically, the classification of the low-lying hadrons into multiplets (the eight-fold way) was derived before the creation of QCD [36, 37].

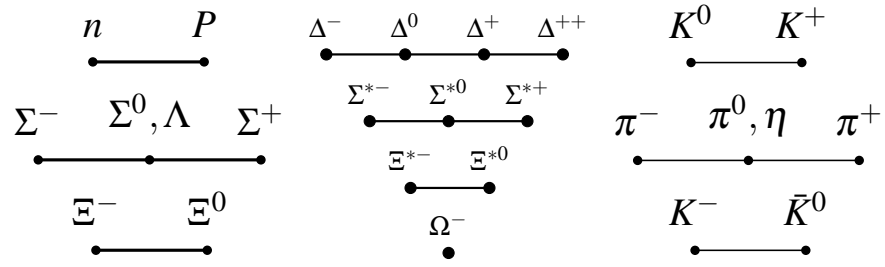

Figure 2.1. The low-lying hadrons classified into multiplets. In (a): The octet-baryons. (b): The decuplet-baryons. (c): The Goldstone bosons of spontaneously broken $\mathrm{SU}(3)_A$.

2.5.1 Chiral symmetry

In the previous section we considered QCD in the limit where we neglected the mass differences of the lightest N_f flavors, yielding the isospin $(N_f = 2)$ and flavor $(N_f = 3)$ symmetries. We now consider the limit where we set the masses of these N_f lightest flavors to zero. The QCD Lagrangian then becomes[9]

$$\mathscr{L}_{0,N_f} = -\frac{1}{2}\,\mathrm{tr}(F_{\mu\nu}F^{\mu\nu}) + \sum_{f=(s,)c,b,t} \bar{f}(\mathrm{i}\not{D} - m_f)f + \bar{q}\mathrm{i}\not{D}q. \tag{2.25}$$

By introducing the left and right handed fields

$$q_{L,R} \equiv P_{L,R}q = \frac{1 \mp \gamma_5}{2}q, \tag{2.26}$$

one finds that the QCD Lagrangian in the chiral limit is invariant under chiral transformations

$$\mathrm{SU}(N_f)_L \times \mathrm{SU}(N_f)_R, \tag{2.27}$$

that act independently on left and right handed fields.

One can further reformulate these symmetries in terms of vector and axial-vector flavor transformations to connect with the isospin and flavor transformations previously discussed in Section 2.5. Applying Noether's theorem, one then finds the conserved currents,

$$(j_A)^\mu_a = \bar{q}_{cfs}(\gamma^\mu\gamma_5)_{ss'}(t_a)_{ff'}q_{cf's'},\ a = 1,\ldots,N_f^2 - 1 \tag{2.28}$$

and

$$(j_V)^\mu_a = \bar{q}_{cfs}(\gamma^\mu)_{ss'}(t_a)_{ff'}q_{cf's'},\ a = 1,\ldots,N_f^2 - 1. \tag{2.29}$$

[9]The notation refers to the cases of setting the mass of the lightest N_f flavors to zero [38].

For $N_f = 2$, i.e. taking only the up and down quarks as massless, one obtains from these currents the corresponding (approximately) conserved charges[10]

$$(I_V)_a = \int \mathrm{d}^3 r\, q^\dagger t_a q, \;\; a = 1, \ldots, 3 \tag{2.30}$$

and

$$(I_A)_a = \int \mathrm{d}^3 r\, q^\dagger \gamma_5 t_a q, \;\; a = 1, \ldots, 3. \tag{2.31}$$

These charges commute with the QCD Hamiltonian $\mathscr{H}_{0,2}$ corresponding to the Lagrangian (2.25) and one can show that one would expect to find parity doublets, that is, particles very close in mass but of opposite parity relative to each other. These parity doublets have not been found in Nature and it seems that they do not exist.[11]

One neat way to explain this lack of parity doublets which at the same time also explains the low mass of the pions is that the axial-vector flavor symmetry $\mathrm{SU}(N_f)_A$ is hidden, or in other words, it is spontaneously broken. Corresponding to a spontaneous breaking of a continuous symmetry is the appearance of Goldstone bosons that in the case of an $\mathrm{SU}(N)$ group number in $N^2 - 1$, which is the number of degrees of freedom of said group. Now, if the chiral symmetry was an exact symmetry, these Goldstone bosons would be massless. Since we know that the chiral symmetry is only approximate, we don't expect exactly massless Goldstone bosons. But in view of the lightness of the up and down quarks as compared to the hadronic scale, we expect 'Goldstone bosons' having small mass.[12] In particular, corresponding to spontaneous breaking of $\mathrm{SU}(2)_A$, one expects to find $2^2 - 1 = 3$ Goldstone bosons. And indeed this is what is found in Nature, namely the three pions π^0, π^+ and π^- are near degenerate in mass and very light compared to other hadrons.

In this thesis we include all the Goldstone bosons corresponding to spontaneous breaking of $\mathrm{SU}(3)_A$. These number in $3^2 - 1 = 8$ and are collected in the meson-octet of Figure 2.1c.

[10] These charges are only approximately conserved in QCD due to the non-vanishing (but yet small compared to hadronic scales) of the up and down quark masses.

[11] For instance, no meson has ever been found in Nature having a mass near that of the pions but having the opposite parity to that of the pions.

[12] The strange quark is kind of *special*. In some instances it can be considered as heavy, e.g. when discussing SU(2) isospin symmetry. And in some other instances it can be considered as light (compared to the c, b, t quarks), as in for instance when considering SU(3) flavor symmetry.

3. Effective theories

In this chapter we will review some important aspects of a way to view a theoretical model that in recent times has gained more appreciation and reverence. It is the concept of an effective theory, more specifically in our case an effective field theory. We give some examples of effective theories such as low-energy QED and show their usability, but also their limitation.

Some references that goes into more detail regarding effective field theories are e.g. [39, 40].

3.1 Newtonian mechanics as an effective theory

The idea of an effective theory is really not that dramatic. For instance, before the birth of Einstein's theories of relativity, Galilean relativity together with Newtonian gravity had been applied with great success to anything from the motion of the planets to everyday things like addition of velocities.[1] It is not until extreme cases such as speeds v close to the speed of light[2] in vacuum c, or very precise measurements of gravitational effects that one notices deviation of Galilean & Newtonian relativity from data. For instance, in Galilean relativity, the addition of two collinear velocities, in the x-direction say, having relative velocity v is given by the simple rule

$$u_x = u'_x + v, \text{ (in Galilean relativity).} \tag{3.1}$$

In the special theory of relativity, the same quantity is given by

$$u_x = \frac{u'_x + v}{1 + \frac{v}{c^2}u'_x} = \left(u'_x + v\right)\left[1 - \frac{vu'_x}{c^2} + \mathscr{O}\left(\left(\frac{vu'_x}{c^2}\right)^2\right)\right], \tag{3.2}$$
$$\text{(in Einsteinian relativity).}$$

As can be seen, for low velocities compared to that of the speed of light c, the two expressions are as good as equal. Thus Newtonian mechanics is a perfectly fine theory for everyday life occurrences where the speeds involved are small compared to that of light. In that sense, it can be seen as a low-speeds effective theory of the more fundamental Einsteinian mechanics. For

[1] The precession of the perihelion of the planet Mercury is something that is difficult to account for with Galilean relativity and Newtonian gravity. It can be calculated using Einstein's general theory of relativity and the result is consistent with experimental data [41].

[2] For the purpose of illustration, we will restore c in the present section.

low speeds, it is much more *economical* to use Newtonian mechanics as can be seen from the simple addition rule of Equation (3.1) as compared to the more involved (3.2). This fact didn't change with the creation of special theory of relativity and will not change tomorrow if an even more fundamental theory of relativity is created.

But we want to stress that for speeds *not small* compared to the speed of light, the effective theory as provided by Newtonian & Galilean mechanics is simply wrong and has to be modified.

3.2 Low-energy light-by-light scattering in effective QED

In particle physics the scale separations are given in the masses and energies involved. For instance, in calculating most atomic processes, where the electron is the main player, one does not need to know even about the existence of the top quark. This is because their respective masses, m_e and m_t, are well separated by a scale Λ. That is, $m_e = 0.511\ \text{MeV} \ll \Lambda \lesssim m_t = 172000\ \text{MeV}$. Similarly, in reactions where the momentum transfers are much smaller than the electron mass, the electron can be integrated out of the theory.[3]

A simple example comes from low-energy light-by-light (γ-γ) scattering in QED. In QED, the only available mass scale is that of the electron mass m_e. Thus in low-energy γ-γ scattering where the energy of the photon E_γ is much less than the mass of the electron $E_\gamma \ll m_e$, the electron can be viewed as a very heavy static particle and its propagator $1/\Delta(p, m_e)$ essentially reduces to its inverse mass:

$$\frac{1}{\Delta(p,m_e)} = \frac{\not{p}+m_e}{p^2-m_e^2} = \frac{\not{p}+m_e}{m_e^2}\frac{1}{\frac{p^2}{m_e^2}-1} = \frac{\not{p}+m_e}{m_e^2}\left(-1-\frac{p^2}{m_e^2}\right)+\cdots \approx \frac{-1}{m_e}. \tag{3.3}$$

This means that the electron has been integrated out of the theory and is no longer a dynamical field. Therefore, one can write down an effective Lagrangian using only the electromagnetic field as a degree of freedom. If we constrain our effective theory to be invariant under Lorentz, gauge and parity transformations, one can write down the most general effective Lagrangian

[3] The term 'integrate out' comes from the act of literally integrating out the electron field from the generating functional, in the setting of path integral formalism of a quantum field theory [39, 40].

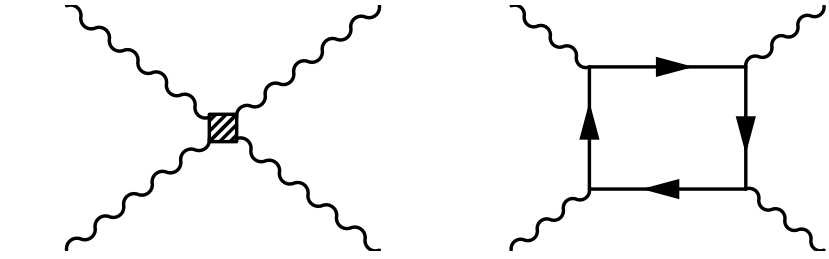

(a) (b)

Figure 3.1. Light-by-light scattering. (a): Low-energy effective theory four-photon contact interaction. (b): Leading-order contribution in QED (one-loop diagram plus permutations).

using the invariants[4] $F_{\mu\nu}F^{\mu\nu}$ and $F_{\mu\nu}\tilde{F}^{\mu\nu}$ [38, 42–44]

$$\mathscr{L}_{\text{eff,temporary}} = -\frac{1}{4}F_{\mu\nu}F^{\mu\nu} + \frac{a}{m_e^4}\left(F_{\mu\nu}F^{\mu\nu}\right)^2 + \frac{b}{m_e^4}F_{\mu\nu}F^{\nu\sigma}F_{\sigma\rho}F^{\rho\mu} + cF_{\mu\nu}\partial^2 F^{\mu\nu} + d(\partial^\mu F_{\mu\nu})(\partial_\alpha F^{\alpha\nu}) + \mathscr{O}(\partial^6), \tag{3.4}$$

where $F \in \mathscr{O}(\partial)$. The effective Lagrangian could in principle include an infinite number of terms, but by using symmetry arguments together with power counting and the approximation that we neglect terms of order $\mathscr{O}(\partial^6)$, we have reduced it down to four terms only! Actually, one can reduce the number of terms even further using information from the equations of motion. Namely

$$\partial_\mu F^{\mu\nu} - (4c-2d)\partial^2\partial_\mu F^{\mu\nu} + \mathscr{O}(\partial F\cdot F^2) + \mathscr{O}(\partial^6) = 0, \tag{3.5}$$

thus $\partial_\mu F^{\mu\nu} \in \mathscr{O}(\partial^4)$ and $\partial^2\partial_\mu F^{\mu\nu} \in \mathscr{O}(\partial^6)$. Therefore the derivative terms in (3.4) are actually not leading-order but higher-order operators and are at least $\mathscr{O}(\partial^6)$. Thus, the leading order effective Lagrangian contains only two unknown low-energy constants a and b,

$$\mathscr{L}_{\text{eff}} = -\frac{1}{4}F_{\mu\nu}F^{\mu\nu} + \frac{a}{m_e^4}\left(F_{\mu\nu}F^{\mu\nu}\right)^2 + \frac{b}{m_e^4}F_{\mu\nu}F^{\nu\sigma}F_{\sigma\rho}F^{\rho\mu} + \mathscr{O}(\partial^6). \tag{3.6}$$

An example of these effective point interactions is shown in the Feynman diagram of Figure 3.1a.

What is important to notice is that the symmetries of the more fundamental theory of QED are present in the effective theory. And that all the information of the physics in this energy regime is contained in the low-energy constants a and b in (3.6).

Suppose now for a moment that we don't know of QED. As it stands, we cannot write down an expression for the low-energy constants a and b. We

[4] Invariance under parity implies that only the square of the dual tensor $\tilde{F}_{\mu\nu} = \varepsilon_{\mu\nu\rho\sigma}F^{\rho\sigma}$ can appear in the Lagrangian.

can only hope to determine them by comparing to experiment, i.e. we measure them by recognizing the different interactions

$$\begin{aligned} F_{\mu\nu}F^{\mu\nu} &\propto \vec{E}^2 - \vec{B}^2, \\ F_{\mu\nu}\tilde{F}^{\mu\nu} &\propto \vec{E}\cdot\vec{B}. \end{aligned} \tag{3.7}$$

The idea is that we use the effective Lagrangian (3.6) in the energy regime where it is valid, until some day we construct a more predictive and more fundamental theory that describes the interaction in even more detail.

Of course we know that in this case the theory is QED. In fact, the value of the low-energy constants a and b can be *derived* in QED by computing the Feynman diagram of Figure 3.1b which can be seen as a zoom in of the effective vertex of the effective Lagrangian shown in Figure 3.1a. The result is [45],

$$a = -\frac{\alpha^2}{36} \qquad \text{and} \qquad b = \frac{7\alpha^2}{90}. \tag{3.8}$$

As seen, they are *both* given in terms of a *single* parameter α, namely the fine structure constant of QED.

We conclude this section by emphasizing that the effective theory as provided by the pure-photon Lagrangian (3.6) has its limitations. It is only valid for momenta much smaller than the electron mass. For larger momenta the effective theory has to be modified.

3.3 Fermi's theory of weak interactions

A similar example to that of Section 3.2 is given by Fermi's theory of weak interactions. For a long time, the energies of the particle accelerators were far below the mass of the Z and the W bosons and there was no knowledge about their existence. From knowledge about the symmetries of the weak interactions as obtained through experiments, one could write down an effective Lagrangian for the flavor-changing reaction $us \to ud$

$$\mathscr{L}_{\text{eff,weak}} = -2\sqrt{2}G_F V_{us}V_{ud}^* \left(\bar{u}\gamma^\mu \frac{1-\gamma_5}{2}s\right)\left(\bar{d}\gamma_\mu \frac{1-\gamma_5}{2}u\right), \tag{3.9}$$

where G_F is Fermi's constant and the V_{ij} are matrix elements of the CKM mixing matrix.[5] The four-fermion contact interaction is depicted in the Feynman diagram of Figure 3.2a. Much later when a theory with better 'resolving power' was constructed in the electroweak theory, one could understand that the vertex consisted of exchanges of very massive Z and W bosons, see Figure 3.2b.

[5] The acronym stands for Cabibbo Kobayashi–Maskawa.

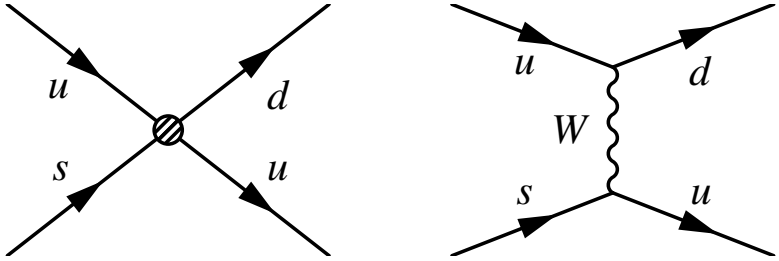

(a) (b)

Figure 3.2. Flavor-changing weak interaction. (a): Fermi's effective four-fermion interaction. (b): W-boson exchange as described by the electroweak theory.

In the electroweak theory, the lowest-order amplitude $\mathscr{M}$ of the reaction is given by

$$\mathscr{M} = \left(\frac{\mathrm{i}g}{\sqrt{2}}\right)^2 V_{us}V_{ud}^* \left(\bar{u}\gamma^\mu \frac{1-\gamma_5}{2}s\right)\left(\bar{d}\gamma^\nu \frac{1-\gamma_5}{2}u\right)\left(\frac{-\mathrm{i}g_{\mu\nu}}{p^2-m_W^2}\right), \quad (3.10)$$

where the propagator of the W-boson is written in Feynman gauge. Expanding the propagator like we did in (3.3) one can make the matching between Fermi's coupling and the weak coupling g,

$$G_F = \frac{g^2}{4\sqrt{2}m_W^2}. \quad (3.11)$$

We conclude by noting that Fermi's effective theory of the weak interactions is only valid for momenta much smaller than the mass of the W boson.

4. A brief introduction to chiral perturbation theory.

Having given some examples of effective theories and their advantages and limitations, we will in this chapter discuss a low-energy effective theory of QCD called chiral perturbation theory (ChPT) [6, 42–44, 46].

In sections 4.1-4.3 the basic building blocks of ChPT are presented. In Section 4.4 we give the full leading-order Lagrangian that we use. For completeness we give in Section 4.5 the Lagrangian for an initial state neutron fluctuating into a baryon-meson pair. The analogous Lagrangian for the initial state proton is given in the papers. We show here that the neutron Lagrangian cannot be obtained by a simple isospin flip.

4.1 An effective low-energy theory of chiral QCD

Consider the Lagrangian of Equation (2.25) with the addition of some external fields v_μ, a_μ, s and p,

$$\begin{aligned}\mathscr{L}_{0,3,\text{ext}} = &-\frac{1}{2}\,\text{tr}(F_{\mu\nu}F^{\mu\nu}) + \sum_{f=c,b,t}\bar{f}(\mathrm{i}\not{D} - m_f)f + \bar{q}\mathrm{i}\not{D}q \\ &+ \bar{q}\not{v}q + \bar{q}\not{a}\gamma_5 q - \bar{q}sq + \mathrm{i}\bar{q}\gamma_5 pq.\end{aligned} \tag{4.1}$$

The external fields are classical Hermitian 3×3 flavor-matrix fields. For instance, one can describe photon-hadron coupling by replacing v_μ by the photon field. Setting all of them equal to zero, $a = v = p = 0$, except $s \to \text{diag}(m_u, m_d, m_s)$, one obtains the full QCD Lagrangian.

To show that the Lagrangian (4.1) has a local chiral symmetry

$$\text{SU}(3)_R \times \text{SU}(3)_L = \text{SU}(3)_V \times \text{SU}(3)_A \tag{4.2}$$

one introduces the fields $r_\mu \equiv v_\mu + a_\mu$, $l_\mu \equiv v_\mu - a_\mu$ and $M \equiv s + \mathrm{i}p$. Inserting these into (4.1) one obtains

$$\begin{aligned}\mathscr{L}_{0,3,\text{ext}} = &-\frac{1}{2}\,\text{tr}(F_{\mu\nu}F^{\mu\nu}) + \sum_{f=c,b,t}\bar{f}(\mathrm{i}\not{D} - m_f)f + \bar{q}_R\mathrm{i}\not{D}q_R + \bar{q}_R\not{r}q_R \\ &+ \bar{q}_L\mathrm{i}\not{D}q_L + \bar{q}_L\not{l}q_L - \bar{q}_R M q_L - \bar{q}_L M^\dagger q_R,\end{aligned} \tag{4.3}$$

which is invariant under local flavor transformations[1] $V_{R,L}(z) \in \mathrm{SU}(3)$

$$\begin{aligned} q_{R,L} &\to V_{R,L} q_{R,L}, \\ r_\mu &\to V_R (r_\mu + \mathrm{i}\partial_\mu) V_R^\dagger, \\ l_\mu &\to V_L (l_\mu + \mathrm{i}\partial_\mu) V_L^\dagger, \\ M &\to V_R M V_L^\dagger. \end{aligned} \tag{4.4}$$

As discussed in Subsection 2.5.1, the $\mathrm{SU}(3)_A$ part is spontaneously broken and the 8 Goldstone bosons[2] are conveniently encoded in the 3×3 flavor matrix $U(z)$ having unit determinant,

$$U(z) = \mathrm{e}^{\mathrm{i}\Phi(z)/F_0}, \tag{4.5}$$

with the condition that it transforms as $U(z) \to V_R(z) U(z) V_L^\dagger(z)$ under local chiral transformations. The Hermitian matrix Φ contains the Goldstone bosons

$$\Phi = \begin{pmatrix} \pi^0 + \frac{1}{\sqrt{3}}\eta & \sqrt{2}\pi^+ & \sqrt{2}K^+ \\ \sqrt{2}\pi^- & -\pi^0 + \frac{1}{\sqrt{3}}\eta & \sqrt{2}K^0 \\ \sqrt{2}K^- & \sqrt{2}\bar{K}^0 & -\frac{2}{\sqrt{3}}\eta \end{pmatrix}. \tag{4.6}$$

At leading order, the parameter F_0 is equal to the pion decay constant $F_\pi = F_0$. The weak decay width of the charged pion is proportional to the pion decay constant which is measured to be

$$F_\pi \approx 92.4 \text{ MeV}. \tag{4.7}$$

4.2 The building blocks of mesonic ChPT

With all this in place, we now have the building blocks of the effective theory. These consist of: The unitary matrix $U(z)$ containing the Goldstone bosons; the matrix M; the chiral gauge covariant derivative

$$D_\mu A \equiv \partial_\mu A - \mathrm{i} r_\mu A + \mathrm{i} A l_\mu, \tag{4.8}$$

where A (and $D_\mu A$) transforms as $A(z) \to V_R(z) A(z) V_L^\dagger(z)$; and the left and right field strength tensors defined respectively as

$$\begin{aligned} f^L_{\mu\nu} &\equiv \partial_\mu l_\nu - \partial_\nu l_\mu - \mathrm{i}[l_\mu, l_\nu], \\ f^R_{\mu\nu} &\equiv \partial_\mu r_\nu - \partial_\nu r_\mu - \mathrm{i}[r_\mu, r_\nu], \end{aligned} \tag{4.9}$$

[1] We have suppressed the spacetime dependence of the fields, i.e. q is $q(z)$ and so on.

[2] These are also sometimes referred to as *pseudo* Goldstone bosons since a true Goldstone boson should be massless.

which transform as $f^L_{\mu\nu} \to V_L f^L_{\mu\nu} V_L^\dagger$ and $f^R_{\mu\nu} \to V_R f^R_{\mu\nu} V_R^\dagger$. In particular we note that the gluons and quarks are no longer the degrees of freedom. Actually not even all hadrons appear as active degrees of freedom at this stage. For the moment we are considering such low energies where only the Goldstone bosons are the active degrees of freedom [cf. Eq. (4.6)].

Obviously, one can build infinitely many combinations out of these building blocks. To make progress one needs a counting scheme that enables one to identify and categorize each building block in terms of importance. For instance such as the example of low-energy QED where we saw that the field strength F is counted as $F \in \mathcal{O}(\partial)$ [cf. Equation (3.4)] and $\partial \leftrightarrow p$ is a typical momentum in a reaction described by the effective theory.

Perturbative QED and pQCD being expansions in coupling constants, are valid as long as the expansion parameters (the coupling constants) are small. By definition then, terms where more powers of the expansion parameter appear, are still smaller. The appearance of the expansion parameter is as good as synonymous with the appearance of many field operators. This is however not the case in ChPT. Here the expansion is in powers of Q, where Q is a typical momentum appearing in a reaction described by ChPT, and terms with many field operators need not be irrelevant. For this reason one assumes no suppression for the Goldstone boson fields i.e.

$$U(z) \sim \mathcal{O}\left(Q^0\right). \tag{4.10}$$

One can show that the mass term actually is counted as the square of the mass of the (pseudo) Goldstone bosons, thus

$$M \sim \mathcal{O}\left(Q^2\right). \tag{4.11}$$

Also from

$$D_\mu \sim \mathcal{O}\left(Q\right), \tag{4.12}$$

one finds that [cf. e.g. Equation (2.17)]

$$f^{L/R}_{\mu\nu} \sim \mathcal{O}\left(Q^2\right). \tag{4.13}$$

4.3 Lowest-order ChPT Lagrangian

From these one can construct the Lagrangian order by order. At order Q^0 we have the trivial terms $UU^\dagger = 1$ and $\det U = 1$. At order Q we only have the building block D_μ but this is forbidden by Lorentz invariance. At order Q^2, there are only two terms (tr = flavor trace),[3]

$$\mathrm{tr}\left[\left(D_\mu U\right)^\dagger D^\mu U\right] \text{ and } \mathrm{tr}\left[U^\dagger M + M^\dagger U\right] \text{ at } \mathcal{O}(Q^2). \tag{4.14}$$

[3]There is also a third term proportional to $\mathrm{tr}\left[U^\dagger M - M^\dagger U\right]$ which has a zero coefficient due to parity invariance of the theory.

Thus, the lowest-order Lagrangian of ChPT is determined by two low-energy constants F_0 and B_0 [recall a similar situation in low-energy QED, Equation (3.6)],

$$\mathscr{L}^{(2)}_{\text{ChPT}} = \frac{1}{4}F_0^2 \,\text{tr}\left[\left(D_\mu U\right)^\dagger D^\mu U\right] + 2B_0 \,\text{tr}\left[U^\dagger M + M^\dagger U\right]. \tag{4.15}$$

Notice that even though this Lagrangian looks very simple (it is written in terms of only two free parameters) it has predictive power to a wide range of Goldstone boson interactions since it is written in terms of U and M, which can be expanded to write very complicated interactions.

4.4 Baryonic ChPT

The outline presented in the previous sections regarding mesonic ChPT can be generalized to also account for baryonic degrees of freedom. We won't go into any details here and refer the reader to [46] for an introduction. Also since the leading-order mesonic + baryonic Lagrangian of ChPT is presented in papers I & II with all the necessary information we won't repeat the details here but simply state the leading-order Lagrangian.

The leading-order Lagrangian that describes the interaction of pseudo Goldstone bosons with octet-baryons and decuplet-baryons is given by[4] [48–51],

$$\begin{aligned}\mathscr{L}_{\text{int}} = {} & \frac{D}{2}\,\text{tr}(\bar{B}\gamma^\mu\gamma_5\{u_\mu, B\}) + \frac{F}{2}\,\text{tr}(\bar{B}\gamma^\mu\gamma_5[u_\mu, B]) \\ & - \frac{h_A}{m_R}\frac{\varepsilon_{ade}\varepsilon^{\rho\mu\alpha\beta}}{2\sqrt{2}}\left[\left(\partial_\alpha \bar{T}^{abc}_\beta\right)\gamma_5\gamma_\rho u_{\mu bd}B_{ce} + \bar{B}_{ec}u_{\mu db}\gamma_5\gamma_\rho\partial_\alpha T^{abc}_\beta\right],\end{aligned} \tag{4.16}$$

where D, F and h_A/m_R are coupling constants with values determined from experiment. In the Lagrangian (4.16) the octet-baryons of Fig. 2.1a, such as for instance the proton and neutron, are encoded in the matrix B. Similarly the decuplet-baryons of Fig. 2.1b such as e.g. Δ^{++}, Δ^{+}, Δ^{0} and Δ^{-} are encoded in the object T^{abc}_β. Finally the pseudo Goldstone bosons such as e.g. the pions π^+, π^0 and π^- are encoded in the matrix u_μ which is related to the matrix U presented in Eq. (4.5) [see papers I & II for details regarding this].

If one expands (4.16) one finds that a typical term in the octet part is given by

$$\left[-\frac{D+F}{\sqrt{2}F_\pi}\right]\bar{n}\gamma^\mu\gamma_5(\partial_\mu\pi^-)P + \text{h.c.} \tag{4.17}$$

where 'h.c.' stands for Hermitian conjugate and F_π is the pion decay constant [cf. Equation (4.7)]. Equation (4.17) can be used to describe an interaction

[4] The next-to-leading-order ChPT Lagrangian for octet & decuplet baryons is presented in [47].

containing the neutron, the pion and the proton represented by the field operators $\bar{n}$, π^- and P, respectively.

Similarly a typical term in the decuplet part of (4.16) is given by

$$\left[\frac{h_A \varepsilon^{\rho\mu\alpha\beta}}{2m_R F_\pi}\right](\partial_\alpha \bar{\Delta}^{++}_\beta)\gamma_5\gamma_\rho(\partial_\mu\pi^+)P + \text{h.c.} \tag{4.18}$$

which can be used to describe the interaction between a Delta baryon (Δ^{++} in this case) with a pion and a proton represented by the field operators $\bar{\Delta}^{++}$, π^+ and P, respectively.

4.5 The Lagrangian describing neutron to baryon-meson fluctuation

In papers I and II we present the Lagrangian for the initial state being a proton state. For completeness we give here the Lagrangian for the case of having an initial-state neutron.

One might think that this should be given by a simple isospin-flip relation. However, this is not the case, there are some sign changes in some of the terms. For many calculations only the magnitude (squared) of the couplings enter each term of the final formula, as for instance in the deep inelastic scattering and the self-energy calculations. But in reactions where interference effects are involved, signs can be important. Therefore, for the convenience of the reader we list here the neutron to baryon-meson Lagrangian. These Lagrangians are all derived from (4.16).

For the case of a neutron fluctuating into a meson and an octet-baryon we find,

$$\begin{aligned}\mathscr{L}^{n\to B_{\rm oct}M} = \Bigg[&-\frac{D+F}{\sqrt{2}F_\pi}\bar{P}\gamma^\mu\gamma_5(\partial_\mu\pi^+) + \frac{D+F}{2F_\pi}\bar{n}\gamma^\mu\gamma_5(\partial_\mu\pi^0) \\ &+\frac{D-3F}{2\sqrt{3}F_\pi}\bar{n}\gamma^\mu\gamma_5(\partial_\mu\eta) + \frac{D-F}{2F_\pi}\bar{\Sigma}^0\gamma^\mu\gamma_5(\partial_\mu\bar{K}^0) \\ &-\frac{D-F}{\sqrt{2}F_\pi}\bar{\Sigma}^-\gamma^\mu\gamma_5(\partial_\mu K^-) + \frac{D+3F}{2\sqrt{3}F_\pi}\bar{\Lambda}\gamma^\mu\gamma_5(\partial_\mu\bar{K}^0)\Bigg] n + \text{h.c.}\end{aligned} \tag{4.19}$$

Table 4.1. *The neutron to baryon-meson fluctuations. Also shown are the couplings and their strength relative to the largest coupling g_{BM}^{max}, where $g_{OM}^{max} = g_{P\pi^-}$ for the octet and $g_{DM}^{max} = g_{\Delta^-\pi^+}$ for the decuplet.*

OM	$P\pi^-$	$n\pi^0$	ΛK^0	$\Sigma^- K^+$	$\Sigma^0 K^0$	$n\eta$
g_{BM}	$-\frac{D+F}{\sqrt{2}F_\pi}$	$\frac{D+F}{2F_\pi}$	$\frac{D+3F}{2\sqrt{3}F_\pi}$	$-\frac{D-F}{\sqrt{2}F_\pi}$	$\frac{D-F}{2F_\pi}$	$\frac{D-3F}{2\sqrt{3}F_\pi}$
$\lvert g_{BM}/g_{OM}^{\max}\rvert^2$	1	0.5	0.5	0.08	0.04	0.03
DM	$\Delta^-\pi^+$	$\Delta^0\pi^0$	$\Delta^+\pi^-$	$\Sigma^{*-}K^+$	$\Sigma^{*0}K^0$	
g_{BM}	$\frac{-h_A}{2m_R F_\pi}$	$\frac{-h_A}{\sqrt{6}m_R F_\pi}$	$\frac{h_A}{2\sqrt{3}m_R F_\pi}$	$\frac{-h_A}{2\sqrt{3}m_R F_\pi}$	$\frac{h_A}{2\sqrt{6}m_R F_\pi}$	
$\lvert g_{BM}/g_{DM}^{\max}\rvert^2$	1	0.67	0.33	0.33	0.17	

For the case of a neutron fluctuating into a meson and a decuplet-baryon we find,

$$\begin{aligned}\mathscr{L}^{n\to B_{\rm dec}M} = \frac{h_A \varepsilon^{\rho\mu\alpha\beta}}{2m_R F_\pi}\Bigg[&\frac{-1}{\sqrt{3}}(\partial_\alpha \bar{\Sigma}^{*-}_\beta)\gamma_5\gamma_\rho(\partial_\mu K^-) + \frac{1}{\sqrt{6}}(\partial_\alpha \bar{\Sigma}^{*0}_\beta)\gamma_5\gamma_\rho(\partial_\mu \bar{K}^0)\\ &-(\partial_\alpha \bar{\Delta}^-_\beta)\gamma_5\gamma_\rho(\partial_\mu \pi^-) - \sqrt{\frac{2}{3}}(\partial_\alpha \bar{\Delta}^0_\beta)\gamma_5\gamma_\rho(\partial_\mu \pi^0)\\ &+\sqrt{\frac{1}{3}}(\partial_\alpha \bar{\Delta}^+_\beta)\gamma_5\gamma_\rho(\partial_\mu \pi^+)\Bigg] n + \text{h.c.}\end{aligned} \tag{4.20}$$

In Table 4.1, we have collected the names of the *BM* pairs in the fluctuation together with their couplings. We have also indicated the coupling strength relative the largest coupling within a multiplet.

4.6 Assets and limitations of ChPT

Since ChPT is an effective theory it also has its range of applicability similar to the effective theories described in Chapter 3. Indeed in the case of ChPT the perturbative expansion is carried out i powers of momenta and the masses of the Goldstone bosons and in practice it is limited by two effects [52]: On the one hand ChPT breaks down where the *not-considered* degrees of freedom become active i.e. when the heavier hadrons can be excited; On the other hand ChPT breaks down when loops become as important as tree-level diagrams. Both of these limits lead to the fact that ChPT does not work for momenta in the 1 GeV range [6, 47]. How we deal with this is discussed in Chapter 6.

One of the advantages ChPT has over a pure phenomenological model such as e.g. the eight-fold way [36, 37] is that one does not need to stick to the leading-order results, but one can calculate the corrections in a systematic way. For example even before the creation of QCD one could use the eight-fold way to derive the Gell-Mann-Okubo mass formula [53],

$$m_\eta^2 = \frac{4}{3} m_K^2 - \frac{1}{3} m_\pi^2. \tag{4.21}$$

The relation (4.21) coincides with the leading-order ChPT result for the same quantity. The difference is that in the case of ChPT one can improve on the result whereas in the phenomenological eight-fold way one does not know how to improve it systematically.

If one plugs in the isospin averaged pion and kaon masses one finds $m_\eta \approx 567$ MeV which is surprisingly close to the experimental value of $m_\eta^{\text{exp}} \approx 547$ MeV, given that the comparison comes from the leading-order Lagrangian.

Another instance where ChPT has proven to be a precision science is the use of ChPT corrections to the quark-mass ratio[5] [54],

$$\frac{m_s}{m_q} = 2\frac{m_K^2}{m_\pi^2} - 1. \tag{4.22}$$

[5]Here $m_q = m_u = m_d$.

5. The structure of the proton

In this chapter we go into the details of deep inelastic scattering (DIS) and introduce the structure functions of the proton. Section 5.1 is a brief history of the investigations of the proton structure. It is aimed at the history-of-science interested reader. In Section 5.2 we introduce the relevant variables used in describing DIS on a proton. Section 5.3 introduces light-cone variables.

In Section 5.4 we investigate the 'small' and large (in the Bjorken limit) components of the photon momentum q and show that DIS takes a snapshot of the proton at light-cone time. In the sections 5.5 - 5.7 we introduce the structure functions of the proton and their interpretation in the naive parton model. The QCD-improved parton model is also discussed here.

The virtual-photon asymmetries and the sum rules for the polarized structure functions, in particular the Bjorken sum-rule are discussed in Section 5.8. We conclude this chapter with sections 5.9 and 5.10 by discussing the SU(6) model of hadrons and how it relates to the spin puzzle of the proton.

5.1 A brief history of the proton structure

With Heisenberg introducing the notion of grouping 'similar' particles into multiplets such that they can be related by some symmetry transformation, a whole new way of looking at the world of particles was established [55]. This was motivated by the discovery of the neutron by Chadwick [56] and its usefulness was further cemented by the fact that the neutron's mass is only slightly larger than that of the proton [57]. In fact it was realized that the proton, P, and the neutron, n, could generally be treated as two states of one and the same particle, the nucleon N. In this way the neutron is then related to the proton by a symmetry transformation called isotopic spin, or simply isospin, the name of which reflects the fact that the group properties are similar to those of 'ordinary' spin. At this time, there was no knowledge of the existence of quarks and in particular no knowledge about where this isospin property of the nucleon came from. Of course, we now know that the isospin symmetry between the proton and the neutron is due to the isospin symmetry between their building blocks, the so called u and d quarks, cf. Section 2.5.

Eventually even more particles were discovered which we now know are bound states of 2 or 3 valence quarks, which we call mesons and baryons, respectively. The discovery that hadrons are made of quarks goes back to the experimental data coming from DIS of electrons on protons. Similar to

the results obtained by Geiger & Marsden [58, 59] leading to the realization that the atom contains a small but compact core [60], the very important DIS experiments at SLAC [61, 62] lead to the conclusion that the protons, and hadrons in general, consist of tiny parts that indeed can carry a big part of the proton's energy & momentum.

Bjorken developed the DIS theory and amongst other introduced a variable ω into the structure functions [63]. When Feynman learned of this he realized that introducing instead the variable $x = 1/\omega = Q^2/(2p \cdot q)$ will allow him to make the parton interpretation, cf. e.g. [64]. Bjorken & Paschos very soon applied it to DIS [65]. An effort that eventually lead to the important notion of scaling, i.e. that in the Bjorken limit, $Q^2 \to \infty$ with $x = Q^2/(2p \cdot q)$ held fixed, the structure functions of the proton F_1 and F_2 are independent of Q^2 but depend only on the dimensionless variable x. Here, Q^2 denotes the square of the momentum transfer from the electron (or lepton in general) to the proton, and $q^2 = -Q^2 < 0$ is the virtuality of the photon and p is the momentum of the proton.

What was found experimentally was that scaling was approximate but only mildly violated. But not long after the derivation of Bjorken scaling it was shown that Bjorken scaling is grossly violated in all but few interacting quantum field theories (QFTs) [66,67]. The only QFTs where a mild scaling violation could occur were asymptotically free ones, i.e. those having an effective coupling approaching zero for the renormalization scale approaching infinity. None of the QFTs around at that time were asymptotically free and a quest to find one had begun. This resulted in the proposal of QCD in 1973 [34, 35] as the theory of strong interactions. The experimental data in favor of QCD as *the* theory of strong interactions soon came through the detection of three-jet events at PETRA in 1979 [68, 69].

Eventually the 'mild' modification of the Bjorken scaling was derived via QCD. The modification introduces a logarithmic energy dependence of the structure functions and it is known as the DGLAP equation also called QCD evolution [7–9]. This set of equations basically describe how the QCD vacuum is populated and evolves as gluons splits to quark-antiquarks pairs ($q\bar{q}$) and the quarks radiate gluons which transform any of their excess energy into $q\bar{q}$-pairs and so on. A very dynamical picture of the inside of hadrons began to emerge as opposed to the very static one proposed in the naive quark model [70, 71], where hadrons are pictured as consisting of 2 or 3 heavy ~ 300 MeV *valence* quarks basically sitting around carrying quantum numbers such as electromagnetic charge and color charge.

The notion of these so called valence quarks of the quark model was not totally abandoned but rather absorbed into the modern QCD improved parton model. It is still true that, for instance, the proton is made up of 2 u and one d quark but it is understood that when we say this, it is with reactions in mind where the momentum transfers are low $Q^2 \lesssim 1$ GeV. Or in other words, where one's resolution is not precise enough to resolve the sea of gluons and $q\bar{q}$-pairs

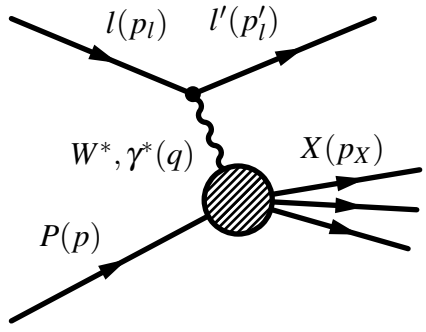

Figure 5.1. Deep inelastic scattering of a lepton $l, l' \in \{e^{\pm}, \mu^{\pm}, \nu\}$ of four-momentum p_l on a proton P of four-momentum p via one-boson exchange carrying the momentum transfer $q = p_l - p'_l$.

inside the proton. Rather, one sees 2 or 3 heavy dressed quarks, dressed by the mentioned partons. As one looks deeper one resolves more and more of the sea structure of the proton.

Once this is established, a plethora of questions arises such as what are the properties of this sea? How much of the proton's energy & momentum is carried by the sea partons? How do the properties of the sea carry over to the properties of the whole proton? To get a better feel for all the terminology just introduced we need to get into some of the details of DIS.

5.2 General deep inelastic scattering

To avoid misunderstandings and confusion when discussing experiments in the natural sciences, but most definitely when it comes to quantum mechanical processes, one needs to be very specific about what it is one is describing and what actually is the information obtained in said experiment. For instance, to get the long-distance properties of the proton, such as its overall electric charge, magnetic moment and spin, one can scatter a lepton l carrying four-momentum p_l on it and measure the recoil of the lepton and the proton. The proton stays intact and the information one extracts can be parametrized by the Pauli and Dirac form factors, cf. e.g. [4, 72]. In this case we say that we have an *elastic* scattering on the proton. These form factors are needed because the proton is not a point-like object.

More generally, there are no point-like objects in any QFT due to quantum fluctuations. For instance, there are also electron form factors in the quantum field theoretical description of electron-electron scattering. But in contrast to the proton form factors, the electron form factors are calculable in perturbative QED [73]. The proton form factors are *not* calculable from QED.

In any case, the physical situation is that plenty of photons are exchanged between the lepton and the proton. To make progress, one describes the reaction with a single photon exchange which is the leading order (in perturbative QED) contribution to the process.[1] The photon carries the momentum transfer

$$q = p_l - p'_l, \tag{5.1}$$

which is absorbed by the proton.

As one puts in more energy into the reaction, larger values of the momentum transfer become available and eventually the proton cannot stay intact and shatters into a shower of hadrons. This final-state hadronic shower carrying four-momentum p_X is denoted by X in Figure 5.1. When this happens, we say that we have an *inelastic* scattering on the proton.

Now, the DIS reaction as depicted in Fig. 5.1 is effectively a two-body reaction. But the mass of X is unspecified. Thus one has three independent kinematical variables, e.g. the square of the center of mass energy s, the momentum transfer (squared) $t = q^2$ and $p \cdot q$. But the QED part (the electron-photon vertex) is calculable whereas the part $\gamma^* + P \to X$ is what we want to explore. This latter part depends only on Q^2 and $p \cdot q$.

One can easily show that in the general scattering reaction, the momentum transfer squared is negative, i.e. $q^2 < 0$. For reasons of convenience then, one chooses to work with the variable

$$Q^2 \equiv -q^2 > 0 \tag{5.2}$$

instead.

Apart from q^2, the only other Lorentz-invariant quantity in the reaction is $p \cdot q$. Introducing the dimensionless quantity known as Bjorken x, defined by

$$x \equiv \frac{Q^2}{2p \cdot q}, \tag{5.3}$$

one can show [63, 75] that the structure functions that parameterize the internal, microscopic structure of the proton are, modulo logarithmic corrections [7–9], independent of the energy scale of the probe Q^2. This occurs in the Bjorken limit, also called the 'deep' inelastic limit. To wit, in the specific case where $Q^2 \to \infty$ with x kept fixed, the reaction is said to be a *Deep Inelastic Scattering* (DIS) on the proton. Obviously this limit is an idealization. A less strict definition of DIS is that 'deep' is when $Q^2 \gg m_P^2$ and 'inelastic' refers to when $p_X^2 = (p+q)^2 \gg m_P^2$, where m_P denotes the mass of the proton.

The cross section for DIS of a lepton on a proton is given by

$$\mathrm{d}\sigma \sim \ell^{\mu\nu} W_{\mu\nu}, \tag{5.4}$$

[1] Of course one does not need to stop at single photon exchange. See for instance [74].

where $\ell^{\mu\nu}$ is the leptonic tensor and is easily calculable.[2] The object of interest here is the hadronic tensor $W_{\mu\nu}$ which can be written as a correlation[3] of the hadronic current $J_\mu(\xi)$ in the ground-state proton, at spacetime points ξ and 0 [76],

$$W_{\mu\nu} = \frac{1}{4\pi}\int \mathrm{d}^4\xi\, \mathrm{e}^{\mathrm{i}q\xi}\, \langle P|[J_\mu(\xi), J_\nu(0)]|P\rangle\,. \tag{5.5}$$

The hadronic tensor can be parametrized in terms of Lorentz-invariant structure functions that exhibit the scaling behavior with logarithmic corrections mentioned above.

DIS is naturally a *light-cone* process. To understand this we will briefly discuss the light-front formalism and with it the light-cone time-ordered perturbation theory.

5.3 Light-front dynamics

The most common quantum mechanics is the instant-form version where one assumes commutation relations for the relevant operators at *equal times*,[4] say at $\xi^0 = 0$. Dirac [77] recognized two other options, the forward hyperboloid form, also more commonly called the 'point form' of dynamics with $\xi^2 =$ const. > 0, $\xi^0 > 0$, and the front form

$$\begin{gathered}\xi^0 + \xi^3 = 0,\\ (\text{quantization sheet for front-form dynamics}).\end{gathered} \tag{5.6}$$

Later on, Leutwyler & Stern completed the construction making it in total five inequivalent forms of relativistic dynamics [78], see also [79] for a review on this subject. These different forms of dynamics are related to hyper-surfaces having tangents pointing into the space-like regions of Minkowski space. Two such surfaces, for the instant form and the front form are shown in Figure 5.2.

The instant form of dynamics is the most common, but application of front form of dynamics is far from rare [80]. This form has its advantages e.g. in the light-front gauge, $A^0 + A^3 = 0$, QCD is ghost-free, and disadvantages (e.g. it is quite unintuitive).[5] Some of its advantages are that it yields the maximum number of the generators of the Poincaré group kinematical, that is, free of interactions [77, 82].[6]

[2] For instance in the case of scattering a muon or electron on a nucleon $\ell^{\mu\nu} = \mathrm{tr}[\not{p}'_l\gamma^\mu \not{p}_l\gamma^\nu]/2$ (we have neglected the mass of the lepton), cf. Figure 5.1.

[3] Only the connected part is included in Equation (5.5), that is, vacuum transitions of the form $\langle 0|J_\mu(\xi)J_\nu(0)|0\rangle\,\langle P|P\rangle$ are excluded.

[4] To avoid confusion with the Bjorken-x variable, we denote the spacetime vector by $\xi^\mu = (\xi^0, \xi^1, \xi^2, \xi^3) = (t, x, y, z)$.

[5] See [81] for an introduction to light-cone variables, rapidity and all that.

[6] The terms 'light-front' and 'light-cone' are synonyms and used throughout and sometimes interchangeably.

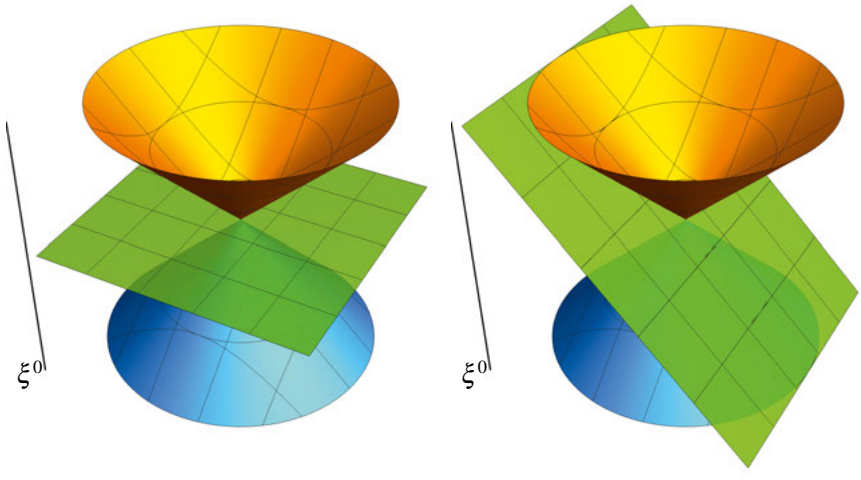

(a) (b)

Figure 5.2. Quantization surfaces for (a) instant form, $t = \xi^0 = 0$ and (b) front form, $t + z = \xi^0 + \xi^3 = 0$.

But it also has its issues, such as those related to so called end-point singularities. For instance, in calculations involving Feynman loops in combination with residue techniques similar to what we do in Paper I, care needs to be taken, see e.g. [83, 84] and the references therein.

The light-cone coordinates of a general four-vector $l = (l^+, l^-, \vec{l}^\perp)$ are given by

$$\vec{l}^\perp \equiv (l^1, l^2) \text{ with } l^\perp \equiv \|\vec{l}^\perp\| \tag{5.7}$$

and

$$l^\pm \equiv l^0 \pm l^3 \leftrightarrow l^0 = \frac{1}{2}(l^+ + l^-) \text{ and } l^3 = \frac{1}{2}(l^+ - l^-). \tag{5.8}$$

Another useful combination that shows up in the light-front spinors is the object

$$l^1 \pm i l^2 = l^\perp e^{\pm i\phi}, \tag{5.9}$$

see Figure 5.3. Including the Jacobian of the transformation (5.8), the volume element is given by

$$d^4 l = \frac{1}{2} dl^+ dl^- d^2 l_\perp. \tag{5.10}$$

From these, one can write down the Lorentzian inner-product of any two four-vectors a and b as

$$a \cdot b = \frac{1}{2}\left(a^+ b^- + a^- b^+\right) - \vec{a}_\perp \cdot \vec{b}_\perp, \tag{5.11}$$

with the obvious special case ($a = b$)

$$a^2 = a^+ a^- - a_\perp^2. \tag{5.12}$$

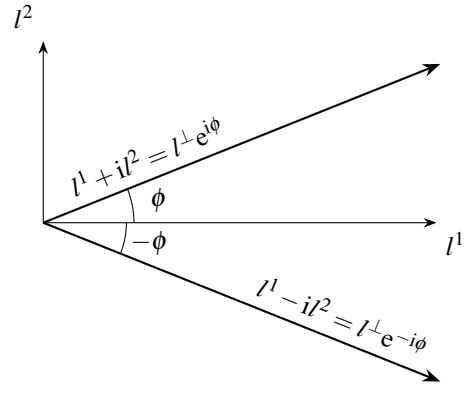

Figure 5.3. Definition of the phase ϕ.

From Equation (5.12) follows that the four-momentum k of an on-shell particle of mass m, satisfies the following dispersion relation

$$k^- = \frac{m^2 + k_\perp^2}{k^+}, \quad \text{(on-shell)}. \tag{5.13}$$

In QFT applications in the instant form (see e.g. [4, 18–20]) one deals with time-ordered correlation functions. At some point in the calculations one has to Fourier transform time-ordered plane-wave factors. An expression that typically appears is

$$\int \mathrm{d}^4x\, \mathrm{e}^{\mathrm{i}px}\, \Theta(t)\, \mathrm{e}^{-\mathrm{i}kx} = (2\pi)^3 \delta^{(3)}(\vec{p} - \vec{k})\, \frac{\mathrm{i}}{p^0 - k^0 + \mathrm{i}\varepsilon}, \tag{5.14}$$

where k denotes again the four-momentum of a one-particle state, i.e. one has $k^2 = m^2$. Obviously, the expression in (5.14) has only support for $\vec{k} = \vec{p}$, but $p^0 \neq k^0$ is possible. One can interpret Equation (5.14) such that in this (ordinary) time-ordered perturbation theory (TOPT) the three-momentum $\vec{k}$ is conserved at a vertex while the energy k^0 is not.

In light-cone time-ordered perturbation theory (LCTOPT), it is the plus-component k^+ and the perpendicular components $\vec{k}_\perp = (k_1, k_2)$ that are conserved while the light-cone energy $k^- = k^0 + k^3$ is not. Taking this and the above changes of variables into account, the transition from TOPT to LCTOPT is straightforward.

A major area of application of light-front dynamics and LCTOPT is in DIS problems. This is because in the Bjorken limit, light-front coordinates separates the variables into large and small components as we now will show.

5.4 DIS takes a snapshot at light-cone time

The canonically conjugate variable to ξ^+ is the light-cone energy $k^- = k^0 - k^3$. The light-cone time ξ^+ multiplies the large component of the photon energy q^- when Fourier transforming [cf. Equation (5.5)].

That q^- is indeed large can be seen by choosing

$$\vec{q} \parallel (-\vec{e}_3) \Rightarrow q = (\nu, 0, 0, -|q^3|). \tag{5.15}$$

Since $Q^2 \equiv -q^2 = q_3^2 - \nu^2$, we have that $|q_3| = \sqrt{Q^2 + \nu^2}$. Then a finite Bjorken-$x$ variable [cf. Equation (5.3)]

$$x = \frac{Q^2}{2p \cdot q} = \frac{Q^2}{2(p^0 \nu + p^3 \sqrt{Q^2 + \nu^2})}, \tag{5.16}$$

where p is the proton momentum, implies $\nu \sim Q^2$ so that

$$|q_3| \approx \nu. \tag{5.17}$$

Thus

$$q^+ = \nu + q^3 = \nu - |q^3| \text{ is small (at least not large)} \tag{5.18}$$

while

$$q^- = \nu - q^3 = \nu + |q^3| \approx 2\nu \sim Q^2 \text{ is large.} \tag{5.19}$$

Now, the the integral in (5.5) has only support for small ξ^+. Everything else is averaged out because of the large q^- that multiplies ξ^+ in the exponential. Naively one might think that DIS takes an instantaneous snapshot of a small spatial region, i.e. that all components of ξ are small. But this is not the case: ξ^- can be sizable. Concerning the smallness of spatial regions, one can show, however, that in the two directions perpendicular to the "collision axis" of proton and γ^* the focus is on small $\xi_\perp$ [76]. This comes about because the commutator in (5.5) has only support for time-like ξ^2 (microcausality) [4]. Thus $\xi^2 > 0$, i.e. $\xi_\perp^2 < \xi^+ \xi^-$. Since ξ^+ must be small [and ξ^- is not large, just normal $\sim 1/(xm_P)$] then $\xi_\perp$ must be small.

5.5 The structure functions

For both the target and the beam unpolarized, the cross section for the DIS reaction $l^\pm P \to l^\pm X$ shown in Figure 5.1, is given by[7] [72, 87]

$$\frac{\mathrm{d}^2\sigma}{\mathrm{d}x\mathrm{d}Q^2} = \frac{4\pi\alpha^2}{Q^4} \left[\left(1 - y - \frac{m_P^2 y^2}{Q^2} \right) \frac{F_2(x, Q^2)}{x} + y^2 F_1(x, Q^2) \right], \tag{5.20}$$

[7] The cross section given in (5.20) refers to the single-photon/boson exchange cross section. Two-photon contribution to the DIS cross section has been measured to be consistent with zero within the uncertainties of the measurement [85]. The interference effects of virtual Z^0 and photon exchange are found to be small [86].

where the functions F_1 and F_2 are called the *unpolarized structure functions* of the proton. They parametrize our ignorance of the proton structure. We will return to their interpretation within the *parton model* in Section 5.6. In Equation (5.20) the term proportional to $m_P^2 y^2/Q^2$ is as good as zero for our purposes and can be omitted. The variable y is defined as [88]

$$y = \frac{q \cdot p}{p_l \cdot p} = 1 - \frac{E'}{E}, \tag{5.21}$$

where the second equality is evaluated in the proton rest frame and E (E') refers to the energy of the initial-state (final-state) lepton in the rest frame of the proton. Another variable widely used in DIS lingua is the energy loss of the incoming particle [cf. Equation (5.1)]

$$\nu = \frac{q \cdot p}{m_P} = E - E'. \tag{5.22}$$

For *both* the target and the lepton beam longitudinally polarized, the difference of cross sections for parallel and antiparallel spins of the proton and the lepton is given by [89],

$$\frac{\mathrm{d}^2\Delta\sigma_{\parallel}}{\mathrm{d}x\mathrm{d}Q^2} = \frac{16\pi\alpha^2 y}{Q^4}\left[\left(1 - \frac{y}{2} - \frac{\gamma^2 y^2}{4} - \frac{m_l^2 y^2}{Q^2}\right) g_1(x,Q^2) - \frac{\gamma^2 y}{2} g_2(x,Q^2)\right]. \tag{5.23}$$

In Equation (5.23), the g_1 & g_2 are the *polarized* structure functions. They parametrize our ignorance about the spin structure of the proton.

Basically, the leptonic tensor $\ell^{\mu\nu}$ of Equation (5.4) contains a symmetric (in $\mu\nu$) and an antisymmetric part (in $\mu\nu$). The antisymmetric part is proportional to the spin vector of the lepton while the symmetric part is not. Similarly for a spin-1/2 target, such as the proton, the hadronic tensor $W_{\mu\nu}$ has a symmetric and an antisymmetric part. The symmetric part is independent of the target's spin vector while the antisymmetric part is proportional to the spin vector of the target. Therefore the contraction $\ell^{\mu\nu}W_{\mu\nu}$ in the DIS cross section (5.4) contains terms that are totally independent of any spin and it contains terms that are proportional to the spins of *both* the lepton and the target proton. Thus to measure the polarized structure functions g_1 and g_2, both the target proton and the lepton beam must be polarized. Obviously then, to measure the unpolarized structure function F_1 and F_2 it suffices to use unpolarized beam and/or target [88].

We will now consider these structure functions in the parton model.

5.6 The naive parton model

In the simple (naive) parton model, one assumes that the constituents of the proton, the partons, are free and pointlike and interact elastically with the lep-

ton. Furthermore, the unpolarized structure function $F_1(x)$ is independent of the momentum transfer Q^2 and it is given by (cf. e.g. [88, 90]),

$$F_1(x) = \frac{1}{2}\sum_q e_q^2 \left[q(x) + \bar{q}(x)\right], \tag{5.24}$$

where e_q denotes the electric charge of the quark q. In Equation (5.24) are defined the *unpolarized* PDFs for a quark and antiquark of flavor q, respectively as

$$q(x) \equiv q^{\uparrow}(x) + q^{\downarrow}(x), \tag{5.25}$$

and

$$\bar{q}(x) \equiv \bar{q}^{\uparrow}(x) + \bar{q}^{\downarrow}(x), \tag{5.26}$$

where $q^{\uparrow(\downarrow)}(x)$ is the number of flavor q quarks carrying a momentum fraction x of the proton having spin parallel (antiparallel) to the spin of the proton.

In the parton model, the polarized structure functions are given by

$$g_2(x) = 0 \tag{5.27}$$

and

$$g_1(x) = \frac{1}{2}\sum_q e_q^2 \left[\Delta q(x) + \Delta\bar{q}(x)\right], \tag{5.28}$$

where the *polarized* PDFs for a quark and antiquark of flavor q are defined as

$$\Delta q(x) \equiv q^{\uparrow}(x) - q^{\downarrow}(x) \tag{5.29}$$

and

$$\Delta\bar{q}(x) \equiv \bar{q}^{\uparrow}(x) - \bar{q}^{\downarrow}(x), \tag{5.30}$$

respectively. These together with the unpolarized ones are the all-important PDFs. They are *universal* in the sense that they are the same for a given hadron no matter what reaction one is considering. They have not yet been calculated from first principles because they are partly (QCD) non-perturbative objects.

In the parton model, the structure functions F_1 and F_2 satisfy the Callan-Gross relation [91]

$$F_2 = 2xF_1. \tag{5.31}$$

In other words $F_2(x)$ is given in terms of $F_1(x)$. To derive the Callan-Gross relation (5.31) in the parton model, one assumes that the electrically charged partons (the quarks) are spin-1/2 particles.[8] The experimental verification of the Callan-Gross relation [92] is indeed strong evidence of the spin-1/2 nature of the confined quarks.

As seen, in the parton model, the PDFs and thus the structure functions are independent of Q^2 [63]. Radiative corrections bring in the Q^2 dependence.

[8]For instance, if one assumes the partons to be spin-0 particles one would get that $F_1(x) = 0$ which is experimentally invalidated.

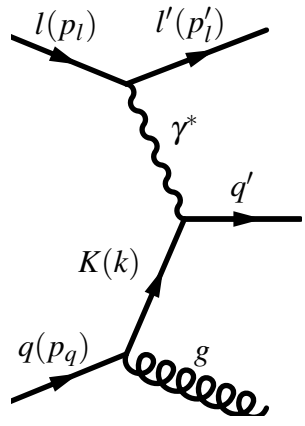

Figure 5.4. Scattering of a lepton on a quark K with momentum $k = zp_q = xp$ where p is the momentum of the proton and p_q is the momentum of the quark before radiation of a gluon g. Another contribution to this process is when the gluon is radiated after the photon-quark interaction.

5.7 QCD-improved parton model

In the QCD-improved parton model, the structure functions gets logarithmic corrections and no longer scale.[9] The quarks can now radiate and absorb gluons and gluons can split into quark-antiquark pairs and so on. Through a process called *factorization*, very similar to renormalization, one can write down the renormalized PDFs at a factorization scale μ_F [93, 94]

$$q(x,\mu_F^2) = q_0(x) + \frac{\alpha_s}{2\pi}\int_x^1 \frac{\mathrm{d}z}{z} q_0\left(\frac{x}{z}\right) P(z) \ln\frac{\mu_F^2}{\kappa^2}. \tag{5.32}$$

Here $q_0(x)$ is the (non-observable) bare parton distribution and κ^2 is an infrared cut-off. Basically, the infrared cut-off κ is the virtuality $\kappa^2 = k^2$ of the quark K and comes from a collinear divergency due to the radiated gluon g of Figure 5.4. This divergency is absorbed into the non-observable bare distribution $q_0(x)$. The variable $z = k/p_q$ is the longitudinal momentum fraction carried by the quark after the radiation, thus $p_q = xp/z$ where p is, as usual, the momentum of the proton.

This yields the Q^2-dependent structure functions the logarithmic dependence of which have been verified experimentally over several orders of magnitude,

$$\begin{aligned} F_1(x,Q^2) = \frac{1}{2}\sum_q e_q^2 \Bigg[& q(x,\mu_F^2) + \frac{\alpha_s}{2\pi}\int_x^1 \frac{\mathrm{d}z}{z} q\left(\frac{x}{z},\mu_F^2\right) \\ & \times \left(P(z)\ln\frac{Q^2}{\mu_F^2} + C(z) + \cdots \right) \Bigg], \end{aligned} \tag{5.33}$$

[9] The structure functions are said to scale if they only depend on x and not on Q^2.

where the ellipsis stand for higher order ($\alpha_s^2, \alpha_s^3, \ldots$) contributions. In equations (5.32) and (5.33), $P(z)$ and $C(z)$ are functions that can be calculated in QCD via diagrams such as the one in Figure 5.4.

We note that it is convenient to choose the factorization scale $\mu_F^2 = Q^2$ because then the explicit logarithm in the structure function is identically zero and all the Q^2 dependency will be put on the PDFs $q(x, Q^2)$.

This is not the end of the story however. Since α_s itself depends on the renormalization scale μ [cf. Equation (2.21)] and it does so as inversely proportional to a logarithm, the factor $\frac{\alpha_s(\mu^2)}{2\pi} \ln(\mu_F^2/\kappa^2)$ is not necessarily small. This problem is solved by a resummation of such terms to a power n. The resulting system of differential equations for the PDFs as functions of x and the momentum transfer Q^2 of the probe are the DGLAP equations. We won't give the full details here, but will state a simpler version of the DGLAP equation where we only take gluon radiation from a parton into account.

Consider the situation of Figure 5.4 only slightly more generalized. Suppose the struck quark radiates n gluons instead of merely one as shown in the figure. Then at each intermediate step the quark carries a momentum fraction x_i and virtuality t_i with presumably $t_0 \ll t_1 \ll \cdots \ll t_{n-1} \ll t_n \ll t = Q^2$ and for sure $x_0 > x_1 > \cdots > x_{n-1} > x_n = x$. One can then show that the resulting differential equation is given by the following simpler DGLAP equation

$$\frac{\partial q(x,t)}{\partial \ln t} = \frac{\alpha_s(t)}{2\pi} \int_x^1 \frac{\mathrm{d}z}{z} P(z) q\left(\frac{x}{z}, t\right). \tag{5.34}$$

Notice that the $\alpha_s(t)$ is evaluated at the same scale as the PDF. We also note that this is a differential equation for $q(x,t)$ in t hence an initial condition needs to be specified. These *starting distributions* have not been derived from first principles and usually they are parametrized with a large set of (~ 25) parameters and fitted to experimental data.

The universality of the PDFs (due to factorization [94]) then implies that one can use the PDFs for other reactions. This way of thinking is understandable from a practical point of view, but it does not provide any insight into the physics of the PDFs and the strongly bound system. In the present work, we promote the idea of using intuition and simple modeling for the starting distributions at some low scale Q_0^2 and then use DGLAP to compare to experiment which usually determines the PDFs at larger scales $Q^2 > Q_0^2$.

5.8 Virtual-photon asymmetries and the Bjorken sum rule

To extract information on the spin-dependent distributions, what one measures experimentally are the so called virtual-photon asymmetries. The imaginary part of the forward Compton amplitude and the virtual-photon absorp-

tion cross-section are related by the optical theorem, enabling one to write the virtual-photon asymmetries as[10] [95]

$$\begin{aligned} A_1 &= \frac{\sigma_{1/2}^T - \sigma_{3/2}^T}{\sigma_{1/2}^T + \sigma_{3/2}^T} = \frac{g_1 - \gamma^2 g_2}{F_1}, \\ A_2 &= \frac{2\sigma^{LT}}{\sigma_{1/2}^T + \sigma_{3/2}^T} = \gamma \frac{g_1 + g_2}{F_1}, \end{aligned} \tag{5.35}$$

where

$$\gamma \equiv \frac{2Mx}{\sqrt{Q^2}}. \tag{5.36}$$

We notice that for a high-energy beam either x is small or Q^2 is large thus $\gamma \equiv 2Mx/\sqrt{Q^2}$ is small. The asymmetry A_2 being proportional to γ is expected to be small at high energies [96]. Thus for our purposes we will be more interested in comparing our results to

$$A_1 \simeq \frac{g_1}{F_1}. \tag{5.37}$$

In Equation (5.35) all the differential cross sections depend on x and Q^2 [97] which we have suppressed. Furthermore $\sigma_{3/2}$ ($\sigma_{1/2}$) is the differential cross-section for the absorption of a transversely polarized photon having spin polarized parallel (antiparallel) to the spin of the longitudinally polarized proton.

Let us consider the following integrals of the proton and neutron structure functions [98–100]

$$\Gamma^{P\pm n}(x_{\min}, Q^2) = \int_{x_{\min}}^1 \mathrm{d}x \left(g_1^P(x, Q^2) \pm g_1^n(x, Q^2) \right). \tag{5.38}$$

The lower limit of the integral represents the fact that for a fixed value of Q^2 the low-x region is difficult to access experimentally. Thus some extrapolation is required. Strictly speaking, also the upper limit involves some extrapolation but here it is more straightforward since $g_1(x, Q^2)$ depends on the difference of quark distributions it must vanish in the $x \to 1$ limit, because the unpolarized distributions are observed to do so [90].

On the theory side Bjorken derived the following Q^2-independent relation using isospin symmetry ($\Delta u^P = \Delta d^n$) and current algebra [98, 99]

$$\Gamma_{\mathrm{Bj}}^{P-n} = \int_0^1 \mathrm{d}x \, [g_1^P(x) - g_1^n(x)] = \frac{|g_A/g_V|}{6}, \tag{5.39}$$

where $|g_A/g_V|$ is the (coupling) strength of the neutron beta decay. In QCD, the structure functions acquire radiative corrections[11] (cf. Section 5.7) and

[10] Due to the smallness of the spin-dependent part of the total cross section, they can be best determined from cross-section asymmetries where the spin-independent parts cancel.

[11] In other words they become Q^2 dependent.

thus so does the Bjorken sum rule. These corrections can be calculated order by order in pQCD. For three active flavors, u, d and s, the expression for the Bjorken sum rule up to and including $\mathscr{O}(\alpha_s^4)$ is given by [101, 102],

$$\Gamma_{\rm Bj}^{P-n}(Q^2) = \frac{|g_A/g_V|}{6}\left[1 - \frac{\alpha_s(Q^2)}{\pi} - \frac{3.5831\ \alpha_s^2(Q^2)}{\pi^2} - \frac{20.2165\ \alpha_s^3(Q^2)}{\pi^3} - \frac{175.673\ \alpha_s^4(Q^2)}{\pi^4} + \mathscr{O}\left(\alpha_s^5\right)\right]. \tag{5.40}$$

Plugging in the numbers $|g_A/g_V| = 1.2723 \pm 0.0023$ from neutron beta decay and $\alpha_s(3\ \text{GeV}^2) = 0.25$ [103] we see that

$$\Gamma_{\rm Bj}^{P-n}(3\ \text{GeV}^2) = 0.187, \tag{5.41}$$

which is in quite good agreement with data [104],

$$\Gamma^{P-n}(3\ \text{GeV}^2) = 0.181 \pm 0.008\ (\text{stat.}) \pm 0.014\ (\text{syst.}). \tag{5.42}$$

We note that the naive quark model gives the value $|g_A/g_V|_{\rm SU(6)} = 5/3 \approx 1.67$, which is much larger that the above quoted experimental value. Obviously to be in agreement with experiment (and the Bjorken sum rule) something more is needed. A more realistic model should also take into account relativistic effects and possibly effects of SU(6) breaking. This is the topic of Paper III.

Starting with the naive quark model expression for the integral

$$\Gamma^{P+n} = \int_0^1 \mathrm{d}x\,[g_1^P(x) + g_1^n(x)], \tag{5.43}$$

and assuming $\mathrm{SU}(3)_f$ flavor symmetry and that the strange quark and sea polarization are zero i.e. that $\Delta s = \Delta\bar{q}_i = 0$ one obtains the so-called Ellis-Jaffe sum rule [100]. This sum rule has been invalidated by experiment and we won't go into more detail here regarding its theoretical aspects, cf. e.g [105].

5.9 The SU(6) model of hadrons

One of the simplest ways to model hadrons is via their SU(6) wavefunction. This consists of a direct product of their quark and spin representations appropriately symmetrized [21]. The simplest hadronic SU(6) wavefunction is that of the Δ^{++} baryon with helicity $\lambda = +3/2$. The Δ^{++} consists of three u quarks and if it is in a helicity $\lambda = 3/2$ configuration the spin of the quarks must all be aligned, say 'up' along the quantization axis. We denote this state by $|\Delta^{++}, 3/2\rangle$. Thus the SU(6) representation of $|\Delta^{++}, 3/2\rangle$ is given by

$$|\Delta^{++}, 3/2\rangle = |u\uparrow u\uparrow u\uparrow\rangle, \tag{5.44}$$

where each 'up arrow' refers to the neighboring quark on its left. The other wavefunctions corresponding to the helicity configurations $\lambda = 1/2$, $-1/2$ and $-3/2$ can be obtained by suitable lowering operators acting on the spin space.

Having the wavefunction at our disposal, one can start calculating and comparing to observables. For instance consider the following expectation value

$$\Delta q_H = \langle H | N_{q\uparrow} - N_{q\downarrow} | H \rangle \,, \tag{5.45}$$

where $N_{q\uparrow}$ counts the number of flavor q quarks with polarization $\uparrow$ and $N_{q\downarrow}$ counts the number of q quarks with polarization $\downarrow$.

Thus in the case of the $|\Delta^{++}, 3/2\rangle$ we have,

$$N_{u\uparrow} |\Delta^{++}, 3/2\rangle = N_{u\uparrow} |u\uparrow u\uparrow u\uparrow\rangle = (1+1+1)\,|u\uparrow u\uparrow u\uparrow\rangle = 3\,|u\uparrow u\uparrow u\uparrow\rangle \tag{5.46}$$

and $N_{u\downarrow} |\Delta^{++}, 3/2\rangle = N_{u\downarrow} |u\uparrow u\uparrow u\uparrow\rangle = 0$. Thus

$$\Delta u = \langle u\uparrow u\uparrow u\uparrow | N_{u\uparrow} - N_{u\downarrow} |u\uparrow u\uparrow u\uparrow\rangle = \langle u\uparrow u\uparrow u\uparrow | N_{u\uparrow} |u\uparrow u\uparrow u\uparrow\rangle = 3 \tag{5.47}$$

for $|\Delta^{++}, 3/2\rangle$. Obviously $\Delta d = 0$ for the same state.

Next we consider a slightly more involved wavefunction, that of the proton. For concreteness let us consider the 'up' polarized proton $|P, 1/2\rangle$. Its SU(6) wavefunction is given by,

$$|P, 1/2\rangle = \frac{\sqrt{2}}{6}\left[2\,|u\uparrow u\uparrow d\downarrow\rangle - |u\uparrow u\downarrow d\uparrow\rangle - |u\downarrow u\uparrow d\uparrow\rangle\right] + \text{permutations}. \tag{5.48}$$

The counting procedure gives,

$$\begin{aligned} &N_{u\uparrow} |P, 1/2\rangle \\ &= \frac{\sqrt{2}}{6}\left[2\cdot 2\,|u\uparrow u\uparrow d\downarrow\rangle - |u\uparrow u\downarrow d\uparrow\rangle - |u\downarrow u\uparrow d\uparrow\rangle\right] + \text{permutations}. \end{aligned} \tag{5.49}$$

Similarly,

$$N_{u\downarrow} |P, 1/2\rangle = \frac{\sqrt{2}}{6}\left[0 - |u\uparrow u\downarrow d\uparrow\rangle - |u\downarrow u\uparrow d\uparrow\rangle\right] + \text{permutations}, \tag{5.50}$$

yielding the result

$$\Delta u = \frac{4}{9} \times 3 = \frac{4}{3}, \tag{5.51}$$

where the factor of 3 comes from the permutations.

Doing a similar calculation for the d quarks one finds,

$$\Delta d = -1/3. \tag{5.52}$$

And since the proton does not contain any valence anti-quarks or valence strange-quarks, we find that the fraction of the proton's spin carried by its quarks is,

$$\Delta\Sigma \equiv \Delta u + \Delta d + \Delta s + \Delta\bar{u} + \Delta\bar{d} + \Delta\bar{s} = \frac{4}{3} - \frac{1}{3} = 1. \tag{5.53}$$

Obviously this is not very surprising since in the SU(6) model the only angular momentum available is provided by the spin degrees of freedom of the quarks. What surprised many in the nuclear and the particle physics community was the result of a measurement done in 1988 by the European Muon Collaboration, which indicated that only a tiny fraction of the proton's spin is carried by the quarks.

5.10 The proton spin crisis

The initial and subsequent measurements by the European Muon Collaboration (EMC) of the proton's axial charge $g_A^{(0)}$ and its spin-dependent parton distributions spawned immense interest from both experimental and the theory side [106]. On the experimental side, the motivation was to check the results and increase on the accuracy of the original data. But also to get a detailed picture of the various distributions of the partons (quarks and gluons), such as their energy-momentum, angular momentum, orbital angular momentum and spin distributions. This impressive effort spanned more than two decades and are collected in the works of e.g. [107–114].

The theoretical activity was mostly motivated by the quest to understand what many interpreted as a surprisingly low value for the obtained axial charge $g_A^{(0)}$. Here, low is in relation to what one would expect from results predicted by the non-relativistic quark model (NRQM). In the NRQM, or as many call it, the naive (static) quark model, the axial charge is given by the sum of the helicities[12] of the quarks of the proton, i.e. $g_A^{(0)} = \Delta\Sigma$ of Equation (5.53). Traditionally, one writes the sum rule for the longitudinal spin structure of the nucleon as (see the reviews [90, 105, 115])

$$\frac{1}{2} = \frac{1}{2}\Delta\Sigma + \Delta g + L_q + L_g, \tag{5.54}$$

where L_g and L_q represent contributions from gluon and quark orbital angular momentum, respectively and Δg is the contribution from any eventual polarized glue.

The 'low' value obtained in experiments would in the NRQM suggest that a large fraction of the proton's spin resides in orbital angular momentum and perhaps in polarized sea, neither of which is accounted for in the NRQM.

[12] Relative to the quantization axis for the proton's spin.

The orbital angular momentum of the partons can contribute to the total proton spin but in general higher orbital angular momentum states belong to higher energy states and not the ground state of the proton. The contribution from polarized sea is not unreasonable due to the fact that approximately 50% of the proton's momentum is carried by electrically neutral, but strongly interacting partons [116]. A result predicted (to hold in the asymptotic limit) in QCD [117–119].

In QCD, this sea and in particular the electrically neutral partons just mentioned are represented by $q\bar{q}$-pairs and gluons. Furthermore, from a theoretical point of view, it is not unreasonable that the gluons can contribute a $\Delta g \neq 0$ to the spin of the proton [120, 121] by virtue of the U(1) axial anomaly, see e.g. [122, 123]. Experimentally, it is challenging to extract Δg, but recent experiments indicate a small value consistent with zero, although with substantial uncertainty [124, 125]. Meanwhile, recent lattice QCD calculations of Δg, together with certain assumptions, indicate a substantial gluonic contribution to the proton spin, see e.g. [126].

What all the above tells us is that the situation is still not resolved to a satisfying degree and that it is in need of some clearance and guidance.

6. The Hadron-Cloud Model

In this chapter we present all parts of the Hadron-Cloud Model. The model consists of three major parts, each applicable in their range of validity. These are in ascending order (in energy) ChPT for low energies, a phenomenological hadronic form factor combined with a physical model for the starting PDFs in intermediate energies and finally pQCD at large energies.

6.1 The HCM

As noted in Section 4.6, ChPT like any other effective theory has its range of applicability. ChPT and in particular leading-order ChPT works for momenta in the range of the Goldstone boson masses $Q \sim 0.5$ GeV, but not for momenta higher up. And we already know from previous chapters that pQCD breaks down around scales of $Q \lesssim 1$ GeV. Thus, there is a gap in energy range $0.5 \text{ GeV} \lesssim Q \lesssim 1$ GeV where neither ChPT nor pQCD is applicable. In our work, we choose to use a phenomenological model that connects these two regions, this is illustrated in Fig. 6.1.

We emphasize in particular that the phenomenological modeling of the intermediate energy range 'connects smoothly' to leading-order ChPT for very low energies, i.e. it shares with ChPT the low-energy limit, which serves to pin down parameters and the overall structure of interactions.

For energies close to 1 GeV the form factor in our model

$$G(\vec{p}_M^{\,2} + \vec{p}_B^{\,2}, \Lambda_H^2) = \mathrm{e}^{-\frac{\vec{p}_M^{\,2}+\vec{p}_B^{\,2}}{2\Lambda_H^2}}, \tag{6.1}$$

which is a decaying Gaussian in the three-momenta of the hadrons in the fluctuation, suppresses the hadronic contributions exponentially. In other words, for energies slightly below ~ 1 GeV the form factor smoothly turns off the hadronic degrees of freedom (d.o.f.). This allows (correctly) for the partonic d.o.f. to be the active ones in this energy range, cf. Fig. 6.1.

It is thus expected that the value of the cut-off parameter Λ_H should be about the energy where the partonic d.o.f. become the correct ones. Indeed this is also what comes out of the fit, cf. Paper II.

Regarding the starting PDFs for a given parton $i = q$, $\bar{q}$ or g (of mass m_i) in a hadron H, we assume that at the starting scale for QCD evolution Q_0, they

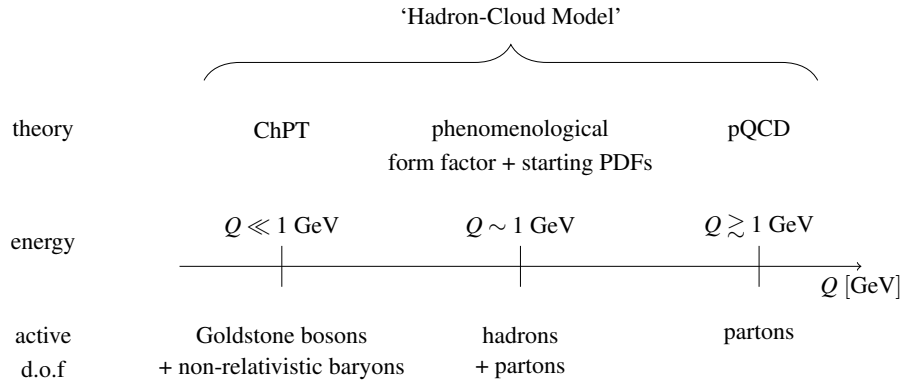

Figure 6.1. The different theory parts of the Hadron-Cloud Model together with the energy range where each part is used: For very low energies $Q \ll 1$ GeV we use leading-order ChPT; in the intermediate region 0.5 GeV $\lesssim Q \lesssim 1$ GeV we use a phenomenological form factor that connects smoothly to the ChPT part (it has ChPT as its low-energy limit). In this range we also use physics motivated starting PDFs. For energies $Q \gtrsim 1$ GeV pQCD is used (DGLAP evolution of the starting PDFs). The bottom row denotes the active d.o.f in each energy range.

are given by a Gaussian in the momentum components of the partons of the probed hadron,

$$f_{i/H}^{\text{bare}}(x) = \int \frac{\mathrm{d}^4 k}{(2\pi)^4}\, \delta\left(\frac{k^+}{p_H^+} - x\right) N_{i/H}(\sigma_i, m_i) \mathrm{e}^{-\frac{(k_0-m_i)^2+k_x^2+k_y^2+k_z^2}{2\sigma_i^2}} \times \Theta(1-x)\,\Theta(x)\,\Theta\left((p_H-k)^2\right). \tag{6.2}$$

The Heaviside functions come from the kinematics of the deep inelastic reaction. The normalization factor $N_{i/H}(\sigma_i, m_i)$ is fixed by valence-quark number and momentum sum rules, cf. Paper II for more details.

These starting PDFs are parametrized using only three parameters, these are the Gaussian widths σ_g, σ_1 and σ_2. The indices refers to the width of the gluon distribution and to the widths of the distributions of quarks appearing once or twice in a hadron, respectively. For instance in the case of the neutron $n(ddu)$ we use σ_1 and σ_2 for the u and d quarks, respectively.

For hadrons containing three quarks of the same flavor such as $\Delta^{++}(uuu)$ we use isospin relations to write down the distributions in terms of the parameters σ_1 and σ_2. To wit: We make use of the relations for the isovector

combination[1] $u-d$,

$$u_{\Delta^{++}} - d_{\Delta^{++}} = 3(u_{\Delta^+} - d_{\Delta^+}), \tag{6.3}$$

$$u_{\Delta^0} - d_{\Delta^0} = -(u_{\Delta^+} - d_{\Delta^+}), \tag{6.4}$$

$$u_{\Delta^-} - d_{\Delta^-} = -(u_{\Delta^{++}} - d_{\Delta^{++}}) \tag{6.5}$$

and for the isoscalar combination $u+d$,

$$u_{\Delta^{++}} + d_{\Delta^{++}} = u_{\Delta^+} + d_{\Delta^+} = u_{\Delta^0} + d_{\Delta^0} = u_{\Delta^-} + d_{\Delta^-}. \tag{6.6}$$

We find,

$$\begin{aligned} u_{\Delta^{++}} &= \frac{1}{2}(u_{\Delta^{++}} + d_{\Delta^{++}}) + \frac{1}{2}(u_{\Delta^{++}} - d_{\Delta^{++}}) = \frac{1}{2}(u_{\Delta^+} + d_{\Delta^+}) + \frac{3}{2}(u_{\Delta^+} - d_{\Delta^+}) \\ &= 2u_{\Delta^+} - d_{\Delta^+}. \end{aligned} \tag{6.7}$$

Thus, the distribution for the u quark in the $\Delta^{++}(uuu)$ baryon can be written as

$$f_{u/\Delta^{++}} = 2f_{u/\Delta^+} - f_{d/\Delta^+}, \tag{6.8}$$

where the first term contains the σ_2 parameter and the second term contains the σ_1 parameter, as discussed above.

We want to emphasize that these parameters are not totally free in the sense that their values should be of the order of the inverse size of the hadrons as given by Heisenberg's uncertainty relation. That is, for a typical hadron size D (diameter) we have

$$\sigma \approx \frac{\hbar}{2D} \approx 0.1 \text{ GeV}. \tag{6.9}$$

Indeed a fit to data on the unpolarized proton structure functions yields such values for the parameters of our model, see Paper II.

Strictly speaking, the HCM has five parameters σ_1, σ_2, σ_g, Q_0 and Λ_H. But as discussed above one would expect that Λ_H and the starting value for QCD evolution Q_0 to be roughly the same. Indeed our results show that they are practically given by the same value

$$\Lambda_H \simeq Q_0 = 0.88 \text{ GeV}, \tag{6.10}$$

effectively reducing the number of parameters to four.

6.2 Spin in the Hadron-Cloud Model

To also describe the spin structure of the nucleon we take as a first ansatz that the polarized distributions are proportional to the unpolarized ones with the

[1] In the following we suppress the notation $f_{u/\Delta^{++}}$ and simply denote this quantity by $u_{\Delta^{++}}$. The other distributions are denoted analogously. We will restore the notation in Eq. (6.8).

constant of proportionality given by the respective SU(6) value. In formulas this reads,

$$\Delta f^{\text{bare}}_{q/H}(x) = \Delta f^{\text{SU(6)}}_{q/H} f^{\text{bare}}_{q/H}(x), \tag{6.11}$$

where $f^{\text{bare}}_{q/H}(x)$ is given by (6.2) and $\Delta f^{\text{SU(6)}}_{q/H}$ is the SU(6) value for a parton q in a hadron H. For instance, in the case of the polarized u distribution inside a proton we use,

$$\Delta f^{\text{SU(6)}}_{u/P} = 4/3, \tag{6.12}$$

as obtained in Section 5.9, Equation (5.51). In (6.11) we also include the relativistic effects of a Melosh transformation [127–131], but this transformation does not introduce any new parameters. The full distributions are given by a convolution as discussed in detail in Paper III.

It turns out that the above ansatz yields a value for the integral of the polarized structure functions that is in disagreement with (5.40, 5.42). This motivates an exploration of a possible breaking of the SU(6) symmetry. We therefore introduce a breaking of the SU(6) symmetry for the nucleon, replacing in (6.11)

$$\Delta f^{\text{SU(6)}}_{q/H} \to \Delta f_{q/H} = \Delta f^{\text{SU(6)}}_{q/H} + \theta^q_H \tag{6.13}$$

for the proton with isospin-flipped values for the neutron, but (as a first approximation) $\theta^q_H = 0$ for all other hadrons.

If one insists on a probabilistic interpretation of the (bare) PDFs, the two parameters θ^u_P and θ^d_P cannot be varied in a completely free way. Rather one has to ensure that the number of quarks with a specific spin orientation does not exceed the total number of quarks. Consequently,

$$-2 \le \Delta f_{u/P} \le 2 \qquad \text{and} \qquad -1 \le \Delta f_{d/P} \le 1. \tag{6.14}$$

This is equivalent to,

$$-10/3 \le \theta^u_P \le 2/3 \qquad \text{and} \qquad -2/3 \le \theta^d_P \le 4/3. \tag{6.15}$$

If one fits the θ parameters to the value of the integral $\Gamma^{P-n}(x_{\min} = 0)$ [cf. Eqs. (5.38) and (5.42)] it turns out that one exhausts the limits put on these parameters, i.e. one finds $\theta^u_P = -\theta^d_P = 2/3$ leading to,

$$\Delta f_{u/P} = 2 \qquad \text{and} \qquad \Delta f_{d/P} = -1. \tag{6.16}$$

The finding (6.16) suggests that in the bare proton a large part of the u quarks have spins parallel to the proton's spin, whereas a large part of the d quarks have spins aligned antiparallel to the proton's spin.

Taking into account all the physical effects of the model: The bare part, the hadronic fluctuations, the Melosh transformation and the values obtained in (6.16) used in (6.11), we obtain a very good agreement with the (measured) full functions $\Gamma^{P\pm n}(x_{\min})$ listed in Equation (5.38).

Finally, we find that the fraction of the proton's spin carried by the quarks to be [cf. Section 5.10],

$$\Delta\Sigma = 0.39. \tag{6.17}$$

This value is in good agreement with the experimental value [104],

$$0.26 \leq \Delta\Sigma^{\text{exp}} \leq 0.36. \tag{6.18}$$

7. Deep inelastic scattering and the proton self-energy in the Hadron-Cloud Model

Deep inelastic scattering of leptons on the proton or more generally on the nucleon, provides an excellent tool to explore the structure of the proton. This is mostly because as far as we know, leptons are elementary particles (cf. Chapter 2). We went through the general DIS formalism in Section 5.2. In the present chapter we will discuss DIS on the proton within the HCM (cf. Section 6.1). In the process we will derive the hadronic distribution functions which are the probability distributions of the fluctuations.

We will here present the hadronic y and $k_\perp$-distributions and present all the various fluctuation probabilities in detail. We will discuss a possible connection between the probabilities obtained in the self-energy and in the DIS calculations.

7.1 Deep inelastic scattering in the Hadron-Cloud Model

To account for the BM fluctuations in accordance with Equation (1.1), we consider the possibility for the probe to interact with either the partons of the bare proton, or those of the baryon (B) or meson (M) in the BM fluctuation. In other words we decompose the hadronic electromagnetic current operator as follows

$$J_\mu(\xi) = J_\mu^{\text{bare}}(\xi) + J_\mu^B(\xi) + J_\mu^M(\xi), \tag{7.1}$$

where each part couples only to the relevant part of the proton wavefunction of Equation (1.1). Due to the decomposition of the current, the hadronic tensor $W_{\mu\nu}$ can similarly be written as a sum depending on whether one probes the bare proton or whether one probes the baryon/meson in the fluctuation i.e.

$$W_{\mu\nu} = W_{\mu\nu}^{\text{bare}} + \sum_{BM} \left[W_{\mu\nu}^{BM} + W_{\mu\nu}^{MB} \right], \tag{7.2}$$

where $W_{\mu\nu}^{BM}$ ($W_{\mu\nu}^{MB}$) refers to probing the baryon (meson) in the fluctuation.

7.2 Probing the bare proton

The different parts of the hadronic tensor can be found by considering how the time-evolution operator acts on the physical proton state. To wit, start with the

hadronic tensor of Equation (5.5) which we write as

$$W_{\mu\nu} = \frac{1}{4\pi}\int \mathrm{d}^4\xi\, \mathrm{e}^{\mathrm{i}q\xi}\left\langle P^{\tilde{\lambda}}(p)\right| J_\mu(\xi)J_\nu(0)\left|P^{\tilde{\lambda}}(p)\right\rangle, \tag{7.3}$$

where we take the proton to be polarized along the $+z$ direction so that $\tilde{\lambda}$ is definite and equals

$$\tilde{\lambda} = +1/2. \tag{7.4}$$

Notice that Equations (7.3) and (5.5) are equivalent since we can write the proton matrix element of $J_\mu(\xi)J_\nu(0)$ as a commutator because the subtracted term vanishes for stable targets [76, 88]. Now, under the time-evolution operator one finds that (T is the time-ordering operator)

$$\begin{aligned} J_\mu(\xi)\,|P^{\tilde{\lambda}}\rangle &= T\{J_\mu(\xi)\mathrm{e}^{\mathrm{i}S_{\mathrm{int}}}\}\,|P^{\tilde{\lambda}}\rangle_{\mathrm{bare}} \\ &\hat{=}\, T\{\left(J_\mu^{\mathrm{bare}}(\xi)+J_\mu^B(\xi)+J_\mu^M(\xi)\right)(1+\mathrm{i}S_{\mathrm{int}})\}\,|P^{\tilde{\lambda}}\rangle_{\mathrm{bare}} \end{aligned} \tag{7.5}$$

where we have only kept the non-trivial leading-order terms in the step '$\hat{=}$'. When contracted with $\langle P^{\tilde{\lambda}}|$, the first term gives the bare tensor, i.e.

$$W_{\mu\nu}^{\mathrm{bare}} = \frac{1}{4\pi}\int \mathrm{d}^4\xi\, \mathrm{e}^{\mathrm{i}q\xi}\left\langle P^{\tilde{\lambda}}\right|\left[J_\mu^{\mathrm{bare}}(\xi), J_\nu^{\mathrm{bare}}(0)\right]\left|P^{\tilde{\lambda}}\right\rangle_{\mathrm{bare}}. \tag{7.6}$$

Terms such as

$$|J_\mu^B(\xi)|P^{\tilde{\lambda}}\rangle_{\mathrm{bare}} \text{ and } |J_\mu^M(\xi)|P^{\tilde{\lambda}}\rangle_{\mathrm{bare}} \tag{7.7}$$

vanish since by definition the bare-proton state $|P^{\tilde{\lambda}}\rangle_{\mathrm{bare}}$ doesn't contain any fluctuations. The non-vanishing terms in (7.5) are what constitutes the baryonic and mesonic tensors $W_{\mu\nu}^{BM}$ and $W_{\mu\nu}^{MB}$, respectively. We will now turn to these terms.

7.3 Probing the baryon in the fluctuation

Consider the case of probing one of the hadrons in the fluctuation. For concreteness let us take the case of probing the baryon in the fluctuation (cf. Figure 1 of Paper II). The tensor for this is given by

$$\begin{aligned} W_{\mu\nu}^{BM} = &\frac{1}{4\pi}\sum_{M,X'}\int \mathrm{d}^4\xi\, \mathrm{e}^{\mathrm{i}q\xi}\,\frac{\mathrm{đ}^3 p_M}{2E_M} \\ &\times\left\langle P^{\tilde{\lambda}}\right| J_\mu^B(\xi)\left|X',M(p_M)\right\rangle\left\langle X',M(p_M)\right| J_\nu^B(0)\left|P^{\tilde{\lambda}}\right\rangle. \end{aligned} \tag{7.8}$$

Here we have inserted a complete set of states with the anticipation that S_{int} annihilates a state M. Therefore we have written down the phase space of M

explicitly, while the sum over X' is kept on a schematic level. We use the notation

$$\text{đ}^n \equiv \mathrm{d}^n/(2\pi)^n \qquad \text{and} \qquad \delta^{(n)} \equiv (2\pi)^n \delta^{(n)}. \tag{7.9}$$

With equations (7.5) and (7.7) in mind, the matrix elements in Eq. (7.8) can be written

$$\left\langle X', M(p_M) \left| T\{J^B_\mu(\xi) \mathrm{i}S_{\mathrm{int}}\} \right| P^{\tilde{\lambda}} \right\rangle_{\mathrm{bare}}. \tag{7.10}$$

We will in the following omit the subscript 'bare', and for the sake of definiteness, we will consider the proton-pion fluctuation. In other words, we will use the following part of the action

$$\mathrm{i}S_{\mathrm{int}} = \mathrm{i}g_{P\pi^0} \int \mathrm{d}^4 z \bar{P}(z) \gamma^\alpha \gamma_5 (\partial^z_\alpha \pi^0(z)) P(z). \tag{7.11}$$

The full leading-order Lagrangian and thus the action is presented in Paper I. The hadronic couplings including $g_{P\pi^0}$ are tabulated in Table I of said paper.

Inserting the action we find

$$\begin{aligned}
&\left\langle X', M(p_M) \left| T\{J^B_\mu(\xi) \mathrm{i}S_{\mathrm{int}}\} \right| P^{\tilde{\lambda}} \right\rangle \\
&= \frac{g_{P\pi^0}}{2} \int \mathrm{d}^2 z_\perp \mathrm{d}z^- \mathrm{d}z^+ \, \theta(\xi^+ - z^+) \int \text{đ}^2 p_{B\perp} \text{đ}p^-_B \int \frac{\text{đ}y}{2y} \delta\left(p^-_B - \frac{p^2_{B\perp} + m^2_B}{y p^+} \right) \\
&\times \theta(y) \exp\left[\frac{-\mathrm{i}}{2} z^+ \left(p^- - p^-_B - p^-_M \right) \right] \exp\left[\frac{-\mathrm{i}}{2} z^- \left(p^+ - p^+_B - p^+_M \right) \right] \\
&\times \exp\left[+\mathrm{i}\vec{z}_\perp \cdot (\vec{p}_\perp - \vec{p}_{B\perp} - \vec{p}_{M\perp}) \right] \sum_\lambda S^\lambda(p_B = y p^+) \left\langle X' \left| J^B_\mu(\xi) \right| B^\lambda(p_B) \right\rangle,
\end{aligned} \tag{7.12}$$

where

$$p^+_B = y p^+, \qquad p^+_M = y_M p^+. \tag{7.13}$$

In (7.12) we have defined the vertex function

$$S^\lambda(\tilde{p}_B) = \bar{u}^\lambda(\tilde{p}_B) \gamma_5 \not{p}_M u^{\tilde{\lambda}}(\tilde{p}), \tag{7.14}$$

with the notation $\tilde{a} \equiv (a^+, \vec{a}_\perp)$ for the momenta.[1] The light-front spinors $u_\lambda(\tilde{p})$ for a spin-1/2 baryon of mass m and polarization λ are given by [132, 133]

$$u_{1/2}(\tilde{p}) = \frac{1}{\sqrt{2p^+}} \begin{pmatrix} p^+ + m \\ p_\perp \mathrm{e}^{\mathrm{i}\phi} \\ p^+ - m \\ p_\perp \mathrm{e}^{\mathrm{i}\phi} \end{pmatrix}, \qquad u_{-1/2}(\tilde{p}) = \frac{1}{\sqrt{2p^+}} \begin{pmatrix} -p_\perp \mathrm{e}^{-\mathrm{i}\phi} \\ p^+ + m \\ p_\perp \mathrm{e}^{-\mathrm{i}\phi} \\ m - p^+ \end{pmatrix}, \tag{7.15}$$

where the angle ϕ is defined in Equation (5.9).

[1] This notation is not to be confused with or applied to $\tilde{\lambda}$, which is helicity and given by (7.4).

The light-front vector-spinors, $u^{\mu}_{\lambda}(\tilde{p})$, of a spin-3/2 particle of mass m and polarization λ are given by the Clebsch-Gordon expansion,

$$\begin{aligned}
u^{\mu}_{3/2}(\tilde{p}) &= \varepsilon^{\mu}_{+1}(\tilde{p})u_{1/2}(\tilde{p}),\\
u^{\mu}_{1/2}(\tilde{p}) &= \sqrt{\frac{2}{3}}\varepsilon^{\mu}_{0}(\tilde{p})u_{1/2}(\tilde{p}) + \sqrt{\frac{1}{3}}\varepsilon^{\mu}_{+1}(\tilde{p})u_{-1/2}(\tilde{p}),\\
u^{\mu}_{-1/2}(\tilde{p}) &= \sqrt{\frac{2}{3}}\varepsilon^{\mu}_{0}(\tilde{p})u_{-1/2}(\tilde{p}) + \sqrt{\frac{1}{3}}\varepsilon^{\mu}_{-1}(\tilde{p})u_{1/2}(\tilde{p}),\\
u^{\mu}_{-3/2}(\tilde{p}) &= \varepsilon^{\mu}_{-1}(\tilde{p})u_{-1/2}(\tilde{p}).
\end{aligned} \tag{7.16}$$

Written on the form $\varepsilon = [\varepsilon^{+}, \varepsilon^{-}, (\vec{\varepsilon}_{\perp})]$, the polarization vectors are given by

$$\begin{aligned}
\varepsilon^{\mu}_{+1}(\tilde{p}) &= \left[0, \quad -\tfrac{\sqrt{2}}{p^{+}}p_{\perp}\mathrm{e}^{\mathrm{i}\phi}, \left(-\tfrac{1}{\sqrt{2}} \quad , -\tfrac{\mathrm{i}}{\sqrt{2}}\right)\right],\\
\varepsilon^{\mu}_{0}(\tilde{p}) &= \frac{1}{m}\left[p^{+}, \quad \tfrac{1}{p^{+}}\left(p^{2}_{\perp} - m^{2}\right), \vec{p}_{\perp}\right],\\
\varepsilon^{\mu}_{-1}(\tilde{p}) &= \left[0, \quad \tfrac{\sqrt{2}}{p^{+}}p_{\perp}\mathrm{e}^{-\mathrm{i}\phi}, \left(\tfrac{1}{\sqrt{2}} \quad , -\tfrac{\mathrm{i}}{\sqrt{2}}\right)\right].
\end{aligned} \tag{7.17}$$

Using the following representation for the Dirac matrices,

$$\gamma^{0} = \begin{pmatrix} \sigma^{0} & 0 \\ 0 & -\sigma^{0} \end{pmatrix}, \quad \gamma^{j} = \begin{pmatrix} 0 & \sigma^{j} \\ -\sigma^{j} & 0 \end{pmatrix}, \quad \gamma^{5} = \begin{pmatrix} 0 & \sigma^{0} \\ \sigma^{0} & 0 \end{pmatrix}, \tag{7.18}$$

expressed in terms of the standard Pauli matrices [4] with $\sigma^{0} \equiv \mathrm{diag}(1,1)$, we obtain the vertex functions listed in Paper II.

Getting back to our Equation (7.12) we notice that the exponentials will turn into delta functions once integrated over. The time-ordered exponential will turn into a 'propagator' via[2]

$$\begin{aligned}
&\int_{-\infty}^{\infty}\mathrm{d}z^{+}\,\theta(\xi^{+} - z^{+})\exp\left[\frac{-\mathrm{i}}{2}z^{+}\left(p^{-} - p^{-}_{B} - p^{-}_{M}\right)\right]\\
&= \frac{2\mathrm{i}}{p^{-} - p^{-}_{B} - p^{-}_{M}}\exp\left[\frac{-\mathrm{i}}{2}\xi^{+}\left(p^{-} - p^{-}_{B} - p^{-}_{M}\right)\right]\\
&= \frac{p^{+}2\mathrm{i}}{m^{2}_{P} - \frac{p^{2}_{B\perp} + m^{2}_{B}}{y} - p^{+}p^{-}_{M}},
\end{aligned} \tag{7.19}$$

where the final equality holds in the Bjorken limit.[3] In (7.19), we have also made use of the on-shell relation $p^{+}p^{-} = m^{2}_{P}$ and used the p^{-}_{B} delta function of Equation (7.12).

[2] We suppress the $\mathrm{i}\varepsilon$ regulator.

[3] Recall the factor $\exp(\mathrm{i}q\xi)$ in the hadronic tensor. Thus, ξ^{+} multiplies $q^{-} \gg p^{-} - p^{-}_{B} - p^{-}_{M}$, in the Bjorken limit. Hence, in the Bjorken limit, the exponential in (7.19) is as good as unity.

We will from now on work in a frame where $\vec{p}_\perp = 0$. The $\vec{z}_\perp$ delta function in (7.12) then implies that

$$\vec{p}_{B\perp} = -\vec{p}_{M\perp} \equiv \vec{k}_\perp. \tag{7.20}$$

Notice also that what we have done so far, holds for any baryon in the fluctuation. The only things that differ for the other baryons are the couplings g_{BM} and the explicit form of the vertex functions S^λ. The vertex functions are identical for all the octet-baryons apart from the masses used. Similarly, they are identical for all the decuplet baryons. Thus, it's just as well to denote the hadronic coupling by the more general g_{BM}. Implementing all this, Equation (7.12) becomes

$$\begin{aligned}\left\langle X', M(p_M) \left| T\{J^B_\mu(\xi) \mathrm{i}S_{\mathrm{int}}\} \right| P^{\tilde{\lambda}} \right\rangle = \frac{\mathrm{i}g_{BM}}{1-y_M} \frac{\sum_\lambda S^\lambda(p_B^+ = (1-y_M)p^+)}{m_P^2 - \frac{k_\perp^2+m_B^2}{1-y_M} - p^+ p_M^-} \\ \times \theta(1-y_M) \langle X'|J^B_\mu(\xi)|B^\lambda\left(p_B^+ = (1-y_M)p^+\right)\rangle,\end{aligned} \tag{7.21}$$

where we have suppressed the mass and $\vec{k}_\perp$ dependence of S^λ. Similarly the Lorentz-invariant integrals become

$$\int \frac{\mathrm{d}^3 p_M}{2E_M} = \int \mathrm{d}^2 k_\perp \int \mathrm{d}p_M^- \int \frac{\mathrm{d}y_M}{2y_M} \delta\left(p_M^- - \frac{p_{M\perp}^2 + m_M^2}{y_M p^+}\right) \theta(y_M), \tag{7.22}$$

which together with $\theta(1-y_M)$ of Equation (7.21) restricts the y_M-integral to the physical range $y_M \in [0,1]$. Doing the p_M^- delta function and summing over all the BM pairs, the baryonic tensor becomes

$$\begin{aligned}W^{BM}_{\mu\nu} &= \sum_{BM,\lambda,\lambda'} |g_{BM}|^2 \frac{1}{4\pi} \int \mathrm{d}^4\xi\, \mathrm{e}^{\mathrm{i}q\xi} \int \mathrm{d}^2 k_\perp \int_0^1 \frac{\mathrm{d}y_M}{2y_M} \frac{1}{(1-y_M)^2} \\ &\times \left\langle B^{\lambda'}\left(p_B^+ = (1-y_M)p^+\right) \left| \left[J^B_\mu(\xi), J^B_\nu(0)\right] \right| B^\lambda\left(p_B^+ = (1-y_M)p^+\right) \right\rangle \\ &\times \frac{S^{*\lambda'}(p_B^+ = (1-y_M)p^+) S^\lambda(p_B^+ = (1-y_M)p^+)}{\left(m_P^2 - \frac{k_\perp^2+m_B^2}{1-y_M} - \frac{k_\perp^2+m_M^2}{y_M}\right)^2},\end{aligned} \tag{7.23}$$

where we have used the completeness of the states X'.

From the explicit form of the vertex functions [cf. Paper II] it is easy to verify that the off-diagonal terms vanish under the ϕ-integration. In other words

$$\int_0^{2\pi} \mathrm{d}\phi \sum_{\lambda,\lambda'} S^{*\lambda'} S^\lambda = \int_0^{2\pi} \mathrm{d}\phi \sum_\lambda |S^\lambda|^2. \tag{7.24}$$

Using this, and making the change of variables $y = 1 - y_M$, the baryonic tensor becomes

$$W_{\mu\nu}^{BM} = \frac{1}{4\pi}\int \mathrm{d}^4\xi\, \mathrm{e}^{\mathrm{i}q\xi} \sum_{BM,\lambda} \int_0^1 \frac{\mathrm{d}y}{y} \left\langle B^\lambda\left(p_B\right)\right| \left[J_\mu^B(\xi), J_\nu^B(0)\right] \left|B^\lambda\left(p_B\right)\right\rangle \Big|_{p_B^+ = yp^+}$$
$$\times \frac{1}{(2\pi)^3\, 2y(1-y)} \int \mathrm{d}^2k_\perp \left| g_{BM} G(y, k_\perp^2, \Lambda_H^2) \frac{S^\lambda(p_B^+ = yp^+, \vec{k}_\perp)}{m_P^2 - \frac{k_\perp^2 + m_B^2}{y} - \frac{k_\perp^2 + m_M^2}{1-y}} \right|^2 , \tag{7.25}$$

where we have included the form factor $G(p_B^+ = yp^+, k_\perp^2, \Lambda_H^2)$ to avoid unphysical contributions [cf. Section 6.1 and Paper II].

7.4 Probing the meson in the fluctuation

We now turn to the case of probing the meson in the fluctuation (cf. Figure 1 of Paper II). The mesonic tensor is given by

$$W_{\mu\nu}^{MB} = \frac{1}{4\pi} \sum_{B,\lambda,X'} \int \mathrm{d}^4\xi\, \mathrm{e}^{\mathrm{i}q\xi} \frac{\bar{\mathrm{d}}^3 p_B}{2E_B}$$
$$\times \left\langle P^{\tilde{\lambda}} \left| J_\mu^M(\xi) \right| X', B^\lambda(p_B) \right\rangle \left\langle X', B^\lambda(p_B) \left| J_\nu^M(0) \right| P^{\tilde{\lambda}} \right\rangle . \tag{7.26}$$

This is very similar to the baryon case with the main difference that we are now probing a spinless meson. Let the baryon and meson carry the momentum fractions y and y_M, respectively. We can then write the matrix element as

$$\left\langle X', B^\lambda(p_B) \left| J_\mu^M(\xi) \right| P^{\tilde{\lambda}} \right\rangle = \left\langle X', B^\lambda(p_B) \left| T\{J_\mu^M(\xi) \mathrm{i}S_{\mathrm{int}}\} \right| P^{\tilde{\lambda}} \right\rangle_{\mathrm{bare}}$$
$$= \mathrm{i}g_{BM} \int \frac{\bar{\mathrm{d}}y_M}{y_M} \theta(y_M) \frac{S^\lambda(p_B^+ = yp^+)\delta(1-y-y_M)}{m_P^2 - \frac{k_\perp^2 + m_M^2}{y_M} - p^+ p_B^-}$$
$$\times \left\langle X' \left| J_\mu^M(\xi) \right| M(y_M p^+, \vec{k}_\perp) \right\rangle$$
$$= \mathrm{i}g_{BM} \frac{\theta(1-y)}{1-y} \frac{S^\lambda(p_B^+ = yp^+)}{m_P^2 - \frac{k_\perp^2 + m_M^2}{1-y} - p^+ p_B^-} \left\langle X' \left| J_\mu^M(\xi) \right| M\left((1-y)p^+, \vec{k}_\perp\right) \right\rangle . \tag{7.27}$$

Now using

$$\int \frac{\bar{\mathrm{d}}^3 p_B}{2E_B} = \int \bar{\mathrm{d}}^2 k_\perp \int \bar{\mathrm{d}} p_B^- \int \frac{\bar{\mathrm{d}}y}{2y} \delta\left(p_B^- - \frac{p_{B\perp}^2 + m_B^2}{yp^+}\right) \theta(y), \tag{7.28}$$

we obtain for the mesonic tensor,

$$
\begin{aligned}
W_{\mu\nu}^{MB} = & \sum_{BM} |g_{BM}|^2 \frac{1}{4\pi} \int \mathrm{d}^4\xi \, \mathrm{e}^{\mathrm{i}q\xi} \int \text{đ}^2 k_\perp \int_0^1 \frac{\text{đ}y}{2y} \frac{1}{(1-y)^2} \\
& \times \left\langle M\left(p_M^+ = (1-y)p^+\right) \middle| \left[J_\mu^M(\xi), J_\nu^M(0)\right] \middle| M\left(p_M^+ = (1-y)p^+\right) \right\rangle \\
& \times \frac{\sum_\lambda S^{*\lambda}(p_B^+ = yp^+) S^\lambda(p_B^+ = yp^+)}{\left(m_P^2 - \frac{k_\perp^2 + m_M^2}{1-y} - \frac{k_\perp^2 + m_B^2}{y}\right)^2}.
\end{aligned}
\tag{7.29}
$$

We now make the change of variables $y \to 1-y$ and find the analogous expression to that in Equation (7.25),

$$
\begin{aligned}
W_{\mu\nu}^{MB} = & \frac{1}{4\pi} \int \mathrm{d}^4\xi \, \mathrm{e}^{\mathrm{i}q\xi} \sum_{BM,\lambda} \int_0^1 \frac{\mathrm{d}y}{y} \left\langle M(p_M) \middle| \left[J_\mu^M(\xi), J_\nu^M(0)\right] \middle| M(p_M) \right\rangle \Big|_{p_M^+ = yp^+} \\
& \times \frac{1}{(2\pi)^3 2y(1-y)} \int \mathrm{d}^2 k_\perp \left| g_{BM} G(1-y, k_\perp^2, \Lambda_H^2) \frac{S^\lambda(p_B^+ = (1-y)p^+, \vec{k}_\perp)}{m_P^2 - \frac{k_\perp^2 + m_M^2}{y} - \frac{k_\perp^2 + m_B^2}{1-y}} \right|^2 .
\end{aligned}
\tag{7.30}
$$

In deriving (7.25,7.30) we have neglected the dependence of the matrix element on $\vec{k}_\perp$. And the form factor $G(1-y, k_\perp^2, \Lambda_H^2)$ is short for $G(p_B^+ = (1-y)p^+, k_\perp^2, \Lambda_H^2)$.

As discussed in the papers I - III we use a Gaussian form factor having the average of the squares of the fluctuation's three-momenta as its argument

$$
\begin{aligned}
& G(y, k_\perp^2, \Lambda_H^2) = \exp\left[-\frac{\vec{p}_B^{\,2} + \vec{p}_M^{\,2}}{2\Lambda_H^2}\right] = \{\text{in the proton's rest frame}\} \\
& = \exp\left[-\frac{\frac{(p\cdot p_B)^2 + (p\cdot p_M)^2}{m_P^2} - m_B^2 - m_M^2}{2\Lambda_H^2}\right] \\
& = \exp\left[-\frac{\left(\frac{m_B^2 + k_\perp^2}{2m_P y}\right)^2 + \left(\frac{m_M^2 + k_\perp^2}{2m_P(1-y)}\right)^2 + k_\perp^2 - \frac{m_B^2 + m_M^2}{2} + \frac{m_P^2}{4}\left[(1-y)^2 + y^2\right]}{2\Lambda_H^2}\right],
\end{aligned}
\tag{7.31}
$$

where we have written the argument of the second exponential in a Lorentz-invariant form.

7.5 The hadronic distribution functions

For convenience, we collect here the the fluctuation part of the hadronic tensor (7.2), $W^H_{\mu\nu} = \sum_{BM}(W^{BM}_{\mu\nu} + W^{MB}_{\mu\nu})$. It is given by

$$\begin{aligned} W^H_{\mu\nu} = \frac{1}{4\pi}\int \mathrm{d}^4\xi\, \mathrm{e}^{\mathrm{i}q\xi} \sum_{BM,\lambda}\int_0^1 \frac{\mathrm{d}y}{y}\Big\{ \\ f^\lambda_{MB}(y)\left\langle M(p^+_M = yp^+)\right|\left[J^M_\mu(\xi), J^M_\nu(0)\right]\left|M(p^+_M = yp^+)\right\rangle \\ + f^\lambda_{BM}(y)\left\langle B^\lambda(p^+_B = yp^+)\right|\left[J^B_\mu(\xi), J^B_\nu(0)\right]\left|B^\lambda(p^+_B = yp^+)\right\rangle\Big\}, \end{aligned} \tag{7.32}$$

where we have defined the hadronic distribution functions,

$$f^\lambda_{BM}(y) = \frac{|g_{BM}|^2}{(2\pi)^3 2y(1-y)}\int \mathrm{d}^2k_\perp \left| G(y,k^2_\perp,\Lambda^2_H)\frac{S^\lambda(y,\vec{k}_\perp)}{m^2_P - m^2(y,k^2_\perp)}\right|^2, \tag{7.33}$$

and

$$f^\lambda_{MB}(y) = \frac{|g_{BM}\,|^2}{(2\pi)^3 2y(1-y)}\int \mathrm{d}^2k_\perp \left| G(1-y,k^2_\perp,\Lambda^2_H)\frac{S^\lambda(1-y,\vec{k}_\perp)}{m^2_P - m^2(1-y,k^2_\perp)}\right|^2. \tag{7.34}$$

In (7.33) and (7.34) $m^2(y,k^2_\perp)$ is given by

$$m^2(y,k^2_\perp) \equiv \frac{m^2_B + k^2_\perp}{y} + \frac{m^2_M + k^2_\perp}{1-y}. \tag{7.35}$$

We note that without a form factor $G(y,k^2_\perp,\Lambda^2_H)$, the hadronic distributions satisfy the relation

$$f^\lambda_{BM}(y) = f^\lambda_{MB}(1-y). \tag{7.36}$$

When introducing a form factor, one has to choose it such that this relation is not spoiled.

7.6 The probabilities obtained from the DIS calculation

Here we want to make a comment regarding the meson momentum in the numerator of the hadronic distribution functions. In other words the meson momentum p_M in the vertex function (7.14). In the framework of LCTOPT there is an ambiguity for the choice of this momentum. Two choices that are common in the literature are given by [12, 16],

$$(A): \quad p_M = \left(p^+_P - p^+_B, p^-_P - p^-_B, \vec{p}_{P\perp} - \vec{p}_{B\perp}\right), \tag{7.37}$$

and

$$(B): \quad p_M = \left(p_P^+ - p_B^+, \frac{m_M^2 + p_{M\perp}^2}{p_M^+}, \vec{p}_{P\perp} - \vec{p}_{B\perp} \right). \tag{7.38}$$

These two choices give very similar results w.r.t. agreement with the unpolarized structure functions without much adjustment in the values of the parameters Λ_H, Q_0 and σ_i introduced in Chapter 6. Hence the interpretation of the results are basically independent of this momentum choice, except for two instances: The $\bar{d}$-$\bar{u}$ asymmetry has a slightly better shape using momentum choice A, we include a plot of this here; the θ parameter needs to be slightly larger when using momentum choice A.

We choose to work with momentum choice B given in (7.38) because this choice is in line with the Goldstone theorem [134] whereas choice A given in (7.37) is not. This can be seen explicitly from the vertex functions listed in Paper II.

The relation (7.36) is shown explicitly in Figure 7.1 where we have plotted the helicity-summed y distributions for the baryons in the fluctuations given by

$$f_{BM}(y) = \sum_\lambda f_{BM}^\lambda(y). \tag{7.39}$$

For the convenience of the reader we have also plotted the y distributions for the mesons in the fluctuations given by $f_{MB}(y)$. Interestingly, the shape of the y distributions differ quite a lot depending on whether one works with momentum choice A or B shown by the left and right panels, respectively of said figure.

Independent of this choice we see that in a given BM fluctuation the baryon takes a much larger momentum fraction than its companion meson. This is due to the larger mass of the baryon relative to its companion meson. For instance since $m_\Delta/m_\pi > m_N/m_\pi$ we see in the top panels of Figure 7.1 that $f_{\Delta\pi}(y)$ peaks at a slightly larger value of y than does $f_{N\pi}(y)$. On the other hand, the distributions for the baryons that have a heavier companion meson peaks at a smaller value of y relative to the nucleon/Delta case, because now the heavier meson also takes a substantial momentum fraction.

We can also study the $k_\perp$ distributions by defining

$$f_{BM}^\lambda(y,k_\perp) \equiv \frac{k_\perp}{(2\pi)^2 2y(1-y)} \left| g_{BM}\, G(y,k_\perp^2,\Lambda_H^2) \frac{S^\lambda(y,\vec{k}_\perp)}{m_P^2 - m^2(y,k_\perp^2)} \right|^2. \tag{7.40}$$

One can then express the y and $k_\perp$ distributions, respectively as

$$f_{BM}^\lambda(y) = \int_0^\infty \mathrm{d}k_\perp\, f_{BM}^\lambda(y,k_\perp) \tag{7.41}$$

and

$$f_{BM}^\lambda(k_\perp) = \int_0^1 \mathrm{d}y\, f_{BM}^\lambda(y,k_\perp). \tag{7.42}$$

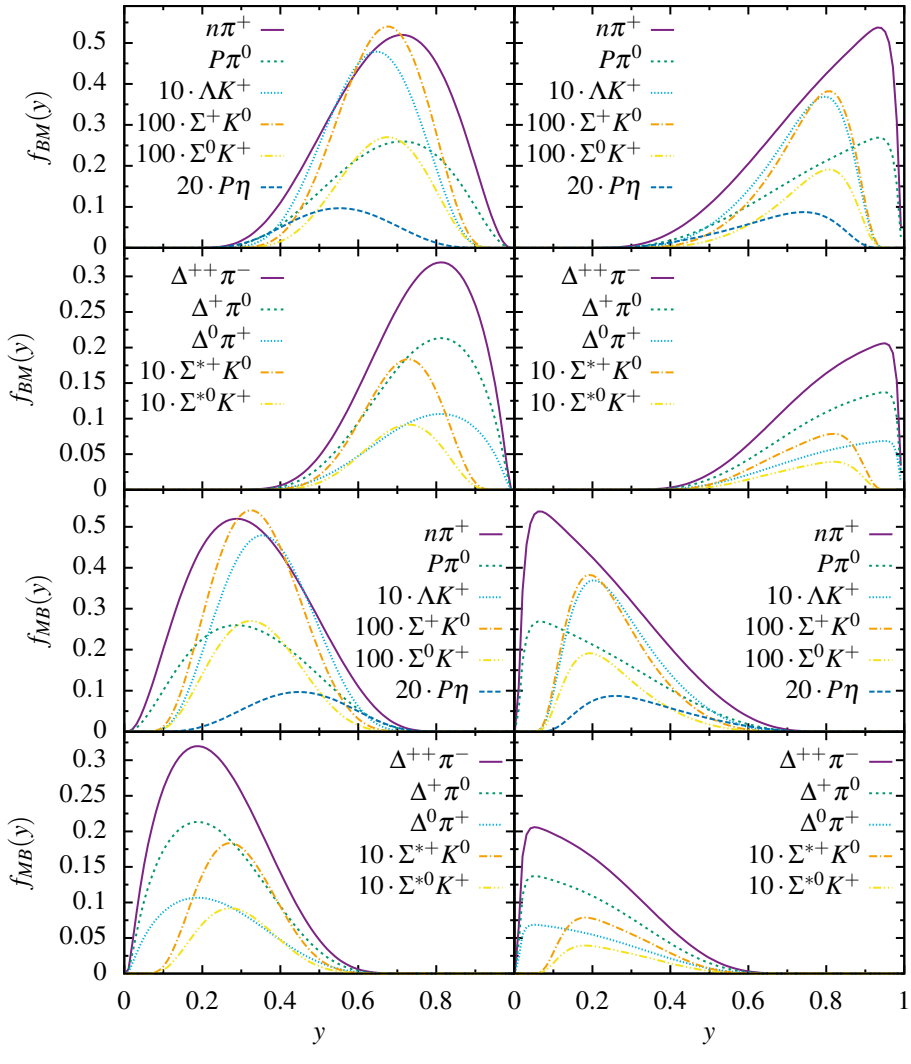

Figure 7.1. The hadronic y distribution functions $f_{BM}(y)$ and $f_{MB}(y)$ in the upper and lower panels, respectively. The left (right) panels are for momentum choice A (B).

Obviously the $k_\perp$ distributions satisfy the relation

$$f^{\lambda}_{BM}(k_\perp) = f^{\lambda}_{MB}(k_\perp). \tag{7.43}$$

In contrast to the y distributions of a BM pair where the baryon carries a fraction y and the companion meson a fraction $1-y$, the baryon and the meson in a given BM pair each carry $k_\perp$. Consequently, the $k_\perp$ distributions of the heavier BM pairs peak at a larger value of $k_\perp$ relative the corresponding ones

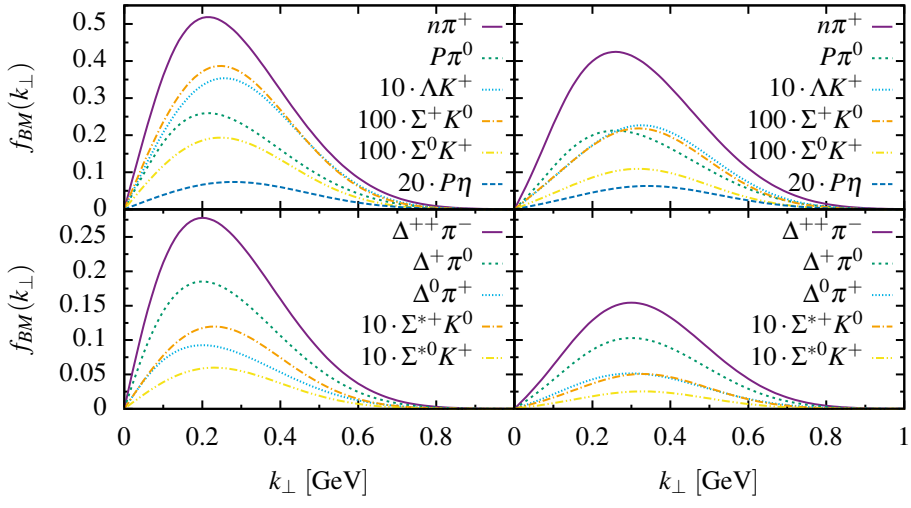

Figure 7.2. The hadronic $k_\perp$ distribution functions $f_{BM}(k_\perp)$ for the octet and decuplet-baryons in the top and bottom panels, respectively. The left and right panels refers to using momentum choice *A* and *B*, respectively.

for the lighter *BM* pairs. This can be seen in Figure 7.2 where we have plotted $f_{BM}(k_\perp)$ for both momentum choices.

The hadronic distribution functions are probability distributions, hence by integrating with respect to y and $k_\perp$ one obtains the fluctuation probabilities $|\alpha_{BM}|^2$ of Equation (1.1),

$$|\alpha^\lambda_{BM}(\Lambda_H)|^2 = \int_0^1 \mathrm{d}y\, f^\lambda_{BM}(y) = \int_0^\infty \mathrm{d}k_\perp\, f^\lambda_{BM}(k_\perp). \tag{7.44}$$

In Figure 7.3 are plotted the helicity-summed probabilities $\sum_\lambda |\alpha^\lambda_{BM}(\Lambda_H)|^2$ as functions of the cut-off parameter Λ_H. As seen, on the octet side the neutron-pion and the proton-pion fluctuations dominate while on the decuplet side the Delta-pion fluctuation dominate.

We can study this closer by looking into the isospin-summed probabilities. This is shown in Figure 7.4 where we have summed the $n\pi^+$ and the $P\pi^0$ contributions and denote it as nucleon-pion ($N\pi$):[4]

$$|\tilde{\alpha}^\lambda_{N\pi}(\Lambda_H)|^2 \equiv |\alpha^\lambda_{n\pi^+}(\Lambda_H)|^2 + |\alpha^\lambda_{P\pi^0}(\Lambda_H)|^2. \tag{7.45}$$

The isospin-summed Delta-pion probability $|\tilde{\alpha}^\lambda_{\Delta\pi}|^2$ is analogously defined. In the same figure we also indicate how the probabilities depend on the helicity of the baryon in question.

[4]By definition the LHS of Equation (7.45) is a positive quantity, so the bars on $|\tilde{\alpha}_{N\pi}(\Lambda_H)|^2$ are not really needed. They serve mainly typographical purposes.

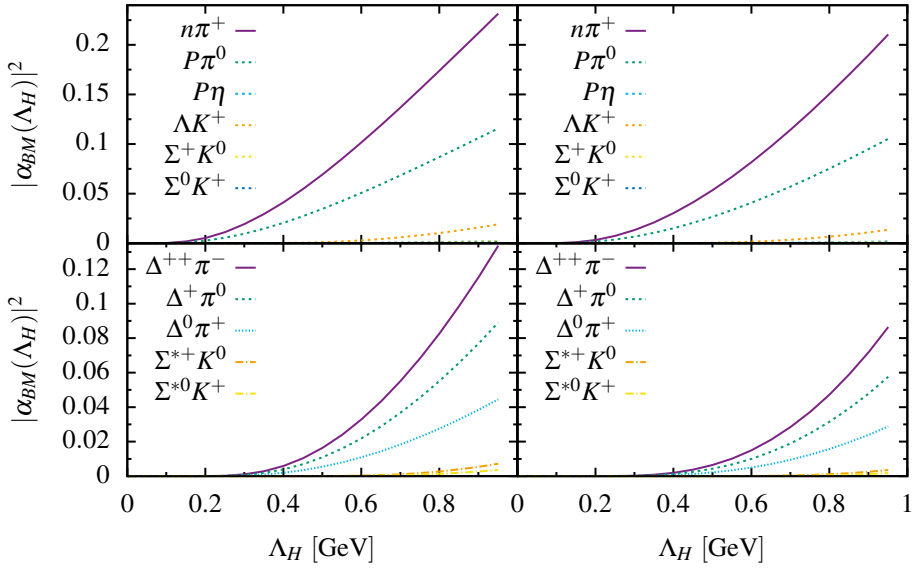

Figure 7.3. The fluctuation probabilities as a function of the cut-off parameter Λ_H. Left and right panels refers to momentum choice *A* and *B*, respectively.

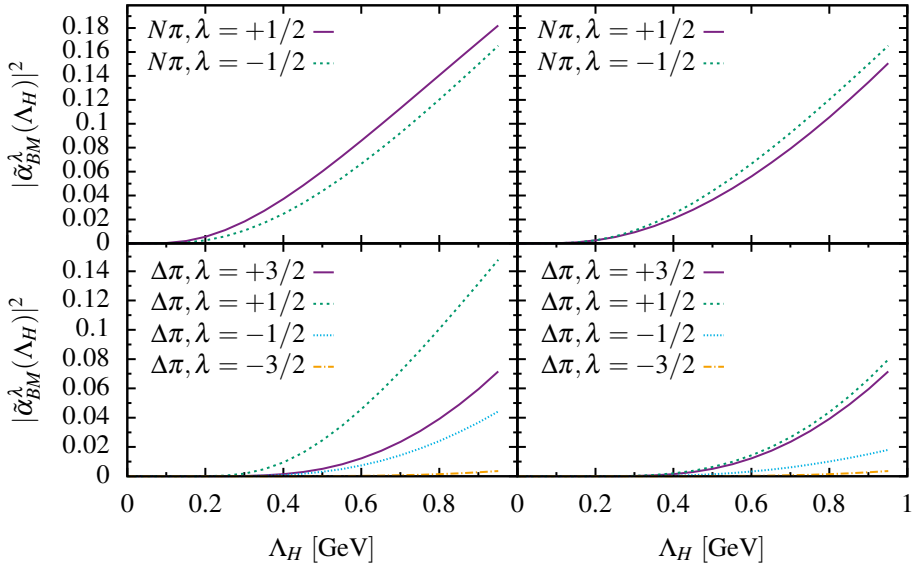

Figure 7.4. The isospin-summed helicity-dependent probabilities of the dominant nucleon-pion and Delta-pion fluctuations. Left and right panels refers to momentum choice *A* and *B*, respectively.

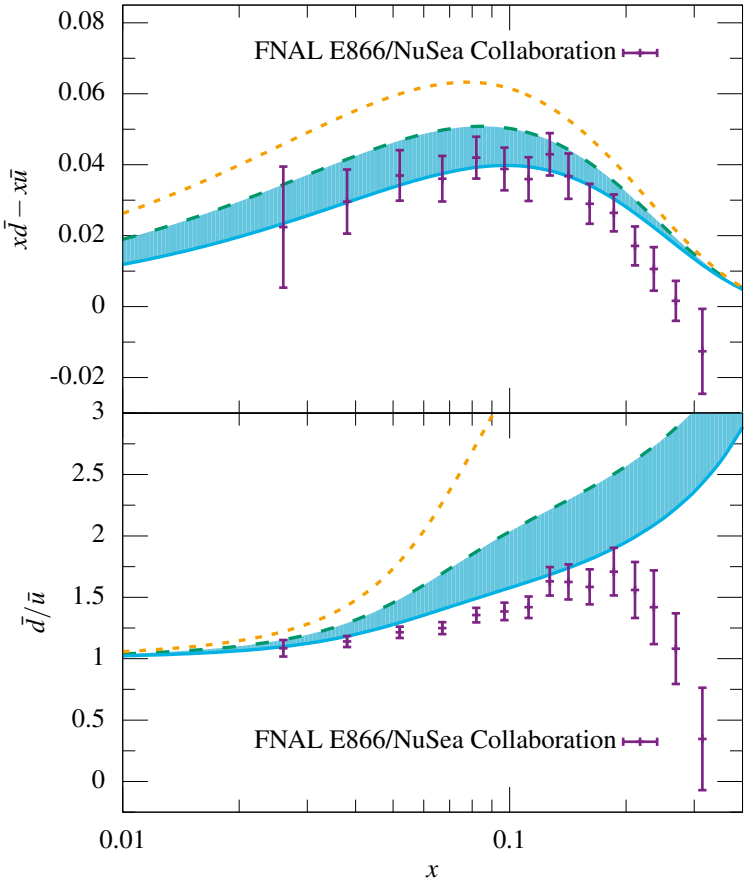

Figure 7.5. The flavor asymmetries $x\bar{d} - x\bar{u}$ (top panel) and $\bar{d}/\bar{u}$ (bottom panel) of the proton sea using momentum choice A and the parameter values (7.46). The band represents a variation in the decuplet coupling where the solid (dashed) curves are for the largest (smallest) value of the decuplet coupling h_A/m_Δ, as discussed in Paper II. The dotted curves only take nucleon-pion fluctuations into account. Data taken from the FNAL E866/NuSea Collaboration [17].

As can be seen from the figure, for the nucleon-pion probabilities there is not much of a difference in using momentum choice A or B as indicated by the left and right panels, respectively. There is a difference for the Delta which leads to the need for a slightly larger SU(6) breaking in the proton to compensate for this when using momentum choice A.

Concerning the flavor asymmetries $x\bar{d} - x\bar{u}$ and $\bar{d}/\bar{u}$, momentum choice A gives a slightly different shape for $x\bar{d} - x\bar{u}$ as can be seen in Figure 7.5. The analogous figure corresponding to using momentum choice B instead can be found in Paper II. We want to emphasize that independent of momentum choice, the values for the parameters of our model that best describe data

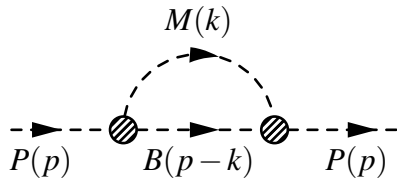

Figure 7.6. Feynman diagram for the scalar self-energy. The blobs denote the form factor.

comes out pretty much the same. To be more explicit, using momentum choice A, the values that best describe data are given by

$$\begin{aligned}&\sigma_1 = 0.13 \text{ GeV}, \sigma_2 = 0.24 \text{ GeV}, \sigma_g = 0.028 \text{ GeV},\\ &\Lambda_H = 0.87 \text{ GeV}, Q_0 = 0.88 \text{ GeV}.\end{aligned} \tag{7.46}$$

7.7 Connecting the DIS and the self-energy probabilities

Since the self-energy calculation of Paper I is done in the instant-form of dynamics [cf. Section 5.3] it is not straightforward to compare the probabilities to those obtained in the DIS formalism which is done in light-front dynamics. Strictly speaking, to make a connection between the probabilities obtained in the two different calculations, they both must be written on the same form of dynamics. Let us illustrate this with a simple example.

7.7.1 Scalar self-energy

In a theory consisting of only scalar fields, the wavefunction renormalization parameter Z (to be defined below) takes on a simpler form than in the case of particles with spin.

A simple scalar theory is described by the following interaction Lagrangian,

$$\mathscr{L}_{\text{int}}^{\text{scalar}} = g\bar{B}MP + \text{h.c.}, \tag{7.47}$$

where the 'baryon' (B), 'meson' (M) and the 'proton' (P) are all scalars and g denotes a coupling. We want to calculate the leading-order BM contribution to the proton self-energy $-\mathrm{i}\Sigma(p)$. This is given by the value of the Feynman diagram shown in Figure 7.6 where the blobs denote the form factor $G(\Lambda_H)$ that comes with every vertex but we will avoid writing it out in the following.

The Feynman propagator is given by,

$$\mathrm{i}S_F(p) = \frac{\mathrm{i}}{p^2 - \mathring{m}_P^2 + \mathrm{i}\varepsilon}, \tag{7.48}$$

where we have denoted the bare mass of the proton by $\mathring{m}_P$. In the case of real protons and non-zero spin baryons the most general Clifford expansion implies that the self-energy operator can be written in terms of two scalar functions [cf. Paper I]. In the present case due to the scalar nature of the fields the most general Clifford expansion of the self-energy is given by a single scalar function

$$\Sigma(p) = \Sigma_s(p^2). \tag{7.49}$$

We will in the following omit the subscript and simply write this as $\Sigma(p^2)$.

Thus the full unrenormalized propagator

$$\mathrm{i}S(p) \equiv \mathrm{i}S_F + \mathrm{i}S_F[-\mathrm{i}\Sigma]\mathrm{i}S_F + \cdots \tag{7.50}$$

can be written as,

$$S(p) = \frac{1}{p^2 - \mathring{m}_P^2 - \Sigma(p^2) + \mathrm{i}\varepsilon}. \tag{7.51}$$

The wavefunction renormalization parameter Z can then be obtained by using the pole mass definition $m_P^2 - \mathring{m}_P^2 - \Sigma_s(m_P^2) = 0$, where m_P denotes the physical mass of the proton, and the definition of the renormalized propagator

$$\begin{aligned} Z \times S_R(p) = S(p) &= \frac{1}{p^2 - \mathring{m}_P^2 - \left[\Sigma(m_P^2) + (p^2 - m_P^2)\Sigma'(m_P^2) + \cdots\right]} \\ &= \frac{1}{1 - \Sigma'(m_P^2)} \times \frac{1}{p^2 - m_P^2}, \end{aligned} \tag{7.52}$$

where

$$\Sigma'(m_P^2) \equiv \left.\frac{\mathrm{d}\Sigma(p^2)}{\mathrm{d}p^2}\right|_{p^2 = m_P^2}. \tag{7.53}$$

Thus, we have

$$Z = \frac{1}{1 - \Sigma'(m_P^2)}. \tag{7.54}$$

The self-energy calculation gives,

$$-\mathrm{i}\Sigma(p^2) = \frac{|g|^2}{(2\pi)^4} \int \mathrm{d}^4k \, \frac{1}{k^2 - m_M^2 + \mathrm{i}\varepsilon} \, \frac{1}{(p-k)^2 - m_B^2 + \mathrm{i}\varepsilon}. \tag{7.55}$$

We now introduce light-cone coordinates and work in the $\vec{p}_\perp = 0$ frame,

$$k^2 = k^+k^- - k_\perp^2, \tag{7.56}$$

$$(p-k)^2 = (p^+ - k^+)(p^- - k^-) - k_\perp^2. \tag{7.57}$$

Let $k^+ = yp^+$, then

$$k^2 - m_M^2 + \mathrm{i}\varepsilon = yp^+ \left(k^- - \frac{m_M^2 + k_\perp^2}{yp^+} + \frac{\mathrm{i}\varepsilon}{yp^+}\right) \tag{7.58}$$

and

$$(p-k)^2 - m_B^2 + \mathrm{i}\varepsilon = p^+(y-1)\left[k^- - p^- + \frac{m_B^2+k_\perp^2}{(1-y)p^+} - \frac{\mathrm{i}\varepsilon}{(1-y)p^+}\right]. \tag{7.59}$$

Thus

$$\Sigma(p^-) = \frac{-\mathrm{i}|g|^2}{(2\pi)^4}\frac{1}{2p^+}\int_{-\infty}^{\infty}\frac{\mathrm{d}y\,\mathrm{d}^2k_\perp}{y(1-y)}\int_{-\infty}^{\infty}\frac{\mathrm{d}k^-}{[k^--\zeta_1][k^--\zeta_2]}, \tag{7.60}$$

where the poles in the complex k^- plane are located at

$$\zeta_1 \equiv \frac{m_M^2+k_\perp^2}{yp^+} - \frac{\mathrm{i}\varepsilon}{yp^+}, \quad \zeta_2(p^-) \equiv p^- - \frac{m_B^2+k_\perp^2}{(1-y)p^+} + \frac{\mathrm{i}\varepsilon}{(1-y)p^+}. \tag{7.61}$$

We notice that the convergence properties of the k^--integral allow us to rewrite it as a closed contour integral in the complex k^- plane. Now, for $y<0$ both the poles $\zeta_{1,2}$ lie in the upper half-plane, hence closing the contour in the lower half-plane yields the integral zero. Similarly if $y>1$ then both poles lie in the lower half-plane and the integral is zero. Thus, this restricts the y-integral to the physical range $0 \le y \le 1$. Picking up the residue we obtain

$$\Sigma(p^-) = \frac{|g|^2}{(2\pi)^3}\frac{1}{2p^+}\int_0^1\frac{\mathrm{d}y\,\mathrm{d}^2k_\perp}{y(1-y)}\frac{1}{\zeta_2(p^-)-\zeta_1}. \tag{7.62}$$

Now

$$\left.\frac{\mathrm{d}\Sigma}{\mathrm{d}p^2}\right|_{p^2=m_P^2} = \frac{1}{p^+}\left.\frac{\mathrm{d}\Sigma}{\mathrm{d}p^-}\right|_{p^+p^-=m_P^2} = \frac{-|g|^2}{16\pi^3}\int_0^1\frac{\mathrm{d}y\,\mathrm{d}^2k_\perp}{y(1-y)}\frac{1}{\left[m_P^2-m^2(1-y,k_\perp^2)\right]^2}, \tag{7.63}$$

where $m^2(y)$ is defined in Equation (7.35).

Now let us reinsert the form factor that comes with every vertex and also to connect with the DIS case we let $y \to 1-y$ so that the baryon carries a momentum fraction y and the meson carries $1-y$. And we can also sum over all possible BM pairs that can contribute to the loop of Fig. 7.6 each having a coupling g_{BM} to the proton. Thus using Eqs. (7.53), (7.54) and (7.63) we find,

$$Z_{\mathrm{SE}}^{\mathrm{scalar}} = \frac{1}{1+\sum_{BM}\frac{|g_{BM}|^2}{16\pi^3}\int_0^1\frac{\mathrm{d}y\,\mathrm{d}^2k_\perp}{y(1-y)}\left|\frac{G(y,k_\perp^2,\Lambda_H^2)}{m_P^2-m^2(y,k_\perp^2)}\right|^2}. \tag{7.64}$$

7.7.2 Scalar DIS

Having the hadronic distribution functions for the realistic DIS case, the scalar case follows trivially with the vertex function of Equation (7.14) replaced by

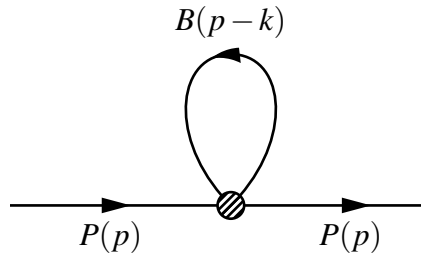

Figure 7.7. Feynman diagram depicting the one-propagator term of Equation (7.67).

unity $S = 1$. Now since $\sum_{BM} |\alpha_{BM}|^2 = \sum_{BM} \int_0^1 \mathrm{d}y f_{BM}(y)$ is the total fluctuation probability, the probability to probe the bare proton is given by

$$Z_{\mathrm{DIS}}^{\mathrm{scalar}} = 1 - \sum_{BM} |\alpha_{BM}|^2 = 1 - \sum_{BM} \frac{|g_{BM|^2}}{16\pi^3} \int_0^1 \frac{\mathrm{d}y\,\mathrm{d}^2k_\perp}{y(1-y)} \left| \frac{G(y,k_\perp^2,\Lambda_H^2)}{m_P^2 - m^2(y,k_\perp^2)} \right|^2 . \tag{7.65}$$

We immediately recognize this as the leading order term in the geometric expansion of Eq. (7.64). Thus

$$Z_{\mathrm{SE}}^{\mathrm{scalar}} = Z_{\mathrm{DIS}}^{\mathrm{scalar}} + \mathscr{O}\left(|\alpha_{BM}|^4\right). \tag{7.66}$$

We note that the result obtained in the self-energy case really is a probability i.e. $0 \leq Z_{\mathrm{SE}}^{\mathrm{scalar}} \leq 1$ whereas $Z_{\mathrm{DIS}}^{\mathrm{scalar}}$ can become negative for unrealistically large values of the cut-off parameter Λ_H. This is not too surprising given the fact that the self-energy result is further away from observables whereas $Z_{\mathrm{DIS}}^{\mathrm{scalar}}$ becoming negative signals that we are operating outside the range of validity of the effective theory. In the self-energy case there is no such signal.

7.7.3 Spin complicates things

Once spin gets involved in the self-energy calculation it is no longer straightforward to make a connection to the probabilities obtained in the DIS calculation. This is due to at least two reasons: The less problematic one is that the Clifford expansion of the self-energy operator now contains two scalar functions one of which is evaluated at the physical proton mass. This is in contrast to the scalar case where it is the derivative of the scalar function that is evaluated at the physical proton mass, cf. Equation (7.54).

The other reason, which is the main issue is that the fermion propagator introduces momenta in the numerator of the self-energy operator. An example

of such a term is given by (cf. Paper I),

$$\begin{aligned}\Sigma &\sim \int \mathrm{d}^4k \frac{k^2}{k^2-m_M^2+\mathrm{i}\varepsilon}\frac{1}{(p-k)^2-m_B^2+\mathrm{i}\varepsilon} \\ &= \int \mathrm{d}^4k \left[\frac{1}{(p-k)^2-m_B^2+\mathrm{i}\varepsilon}+\frac{m_M^2}{k^2-m_M^2+\mathrm{i}\varepsilon}\frac{1}{(p-k)^2-m_B^2+\mathrm{i}\varepsilon}\right],\end{aligned} \tag{7.67}$$

where we have added $0 = m_M^2 - m_M^2$ to the numerator and rewritten. Notice that the first term is a one-propagator term similar to a contact interaction (cf. Figure 7.7) and it is not trivial to relate it to the DIS calculation where only two-propagator terms appear.

To compare with the DIS case we need to rewrite Equation (7.67) in light-cone coordinates and perform the k^- contour integration like we did in the scalar case. But this is not possible for the one-propagator term since the k^--integral is not convergent.

If one still presses on and keeps only the two-propagator terms in the expression for the self-energy one can obtain a relation similar to what we found in the scalar case Equation (7.66) on one condition: That is if one makes the same substitution for the momenta appearing in the numerator as one makes for the momentum choices A and/or B. In other words, one does not integrate over the momenta appearing in the numerator, but instead takes the momenta on-shell. This appears awkward and most likely the resolution of this lies in another approach. Further investigations on this is beyond the scope of this thesis, but the above example shows that the issue is related to the momenta in the numerator as introduced by the effective theory. The problem is less severe in classically renormalizable theories such as QED, cf. e.g. [83, 84, 135].

8. Conclusions and outlook

In this thesis we present our Hadron-Cloud Model (HCM) from which we derive the hadronic distribution functions and present in detail how this is done. Due to the light mass of the pions, naturally the pions play a big role in the hadronic description of nuclear and particle physics. Indeed, we show that a large part of the proton's hadronic wavefunction consists of the wavefunctions of the pions and their companion baryons, the nucleon and the Delta baryon.

With our simple model, which consists of a few physically-constrained parameters the values of which come out as expected from general arguments, we are in agreement with a large set of data on the unpolarized structure functions of the proton.

We also investigate a possible asymmetry in the strange-sea of the proton. Thus we include hadrons containing strangeness into our HCM. These are heavier and have much smaller coupling to the proton, meaning that their fluctuation probabilities are much smaller compared to those of the nucleon-pion or Delta-pion fluctuations. Regardless of this we are able to compare to two available data sets on the strange-sea of the proton. We are in good agreement with the strange-sea data from the HERMES collaboration which shows a small strange-sea content in the proton. The older data from the CCFR collaboration suggest a slightly larger strange-sea content in the proton. In this regard we comment on the possibility to include more strangeness into the model. This may be through the inclusion of the $\Lambda^* K$ fluctuation. We refrain from exploring this possibility mainly because there is no clear indication from experimental data that this is needed.

The model results are in good agreement with data on the flavor asymmetry and the spin structure of the proton. Moreover, exploring a possible SU(6) breaking we show that the polarized structure functions of both the proton and the neutron can be reproduced. Thus we also get good agreement with the measured sum rules of the structure functions, in particular the very important Bjorken sum rule.

The PDFs of our model are global functions which means that their application is not restricted to the reactions we present here. They can be used in various other reactions such as e.g. in proton-proton collisions. In this regard, it would be interesting to see what other insights the HCM has to offer.

9. Summary in Swedish – Populärvetenskaplig sammanfattning

Avhandlingens titel på svenska: *Samspelet mellan kvark och hadronska frihetsgrader och protonens struktur*

Nyfikenhet och grundvetenskapernas nytta

Ett av de utmärkande dragen hos oss människor är vår råa vetgirighet. Vi kan ibland vilja lära oss mer om ett fenomen enbart för nyfikenhetens skull. Lyckligtvis har det genom historien visat sig att denna törst efter kunskap nästan alltid kommit allmänheten till nytta. Ett av de mest självklara exempel på detta ges av Michael Faradays experimenterande med elektricitet och magneter i mitten av 1800-talet. *En dag kan du beskatta det* – så säger legenden att Faraday svarade när han fick frågan av en politiker vari ligger elektricitetens praktiska nytta. Vi är nog de allra flesta överens om att vår förståelse och kontroll av elektricitetens kraft har förhöjt vår livskvalitet avsevärt.

Detta synsätt på grundvetenskaperna, vilket denna avhandling faller under, är ännu mer cementerad idag än någonsin förr. Idag forskar vi om än mer abstrakta fenomen än ovan nämnda exempel från 1800-talets mitt. I detta arbete har vi studerat några finurliga egenskaper hos två partiklar som praktiskt taget hela vår materiella värld består av. Dessa partiklar kallas för *protonen* och *neutronen* och de är i många avseende så otroligt lika att de kan ses som två sidor hos ett och samma mynt. Med andra ord, förstår man ena så förstår man mycket om den andra också.

De allra vanligaste partiklarna

Allt vi kan ta i och känna på är uppbyggd av protoner och neutroner, omgivna av en gas av elektroner. Tillsammans utgör dessa det vi kallar för *atomen*. Om du kunde dela bredden hos ett hårstrå i en miljon lika stora delar så skulle varje del vara en atom bred. I och med denna ‘inzoomning’ så har du alltså gått från ett hårstrå och kommit fram till en atom, dvs till gasmolnet av elektroner. Man skulle kunna tro att protonen och neutronen gömmer sig strax under detta moln av elektroner och att man bara behöver zooma lite till så kommer man fram till atomkärnan. Men det visar sig att kärnan är extremt liten och kompakt. Om atomkärnan skulle var lika stor som ett äpple i din hand så skulle det innebära att elektronmolnet ligger på en höjd av 10 km. Då kan man bara tänka sig hur liten atomkärnan är jämfört med bredden av ett hårstrå!

Kvarkar, gluoner, partoner och färgladdning

Till skillnad från elektronen som är en elementarpartikel, så består protoner och neutroner själva av mindre beståndsdelar. Dessa beståndsdelar är dels materiepartiklar som kallas för *kvarkar* som är elementarpartiklar precis som elektronen, dels består de av förmedlarpartiklar som kallas *gluoner*. En förmedlarpartikel förmedlar kraften mellan andra partiklar. Vanligt ljus som vi bl.a. ser med ögonen är en förmedlarpartikel, den förmedlar den elektromagnetiska kraften mellan partiklar som bär på elektrisk laddning. Gluoner förmedlar något som vi kallar för *färgladdning* mellan partiklar som bär på färgladdning. De partiklar som bär färgladdning är kvarkar och faktiskt gluoner själva. Eftersom både kvarkar och gluoner finns i protonen så brukar man kollektivt kalla dem för *partoner*.

Det finns tre olika färgladdningar, vi kallar dem för röd, grön och blå som kortare skrivs r, g och b. Det finns också motsvarande antifärger som vi skriver som $\bar{r}$, $\bar{g}$ och $\bar{b}$ som tillsammans med deras respektive färger bildar ett färgneutralt tillstånd, dvs ett vitt tillstånd. Varje partikel har dessutom en motsvarande antipartikel. Exempel på dessa är antiprotonen och antineutronen. Det häftiga är att protoner och neutroner, som ju består av färgladdade partoner, själva är *vita* dvs de är färgneutrala. Kan vi beskriva protonen och neutronen i termer av färgladdade kvarkar sådan att 'summan' av alla färger och antifärger på något sätt blir färgneutral? Det visar sig att det går om vi beskriver protonen med tre kvarkar. Detsamma gäller även för neutronen.

Baryoner, mesoner, hadroner

Alla partiklar som består av tre kvarkar kallas för *baryoner*. Det finns dessutom partiklar som består av ett kvark-antikvark par, dessa kallas för *mesoner*. Den allra vanligaste mesonen är pionen som man betecknar π. Mer generellt brukar man kalla både baryoner och mesoner och andra färgneutrala komposita objekt av kvarkar för *hadroner*.

Partikelfysikens standardmodell

I naturen finns det fyra fundamentala krafter eller växelverkan som man numera kallar dem. Dessa är *gravitationskraften*, den *svaga* kraften, *elektromagnetiska* kraften och den *starka* kraften. Den förstnämnda är i många fall gällande mikroskopiska/små massor totalt försumbar. T.ex. så vinner den elektromagnetiska kraften hos ett kylskåpsmagnet över hela jordens gravitationskraft på en liten bit metall!

De övriga tre krafterna beskrivs mycket väl av det som kallas för partikelfysikens standardmodell eller också bara Standardmodellen. Standardmodellen har varit otroligt framgångsrikt och den sista pusselbiten, Higgspartikeln, som enligt Standardmodellen borde finnas hittades till slut mer än 40 år

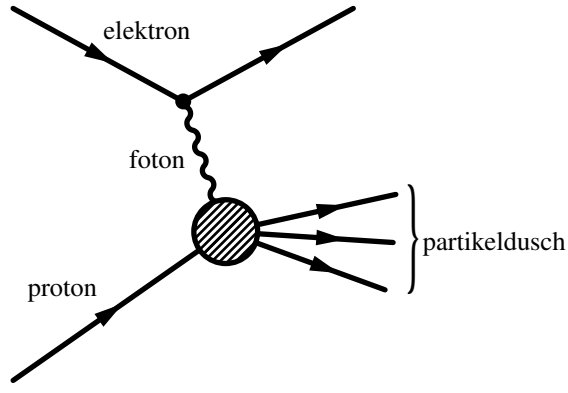

Figur 9.1. Diagram föreställande djupt inelastisk spridning av en elektron på en proton.

efter dess förutsägelse. Men en del av Standardmodellen är mycket mer svårbegriplig än de två övriga och det är delen som behandlar den starka kraften. Den starka kraften beskrivs av teorin som kallas för kvantkromodynamik. Namnet härleder från att den är en kvantmekanisk teori om färgladdningarna r, g, b och deras antifärger $\bar{r}$, $\bar{g}$ och $\bar{b}$.

Observation och djupt inelastisk spridning

Bilden av naturen och hur vi observerar den såsom vi beskrivit den ovan är en någon förenklad variant. Generellt så kan man säga att för att observera något så måste man sprida ljus på det och sedan fånga upp reflektionen av objektet. Som t.ex. när våra ögon fångar upp ljus som reflekterats på ett objekt, så tolkar våra hjärnor om den informationen och skapar oss en bild av objektet. Men människoögat ser bara ytan av saker. Vill man t.ex. se vad som finns under huden kan man bl.a. använda röntgenljus för att fotografera människoskelettet. Röntgenljus är mycket mer energirikt, därför mycket farligare, än det ljus vi kan se. På samma sätt kan man säga att vill man se protonens skelett dvs protonens byggstenar, kvarkarna, så måste man sprida väldigt energirikt ljus på protonen. Det är precis det som görs vid experiment av *djupt inelastisk spridning*. Inelastisk betyder i det här fallet att protonen slås sönder och samman i och med spridningen och 'förvandlas' till en dusch av partiklar, se Figur 9.1. Omvänt kan man säga att om man istället vrider ner energin hos fotonen så sprids den *elastiskt* på protonen och då ser man protonen som en helhet istället för kvarkarna inuti. Man kan då fråga sig om dessa två olika sorters av experiment, elastiskt och inelastisk spridning, ger samma svar om protonens olika egenskaper?

Asymmetrin i sjön och protonens spinn

En kvantmekanisk egenskap hos protonen som kallas för *spinn* har sedan mitten av 1980-talet gäckat forskarvärlden i det som blivit döpt till *protonens spinn-kris*. Då fann man nämligen att de tre kvarkarnas spinn utgör bara en liten bråkdel av protonens spinn vilket var i motsägelse till den enklaste modellen av protonen som dittills gett en bra förståelse. Protonen och hadroner i allmänhet tycks alltså vara mycket mera komplicerade än att bestå av några stillastående kvarkar.

En mera korrekt beskrivning av protonen är att inuti den finns förutom de tre kvarkarna vi beskrev ovan en hel uppsjö av kvark-antikvark par och gluoner i massor som alla bär en liten del av protonens energi. Experimentellt söker man också finna om denna sjö är polariserad dvs om den bär en del av protonens spinn. Vidare finns data på den så kallade *asymmetrin* i sjön i en proton dvs att en viss sorts antikvark som kallas $\bar{d}$ bär mera av protonens impuls & energi än en liknande antikvark kallad $\bar{u}$. Detta är mycket oväntat då dessa antikvarkar båda är väldigt lätta jämfört med kvantkromodynamikens skala kallad Λ_{QCD}.

Störningsteori

I de flesta fall av problemlösning inom fysiken så brukar man tillämpa en viss beräkningsmetod kallad störningsteori. Störningsteori fungerar på så sätt att man delar in problemet i två delar. Ena delen kan man lösa på ett exakt sätt medan den andra delen antar man är litet jämfört med den exakta delen dvs att den är en liten störning. Inom kvantkromodynamik så inser man att störningen är proportionell mot α_s (alpha-s) som är styrkan i en stark växelverkan. Två starka växelverkan är då proportionell mot $\alpha_s \times \alpha_s$ och tre växelverkan är proportionell mot $\alpha_s \times \alpha_s \times \alpha_s$ osv. Om nu α_s är litet jämfört med 1 så är två växelverkan ännu mindre. Som exempel om $\alpha_s = 1/10 = 0.1$ så är $\alpha_s \times \alpha_s = 1/100 = 0.01$ som ju är 10 gånger mindre än α_s. Alltså kan man i de flesta fallen nöja sig med att beräkna de delar som är proportionella mot α_s och anta att de andra delarna är försumbara. Detta fungerar utmärkt så länge α_s är litet jämfört med 1. Det som gör kvantkromodynamiken så komplicerad, som benämndes i samband med diskussionen om Standardmodellen ovan, är att α_s blir stor för låga energier och då kan man inte tillämpa störningsmetoder för att lösa problemen. För att göra framsteg har man konstruerat metoder som använder en annan störningsparameter än ovan nämnda α_s. Den främsta teorin i det här avseendet kallas för *kiral störningsteori* som är en låg-energi variant av kvantkromodynamik.

Hadroner som frihetsgrader

Till skillnad från kvantkromodynamiken som har kvarkar och gluoner som frihetsgrader så har kiral störningsteori hadroner som frihetsgrader. I vår

beskrivning av protonen tar vi hänsyn till detta. Som exempel visar vi i artikel I att protonens vågfunktion (den som teoretiskt beskriver protonens tillstånd), som man skriver $|\text{proton}\rangle$, består till stora delar av andra hadroners vågfunktioner. I enkelhet kan man säga att vi delar in protonens vågfunktion i en del som enbart består av en proton medan de andra delarna består av hadronska fluktuationer.

Generellt så kan man säga att partikel-fluktuationer är något som är tillåtet inom kvantmekanikens värld. Protonens fluktuationer har protonens kvanttal, som t.ex. samma elektriska laddning. Med andra ord skriver vi protonens vågfunktion som

$$|\text{proton}\rangle = \alpha_{\text{bar}} \times |\text{proton}\rangle_{\text{bar}} + \alpha_{n\pi} \times |\text{neutron+pion}\rangle + \text{andra fluktuationer}, \tag{9.1}$$

där den första termen representerar den bara (nakna) protonen medan den andra termen representerar ett neutron-pion par. Parametrarna α_{bar} och $\alpha_{n\pi}$ är sannolikhetsamplituder för respektive term, dvs de är relaterade till hur stor sannolikhet respektive term har i protonens vågfunktion. I vårt arbete har vi också tagit hänsyn till många andra fluktuationer som vi inte skrivit ut i ovan ekvation.

Från modellen som ges av vågfunktionen (9.1) följer alltså att när man sprider en foton på en proton som i Figur 9.1 finns en betydande chans att man egentligen sprider på en fluktuation istället. När man då sprider på en fluktuation måste man tag hänsyn till kvark- och gluon-fördelningarna i fluktuationen. Dessa fördelningar brukar man parametrisera med ett stort antal (cirka 30 st.) parametrar som man anpassar till data från experiment. Detta ger ett effektivt sätt att beskriva andra experiment där samma fördelningar ingår, men det ger inte så mycket för själva förståelsen av protonen. Vi använder istället en mycket enklare model för dessa fördelningar som utgår från en fysikalisk modell av protonen och som ges av få parametrar.

Genom att lägga ihop denna modell för kvark- och gluon-fördelningarna tillsammans med fördelningarna för hadronerna får vi resultat som överensstämmer med en stor mängd data från experiment

Resultat

I denna avhandling presenterar vi vår modell kallad HCM (Hadron-Cloud Model) varifrån vi härleder de hadronska fördelningsfunktionerna. Vi visar i detalj hur detta går till. På grund av pionernas lätta massa så spelar de en stor roll i hadronska reaktioner i kärn- och partikelfysik. Vi visar att stora delar av protonens hadronska vågfunktion består av andra hadroners vågfunktioner, i synnerhet de tillhörande pioner, nukleoner och Delta-baryoner.

Vi undersöker en eventuell asymmetri i särkvarksjön, varför vi även inkluderar tyngre hadroner i vår beskrivning av de hadronska fluktuationerna. Dessa tyngre hadroner har mycket mindre sannolikhetsamplituder på grund av deras större massa och mindre kopplingar till protonen. Med avseende på asymmetrin i särkvarksjön jämför vi med data från två olika experiment varav vår modell är i bra överensstämmelse med det nya experimentet. Data från det äldre experimentet visar på lite mera särkvarkar i sjön. Vi ger förslag på en utveckling av modellen där man också tar hänsyn till andra hadronska frihetsgrader innehållande särkvarkar, som t.ex. $\Lambda^* K$ fluktuationen. Men vi avstår från en vidareutveckling av detta på grund av att det inte finns tillräckligt mycket indikation från experiment att det behövs.

Med vår enkla modell vars få parametrar är i princip bestämda av fysikaliska randvillkor får vi resultat som överensstämmer med en stor mängd data på protonens opolariserade strukturfunktioner. Våra resultat överensstämmer också med data på $\bar{d}$-$\bar{u}$ asymmetrin i sjön.

Genom att utforska ett brott i SU(6) symmetrin hos protonen och neutronen visar vi att våra resultat också överensstämmer med data på de polariserade strukturfunktionerna och därmed summareglerna, i synnerhet Bjorkens summaregel.

Modellen är väldigt generell i att den kan tillämpas på andra reaktioner inom kärn- och partikelfysiken som t.ex. proton-proton kollisioner.

List of abbreviations

QCD	quantum chromodynamics
pQCD	perturbative QCD
QED	quantum electrodynamics
PDF	parton distribution function
PDFs	parton distribution functions
HCM	Hadron-Cloud Model
ChPT	chiral perturbation theory
DIS	deep inelastic scattering
DGLAP	Dokshitzer-Gribov-Lipatov-Altarelli-Parisi
TOPT	time-ordered perturbation theory
LCTOPT	light-cone time-ordered perturbation theory

Acknowledgements

First and foremost, I would like to extend my gratitude to my supervisors Stefan Leupold and Gunnar Ingelman. You have been great mentors and I feel that I have learned a lot from both of you. Thank you for giving me this opportunity and for your guidance.

I give a shout-out to all my awesome colleagues at the Nuclear Physics division and at the Division for High Energy Physics at UU. *Ingen nämnd och ingen glömd.*

I send thanks out to my family and friends and to all those who supported me and encouraged me throughout the years.

References

[1] J. Lilley, *Nuclear physics: principles and applications*. Manchester physics series, J. Wiley, 2001.

[2] C. G. Tully, *Elementary particle physics in a nutshell*. 2011.

[3] S. L. Olsen, T. Skwarnicki, and D. Zieminska, "Nonstandard heavy mesons and baryons: Experimental evidence," *Rev. Mod. Phys.*, vol. 90, no. 1, p. 015003, 2018.

[4] M. E. Peskin and D. V. Schroeder, *An introduction to quantum field theory*. Boulder, CO: Westview, 1995.

[5] R. Gupta, "Introduction to lattice QCD: Course," in *Probing the standard model of particle interactions. Proceedings, Summer School in Theoretical Physics, NATO Advanced Study Institute, 68th session, Les Houches, France, July 28-September 5, 1997. Pt. 1, 2*, pp. 83–219, 1997.

[6] S. Scherer, "Introduction to chiral perturbation theory," *Adv. Nucl. Phys.*, vol. 27, p. 277, 2003.

[7] G. Altarelli and G. Parisi, "Asymptotic Freedom in Parton Language," *Nucl. Phys.*, vol. B126, pp. 298–318, 1977.

[8] Y. L. Dokshitzer, "Calculation of the Structure Functions for Deep Inelastic Scattering and e^+e- Annihilation by Perturbation Theory in Quantum Chromodynamics.," *Sov. Phys. JETP*, vol. 46, pp. 641–653, 1977.

[9] V. N. Gribov and L. N. Lipatov, "Deep inelastic ep scattering in perturbation theory," *Sov. J. Nucl. Phys.*, vol. 15, pp. 438–450, 1972.

[10] J. D. Sullivan, "One pion exchange and deep inelastic electron - nucleon scattering," *Phys. Rev.*, vol. D5, pp. 1732–1737, 1972.

[11] M. Ericson and A. W. Thomas, "Pionic Corrections and the EMC Enhancement of the Sea in Iron," *Phys. Lett.*, vol. 128B, pp. 112–116, 1983.

[12] H. Holtmann, A. Szczurek, and J. Speth, "Flavor and spin of the proton and the meson cloud," *Nucl. Phys.*, vol. A596, pp. 631–669, 1996.

[13] A. Edin and G. Ingelman, "A Model for the parton distributions in hadrons," *Phys. Lett.*, vol. B432, pp. 402–410, 1998.

[14] J. Alwall and G. Ingelman, "Quark asymmetries in the proton from a model for parton densities," *Phys. Rev.*, vol. D71, p. 094015, 2005.

[15] W.-C. Chang and J.-C. Peng, "Flavor Structure of the Nucleon Sea," *Prog. Part. Nucl. Phys.*, vol. 79, pp. 95–135, 2014.

[16] S. Kofler and B. Pasquini, "Collinear parton distributions and the structure of the nucleon sea in a light-front meson-cloud model," *Phys. Rev.*, vol. D95, no. 9, p. 094015, 2017.

[17] R. S. Towell *et al.*, "Improved measurement of the $\bar{d}/\bar{u}$ asymmetry in the nucleon sea," *Phys. Rev. D*, vol. 64, p. 052002, Aug 2001.

[18] T.-P. Cheng and L.-F. Li, *Gauge theory of elementary particle physics*. Oxford: Clarendon, 1984.

[19] M. Srednicki, *Quantum Field Theory*. Cambridge University Press, 2007.
[20] M. Schwartz, *Quantum Field Theory and the Standard Model*. Quantum Field Theory and the Standard Model, Cambridge University Press, 2014.
[21] D. J. Griffiths, *Introduction to elementary particles; 2nd rev. version*. Physics textbook, New York, NY: Wiley, 2008.
[22] H. Georgi, *Lie Algebras In Particle Physics: from Isospin To Unified Theories*. CRC Press, 2018.
[23] H. Liu, *8.324 Relativistic Quantum Field Theory II*. Massachusetts Institute of Technology: MIT OpenCourseWare, 2010.
[24] F. Englert and R. Brout, "Broken symmetry and the mass of gauge vector mesons," *Phys. Rev. Lett.*, vol. 13, pp. 321–323, Aug 1964.
[25] P. W. Higgs, "Broken symmetries and the masses of gauge bosons," *Phys. Rev. Lett.*, vol. 13, pp. 508–509, Oct 1964.
[26] G. 't Hooft, "Renormalization of Massless Yang-Mills Fields," *Nucl. Phys.*, vol. B33, pp. 173–199, 1971.
[27] G. 't Hooft, "Renormalizable Lagrangians for Massive Yang-Mills Fields," *Nucl. Phys.*, vol. B35, pp. 167–188, 1971.
[28] G. 't Hooft and M. J. G. Veltman, "Regularization and Renormalization of Gauge Fields," *Nucl. Phys.*, vol. B44, pp. 189–213, 1972.
[29] C. Itzykson and J. B. Zuber, *Quantum Field Theory*. International Series in Pure and Applied Physics, New York: McGraw-Hill, 1980.
[30] Y. Aharonov and D. Bohm, "Significance of electromagnetic potentials in the quantum theory," *Phys. Rev.*, vol. 115, pp. 485–491, Aug 1959.
[31] L. D. Faddeev and V. N. Popov, "Feynman Diagrams for the Yang-Mills Field," *Phys. Lett.*, vol. B25, pp. 29–30, 1967.
[32] T. van Ritbergen, J. A. M. Vermaseren, and S. A. Larin, "The four-loop beta-function in quantum chromodynamics," *Phys. Lett.*, vol. B400, pp. 379–384, 1997.
[33] F. Herzog, B. Ruijl, T. Ueda, J. A. M. Vermaseren, and A. Vogt, "The five-loop beta function of Yang-Mills theory with fermions," *JHEP*, vol. 02, p. 090, 2017.
[34] D. J. Gross and F. Wilczek, "Ultraviolet behavior of non-abelian gauge theories," *Phys. Rev. Lett.*, vol. 30, pp. 1343–1346, Jun 1973.
[35] H. D. Politzer, "Reliable perturbative results for strong interactions?," *Phys. Rev. Lett.*, vol. 30, pp. 1346–1349, Jun 1973.
[36] M. Gell-Mann, "The Eightfold Way: A theory of strong interaction symmetry," Tech. Rep. CTSL-20, TID-12608, 1961.
[37] M. Gell-Mann and Y. Ne'eman, *The Eightfold Way: a review - with a collection of reprints*. W.A. Benjamin, 1964.
[38] S. Leupold, *Lecture notes for Quantum Chromodynamics and Effective Field Theory*. Unpublished, 2017.
[39] H. Georgi, "Effective field theory," *Ann. Rev. Nucl. Part. Sci.*, vol. 43, pp. 209–252, 1993.
[40] I. Stewart, *8.851 Effective Field Theory, Lecture Notes*. Massachusetts Institute of Technology: MIT OpenCourseWare, 2013.
[41] B. Schutz, *A First Course in General Relativity*. Cambridge University Press, 2009.

[42] A. Pich, "Chiral perturbation theory," *Rept. Prog. Phys.*, vol. 58, pp. 563–610, 1995.
[43] B. Kubis, "An Introduction to chiral perturbation theory," in *Workshop on Physics and Astrophysics of Hadrons and Hadronic Matter, Shantiniketan, India, November 6-10, 2006*, 2007.
[44] B. Borasoy, "Introduction to Chiral Perturbation Theory," *Springer Proc. Phys.*, vol. 118, pp. 1–26, 2008.
[45] R. Karplus and M. Neuman, "The scattering of light by light," *Phys. Rev.*, vol. 83, pp. 776–784, Aug 1951.
[46] S. Scherer and M. R. Schindler, "A Primer for Chiral Perturbation Theory," *Lect. Notes Phys.*, vol. 830, pp. pp.1–338, 2012.
[47] M. Holmberg and S. Leupold, "The relativistic chiral Lagrangian for decuplet and octet baryons at next-to-leading order," *Eur. Phys. J.*, vol. A54, no. 6, p. 103, 2018.
[48] E. E. Jenkins and A. V. Manohar, "Chiral corrections to the baryon axial currents," *Phys. Lett.*, vol. B259, pp. 353–358, 1991.
[49] V. Pascalutsa and R. Timmermans, "Field theory of nucleon to higher spin baryon transitions," *Phys. Rev.*, vol. C60, p. 042201, 1999.
[50] V. Pascalutsa, M. Vanderhaeghen, and S. N. Yang, "Electromagnetic excitation of the Delta(1232)-resonance," *Phys. Rept.*, vol. 437, pp. 125–232, 2007.
[51] T. Ledwig, J. Martin Camalich, L. S. Geng, and M. J. Vicente Vacas, "Octet-baryon axial-vector charges and SU(3)-breaking effects in the semileptonic hyperon decays," *Phys. Rev.*, vol. D90, no. 5, p. 054502, 2014.
[52] U. Aydemir, M. M. Anber, and J. F. Donoghue, "Self-healing of unitarity in effective field theories and the onset of new physics," *Phys. Rev.*, vol. D86, p. 014025, 2012.
[53] S. Okubo, "Note on unitary symmetry in strong interactions," *Prog. Theor. Phys.*, vol. 27, pp. 949–966, 1962.
[54] J. Gasser and H. Leutwyler, "Quark Masses," *Phys. Rept.*, vol. 87, pp. 77–169, 1982.
[55] W. Heisenberg, "Über den Bau der Atomkerne. I," *Zeitschrift für Physik*, vol. 77, pp. 1–11, Jan 1932.
[56] J. Chadwick, "The Existence of a Neutron," *Proc. Roy. Soc. Lond.*, vol. A136, no. 830, pp. 692–708, 1932.
[57] J. Chadwick and M. Goldhaber, "The nuclear photoelectric effect," *Proceedings of the Royal Society of London A: Mathematical, Physical and Engineering Sciences*, vol. 151, no. 873, pp. 479–493, 1935.
[58] H. Geiger, "On the scattering of the α-particles by matter," *Proceedings of the Royal Society of London A: Mathematical, Physical and Engineering Sciences*, vol. 81, no. 546, pp. 174–177, 1908.
[59] H. Geiger and E. Marsden, "On a diffuse reflection of the α-particles," *Proceedings of the Royal Society of London A: Mathematical, Physical and Engineering Sciences*, vol. 82, no. 557, pp. 495–500, 1909.
[60] E. Rutherford, "The scattering of alpha and beta particles by matter and the structure of the atom," *Phil. Mag. Ser.6*, vol. 21, pp. 669–688, 1911.
[61] E. D. Bloom, D. H. Coward, H. DeStaebler, J. Drees, G. Miller, L. W. Mo, R. E. Taylor, M. Breidenbach, J. I. Friedman, G. C. Hartmann, and H. W.

Kendall, "High-energy inelastic $e - p$ scattering at 6° and 10°," *Phys. Rev. Lett.*, vol. 23, pp. 930–934, Oct 1969.
[62] M. Breidenbach, J. I. Friedman, H. W. Kendall, E. D. Bloom, D. H. Coward, H. DeStaebler, J. Drees, L. W. Mo, and R. E. Taylor, "Observed behavior of highly inelastic electron-proton scattering," *Phys. Rev. Lett.*, vol. 23, pp. 935–939, Oct 1969.
[63] J. D. Bjorken, "Current algebra at small distances," *Proc. of Int. School of Physics, Enrico Fermi, 41st Course*, vol. C670717, pp. 55–81, 1967.
[64] R. P. Feynman, "The behavior of hadron collisions at extreme energies," *Conf. Proc. 3rd International Conference on High Energy Collisions Stony Brook, N.Y., September 5-6, 1969*, vol. C690905, pp. 237–258, 1969.
[65] J. D. Bjorken and E. A. Paschos, "Inelastic electron-proton and γ-proton scattering and the structure of the nucleon," *Phys. Rev.*, vol. 185, pp. 1975–1982, Sep 1969.
[66] S. L. Adler and W.-K. Tung, "Breakdown of asymptotic sum rules in perturbation theory," *Phys. Rev. Lett.*, vol. 22, pp. 978–981, May 1969.
[67] R. Jackiw and G. Preparata, "Probes for the constituents of the electromagnetic current and anomalous commutators," *Phys. Rev. Lett.*, vol. 22, pp. 975–977, May 1969.
[68] C. Berger *et al.*, "Jet Analysis of the Υ (9.46) Decay Into Charged Hadrons," *Phys. Lett.*, vol. 82B, pp. 449–455, 1979.
[69] C. Berger *et al.*, "Topology of the υ-decay," *Zeitschrift für Physik C Particles and Fields*, vol. 8, pp. 101–114, Jun 1981.
[70] M. Gell-Mann, "A Schematic Model of Baryons and Mesons," *Phys. Lett.*, vol. 8, pp. 214–215, 1964.
[71] G. Zweig, "An SU_3 model for strong interaction symmetry and its breaking; Version 1," Tech. Rep. CERN-TH-401, CERN, Geneva, Jan 1964.
[72] A. W. Thomas and W. Weise, *The Structure of the Nucleon*. Berlin, Germany: Wiley-VCH, 2001.
[73] J. S. Schwinger, "On Quantum electrodynamics and the magnetic moment of the electron," *Phys. Rev.*, vol. 73, pp. 416–417, 1948.
[74] P. G. Blunden, W. Melnitchouk, and J. A. Tjon, "Two photon exchange and elastic electron proton scattering," *Phys. Rev. Lett.*, vol. 91, p. 142304, 2003.
[75] J. D. Bjorken, "Asymptotic Sum Rules at Infinite Momentum," *Phys. Rev.*, vol. 179, pp. 1547–1553, 1969.
[76] R. L. Jaffe, "Deep inelastic scattering with application to nuclear targets," Tech. Rep. MIT-CTP-1261, MIT. Cent. Theor. Phys., Cambridge, MA, Jul 1985.
[77] P. A. M. Dirac, "Forms of relativistic dynamics," *Rev. Mod. Phys.*, vol. 21, pp. 392–399, Jul 1949.
[78] H. Leutwyler and J. Stern, "Relativistic Dynamics on a Null Plane," *Annals Phys.*, vol. 112, p. 94, 1978.
[79] F. Coester, "Null plane dynamics of particles and fields," *Prog. Part. Nucl. Phys.*, vol. 29, pp. 1–32, 1992.
[80] T. Heinzl, "Light cone quantization: Foundations and applications," *Lect. Notes Phys.*, vol. 572, pp. 55–142, 2001.
[81] J. C. Collins, "Light cone variables, rapidity and all that," 1997.

[82] B. L. Bakker, "Forms of relativistic dynamics," *Lect. Notes Phys.*, vol. 572, pp. 1–54, 2001.
[83] N. C. J. Schoonderwoerd and B. L. G. Bakker, "Equivalence of renormalized covariant and light-front perturbation theory. 1. Longitudinal divergences in the Yukawa model," *Phys. Rev.*, vol. D57, pp. 4965–4975, 1998.
[84] B. L. G. Bakker, M. A. DeWitt, C.-R. Ji, and Y. Mishchenko, "Restoring the equivalence between the light-front and manifestly covariant formalisms," *Phys. Rev.*, vol. D72, p. 076005, 2005.
[85] A. Airapetian *et al.*, "Search for a Two-Photon Exchange Contribution to Inclusive Deep-Inelastic Scattering," *Phys. Lett.*, vol. B682, pp. 351–354, 2010.
[86] A. Argento *et al.*, "Electroweak Asymmetry in Deep Inelastic Muon - Nucleon Scattering," *Phys. Lett.*, vol. 120B, p. 245, 1983.
[87] F. Halzen and A. D. Martin, *Quarks and Leptons: An introductory course in modern particle physics*. New York, USA: Wiley, 1984.
[88] A. V. Manohar, "An Introduction to spin dependent deep inelastic scattering," in *Lake Louise Winter Institute: Symmetry and Spin in the Standard Model Lake Louise, Alberta, Canada, February 23-29, 1992*, pp. 1–46, 1992.
[89] B. Adeva *et al.*, "Spin asymmetries A_1 of the proton and the deuteron in the low x and low $Q2$ region from polarized high-energy muon scattering," *Phys. Rev.*, vol. D60, p. 072004, 1999. [Erratum: Phys. Rev.D62,079902(2000)].
[90] B. W. Filippone and X.-D. Ji, "The Spin structure of the nucleon," *Adv. Nucl. Phys.*, vol. 26, p. 1, 2001.
[91] C. G. Callan and D. J. Gross, "High-energy electroproduction and the constitution of the electric current," *Phys. Rev. Lett.*, vol. 22, pp. 156–159, Jan 1969.
[92] A. Bodek, M. Breidenbach, D. L. Dubin, J. E. Elias, J. I. Friedman, H. W. Kendall, J. S. Poucher, E. M. Riordan, M. R. Sogard, D. H. Coward, and D. J. Sherden, "Experimental studies of the neutron and proton electromagnetic structure functions," *Phys. Rev. D*, vol. 20, pp. 1471–1552, Oct 1979.
[93] T. Muta, *Foundations of Quantum Chromodynamics: An Introduction to Perturbative Methods in Gauge Theories, (3rd ed.)*, vol. 78 of *World scientific Lecture Notes in Physics*. Hackensack, N.J.: World Scientific, 2010.
[94] J. C. Collins, D. E. Soper, and G. F. Sterman, "Factorization of Hard Processes in QCD," *Adv. Ser. Direct. High Energy Phys.*, vol. 5, pp. 1–91, 1989.
[95] M. Anselmino, A. Efremov, and E. Leader, "The Theory and phenomenology of polarized deep inelastic scattering," *Phys. Rept.*, vol. 261, pp. 1–124, 1995. [Erratum: Phys. Rept.281,399(1997)].
[96] D. Adams *et al.*, "Spin structure of the proton from polarized inclusive deep-inelastic muon-proton scattering," *Phys. Rev. D*, vol. 56, pp. 5330–5358, Nov 1997.
[97] A. Airapetian *et al.*, "Measurement of the virtual-photon asymmetry A_2 and the spin-structure function g_2 of the proton," *Eur. Phys. J.*, vol. C72, p. 1921, 2012.
[98] J. D. Bjorken, "Applications of the chiral $u(6) \bigotimes u(6)$ algebra of current densities," *Phys. Rev.*, vol. 148, pp. 1467–1478, Aug 1966.
[99] J. D. Bjorken, "Inelastic scattering of polarized leptons from polarized nucleons," *Phys. Rev. D*, vol. 1, pp. 1376–1379, Mar 1970.

[100] J. R. Ellis and R. L. Jaffe, "Sum Rule for Deep Inelastic Electroproduction from Polarized Protons," *Phys. Rev.*, vol. D9, p. 1444, 1974. [Erratum: Phys. Rev. D10, 1669 (1974)].
[101] S. A. Larin, T. van Ritbergen, and J. A. M. Vermaseren, "The Alpha-s**3 approximation of quantum chromodynamics to the Ellis-Jaffe sum rule," *Phys. Lett.*, vol. B404, pp. 153–160, 1997.
[102] P. A. Baikov, K. G. Chetyrkin, and J. H. Kuhn, "Adler Function, Bjorken Sum Rule, and the Crewther Relation to Order α_s^4 in a General Gauge Theory," *Phys. Rev. Lett.*, vol. 104, p. 132004, 2010.
[103] C. Patrignani *et al.*, "Review of Particle Physics," *Chin. Phys.*, vol. C40, no. 10, p. 100001, 2016.
[104] C. Adolph *et al.*, "The spin structure function g_1^{p} of the proton and a test of the Bjorken sum rule," *Phys. Lett.*, vol. B753, pp. 18–28, 2016.
[105] C. A. Aidala, S. D. Bass, D. Hasch, and G. K. Mallot, "The Spin Structure of the Nucleon," *Rev. Mod. Phys.*, vol. 85, pp. 655–691, 2013.
[106] J. Ashman *et al.*, "A Measurement of the Spin Asymmetry and Determination of the Structure Function g_1 in Deep Inelastic Muon-Proton Scattering," *Phys. Lett.*, vol. B206, p. 364, 1988.
[107] B. Adeva *et al.*, "Spin asymmetries A_1 and structure functions g_1 of the proton and the deuteron from polarized high-energy muon scattering," *Phys. Rev.*, vol. D58, p. 112001, 1998.
[108] E. S. Ageev *et al.*, "Measurement of the spin structure of the deuteron in the DIS region," *Phys. Lett.*, vol. B612, pp. 154–164, 2005.
[109] V. Yu. Alexakhin *et al.*, "The Deuteron Spin-dependent Structure Function g_1^d and its First Moment," *Phys. Lett.*, vol. B647, pp. 8–17, 2007.
[110] A. Airapetian *et al.*, "Precise determination of the spin structure function g_1 of the proton, deuteron and neutron," *Phys. Rev.*, vol. D75, p. 012007, 2007.
[111] K. V. Dharmawardane *et al.*, "Measurement of the x- and Q^2-dependence of the asymmetry A_1 on the nucleon," *Phys. Lett.*, vol. B641, pp. 11–17, 2006.
[112] B. I. Abelev *et al.*, "Longitudinal double-spin asymmetry for inclusive jet production in $p+p$ collisions at $\sqrt{s} = 200$ GeV," *Phys. Rev. Lett.*, vol. 100, p. 232003, 2008.
[113] A. Adare *et al.*, "Inclusive cross-section and double helicity asymmetry for π^0 production in $p+p$ collisions at $\sqrt{s} = 200$ GeV: Implications for the polarized gluon distribution in the proton," *Phys. Rev.*, vol. D76, p. 051106, 2007.
[114] V. W. Hughes, "High-energy physics with polarized electrons and muons," *Nucl. Phys.*, vol. A518, pp. 371–388, 1990.
[115] F. Myhrer and A. W. Thomas, "Understanding the proton's spin structure," *J. Phys.*, vol. G37, p. 023101, 2010.
[116] T. Sloan, R. Voss, and G. Smadja, "The Quark Structure of the Nucleon from the CERN Muon Experiments," *Phys. Rept.*, vol. 162, pp. 45–167, 1988.
[117] H. D. Politzer, "Asymptotic Freedom: An Approach to Strong Interactions," *Phys. Rept.*, vol. 14, pp. 129–180, 1974.
[118] D. J. Gross and F. Wilczek, "Asymptotically free gauge theories. 2.," *Phys. Rev.*, vol. D9, pp. 980–993, 1974.
[119] H. Georgi and H. D. Politzer, "Electroproduction scaling in an asymptotically free theory of strong interactions," *Phys. Rev.*, vol. D9, pp. 416–420, 1974.

[120] A. V. Manohar, "The Polarized gluon distribution and large transverse momentum jets," *Phys. Lett.*, vol. B255, pp. 579–582, 1991.
[121] X. Ji, J.-H. Zhang, and Y. Zhao, "Physics of the Gluon-Helicity Contribution to Proton Spin," *Phys. Rev. Lett.*, vol. 111, p. 112002, 2013.
[122] G. Altarelli and G. G. Ross, "The Anomalous Gluon Contribution to Polarized Leptoproduction," *Phys. Lett.*, vol. B212, pp. 391–396, 1988.
[123] R. D. Carlitz, J. C. Collins, and A. H. Mueller, "The Role of the Axial Anomaly in Measuring Spin Dependent Parton Distributions," *Phys. Lett.*, vol. B214, pp. 229–236, 1988.
[124] A. Airapetian *et al.*, "Leading-Order Determination of the Gluon Polarization from high-p_T Hadron Electroproduction," *JHEP*, vol. 08, p. 130, 2010.
[125] C. Adolph *et al.*, "Leading and Next-to-Leading Order Gluon Polarization in the Nucleon and Longitudinal Double Spin Asymmetries from Open Charm Muoproduction," *Phys. Rev.*, vol. D87, no. 5, p. 052018, 2013.
[126] Y.-B. Yang, R. S. Sufian, A. Alexandru, T. Draper, M. J. Glatzmaier, K.-F. Liu, and Y. Zhao, "Glue Spin and Helicity in the Proton from Lattice QCD," *Phys. Rev. Lett.*, vol. 118, no. 10, p. 102001, 2017.
[127] H. J. Melosh, "Quarks: Currents and constituents," *Phys. Rev.*, vol. D9, p. 1095, 1974.
[128] B.-Q. Ma, "Melosh rotation: Source for the proton's missing spin," *J. Phys.*, vol. G17, pp. L53–L58, 1991.
[129] M. Beyer, C. Kuhrts, and H. J. Weber, "Relativistic spin - flavor states in light front dynamics," *Annals Phys.*, vol. 269, pp. 129–158, 1998.
[130] X.-p. Sun and H. J. Weber, "Melosh construction of relativistic three-quark baryon wave functions," *Int. J. Mod. Phys.*, vol. A17, pp. 2535–2554, 2002.
[131] I. Schmidt and J. Soffer, "Melosh rotation and the nucleon tensor charge," *Physics Letters B*, vol. 407, no. 3, pp. 331 – 334, 1997.
[132] S. J. Brodsky, H.-C. Pauli, and S. S. Pinsky, "Quantum chromodynamics and other field theories on the light cone," *Phys. Rept.*, vol. 301, pp. 299–486, 1998.
[133] B. Pasquini and S. Boffi, "Virtual meson cloud of the nucleon and generalized parton distributions," *Phys. Rev.*, vol. D73, p. 094001, 2006.
[134] J. Goldstone, A. Salam, and S. Weinberg, "Broken symmetries," *Phys. Rev.*, vol. 127, pp. 965–970, Aug 1962.
[135] A. Misra and S. Warawdekar, "Equivalence of covariant and light front QED at one loop level," *Phys. Rev.*, vol. D71, p. 125011, 2005.

Acta Universitatis Upsaliensis

Digital Comprehensive Summaries of Uppsala Dissertations from the Faculty of Science and Technology 1711

Editor: The Dean of the Faculty of Science and Technology

A doctoral dissertation from the Faculty of Science and Technology, Uppsala University, is usually a summary of a number of papers. A few copies of the complete dissertation are kept at major Swedish research libraries, while the summary alone is distributed internationally through the series Digital Comprehensive Summaries of Uppsala Dissertations from the Faculty of Science and Technology. (Prior to January, 2005, the series was published under the title "Comprehensive Summaries of Uppsala Dissertations from the Faculty of Science and Technology".)

Distribution: publications.uu.se
urn:nbn:se:uu:diva-357911

ACTA
UNIVERSITATIS
UPSALIENSIS
UPPSALA
2018